EXTRACTION OF CAPROLACTAM IN A ROTATING DISK CONTACTOR EXTRACTOR

by

DAVID A. CATO

B.S., Georgia Southern University, 2001
M.S., University of Georgia, 2005
B.S., Michigan State University, 2010

A REPORT

submitted in partial fulfillment of the requirements for the degree

MASTER OF SCIENCE

Department of Chemical Engineering
College of Engineering

KANSAS STATE UNIVERSITY
Manhattan, Kansas

2016

Approved by:

Major Professor
Larry Erickson

Copyright

Abstract

Caprolactam ($C_6H_{11}NO$) is produced in industry primarily as a monomer to be converted to nylon-6 via a polymerization reaction. More demanding purity requirements for nylon-6 have increased the performance requirements of extraction columns in the purification train of caprolactam production. Caprolactam is produced by performing a Beckmann Rearrangement on cyclohexanone oxime followed by a neutralization of the excess oleum post reaction. The resulting side product is ammonium sulfate in water with a residual amount of caprolactam that has to be extracted with benzene from the aqueous ammonium sulfate solution to reduce product losses. The aqueous caprolactam liquor is extracted in another column into benzene which purifies the product from water soluble impurities. The resulting caprolactam dissolved in benzene is back extracted into water where the final purification steps are completed prior to storage.

Rotating disk contactor (RDC) extraction columns were invented by Royal Dutch Shell in the early 1950's. The columns have a rotor in the center that is driven by an electric motor to rotate equally spaced flat disks inside the column. There are equally spaced annulus shaped stators that serve to provide mixing-separation compartments for each of the mounted disks on the rotor. Of the variables to consider for the optimum performance of the extraction in the RDC extraction column is the rotor speed. Rotor speed curves are generated for the 3 RDC extraction columns of the caprolactam purification as well as calculations of the number of theoretical stages for each of the columns based on actual performance data.

Benzene is the solvent of choice in this purification process however recent push by environmental groups and agencies as well as tightening regulations have driven a desire to find a more benign alternative to benzene for this process. A review of the research and literature on

potential alternative solvents for caprolactam purification is summarized with positives and drawbacks for each possible alternative.

Table of Contents

List of Figures

List of Tables

Acknowledgements

First I would like to acknowledge Felice Cato, my wife, for being so patient and supportive over the past few years while I spent many nights and weekends consumed in coursework. Second, my children Brianna and Evan for being supportive as well, and I hope that I set a good example of how you can accomplish anything you want as long as you are dedicated to doing so. I would like to acknowledge my committee members Dr. Bin Liu and Dr. Jennifer Anthony, my advisor Dr. Larry Erickson and the entire staff at the Department of Chemical Engineering at Kansas State University.

Chapter 1 - Introduction

Solvent Extraction

Liquid-liquid extraction, also known as solvent extraction, is the chemical process of transferring a solute from one solvent into another in a system where the solvents are immiscible. The efficiency of the mass transfer in solvent extraction is dependent upon a number of parameters of each fluid and of the system in whole including density and viscosity of each phase, droplet size of the dispersed phase which equilibrates to surface area for mass transfer, interfacial tension of the system, and partitioning coefficients for mass transfer among others[1]. Two of the most important parameters in this list include the amount of surface area of contact for mass transfer between the two solvents and the relative solubility of the solute in each solvent. The solvent (B) that is used to extract the solute from another solvent (A) becomes the solute rich extract and the solvent (A) that is depleted of solute becomes the raffinate as shown in Figure 1-1.

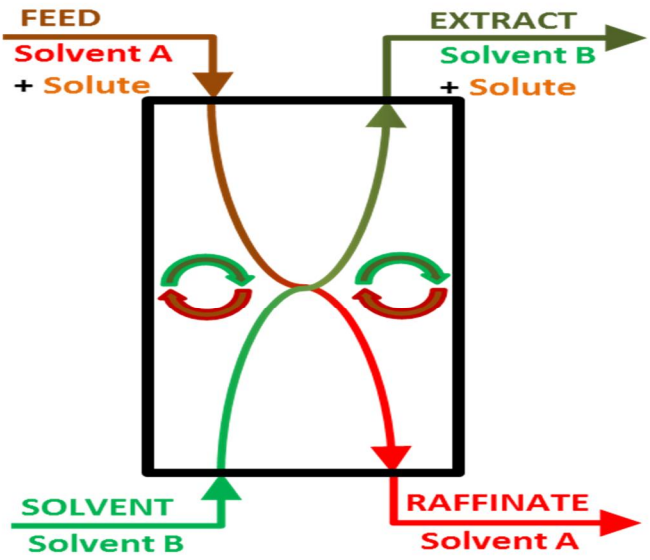

Figure 1-1 Liquid-liquid extraction

Solvent extraction is a purification technique where the solute transfers from the feed solvent to the extract solvent while impurities remain in the raffinate where they have a higher solubility. Extractions on the laboratory scale are typically done with separatory funnels, whereas in industry a large number of extractions are typically done in mixer-settlers or extraction columns.

Surface Area

Solute transfer occurs at the interface between the two immiscible solvents. Therefore solute transfer is highly dependent upon the surface area between the solvents where the transfer of the solute occurs. As two immiscible solvents are fed countercurrent to one another, there is a driving force of the dispersed phase to coalesce into a single stream with the lowest possible surface area. This driving force is the free energy reduction by minimization of surface area. The Helmholtz free energy (A^H) Equation 1-1 shows:

Equation 1-1

$$A^H = U - TS$$

Equation 1-2

$$dA^H = dU - dTS$$

For an isothermal extraction (dQ = 0), the internal energy is shown in Equation 1-3:

Equation 1-3

$$dU = -PdV + \gamma dA$$

Substituting the internal energy dU into Equation 1-2 results in the Helmholtz free energy Equation 1-4:

Equation 1-4

$$dA^H = -PdV - TdS + \gamma dA$$

Since the volume will not change on the incompressible liquids and the entropy is constant, the resulting Helmholtz free energy becomes Equation 1-5:

Equation 1-5

$$dA^H = \gamma dA$$

γ is the surface tension and dA is the change in surface area, therefore any increase in surface area will be proportional to an increase in the free energy of the system[2].

Surface Tension/Interfacial Tension

Surface tension is caused by the attraction between molecules of the liquid by one or more intermolecular forces such as hydrogen bonding or van der Waals forces. Interfacial tension is the driving force for coalescence of the dispersed droplets immersed in another immiscible liquid in order to reduce the interfacial area between the two liquids. The internal energy of an extraction system is a function of the interfacial area and interfacial tension between the two fluids as shown in the Helmholtz equation above. The energy of the system is proportional to interfacial area and therefore smaller droplets means increased interfacial area which results in a higher energy system[3]. A low interfacial tension will favor dispersion and smaller dispersed phase droplets whereas a high interfacial tension will require more energy input into the system in order to maintain the proper droplet dispersion required for efficient solute transfer. Stable emulsions may occur when the interfacial tension of the dispersed phase is low enough and large enough energy per area that continued energy input into the system will result in maintaining the emulsion which is not desirable in most liquid extractions. Extraction columns have a set residence time based on feed rates and stable emulsions can lead to very poor separation and carryover of the dispersed phase.

Extraction is dependent upon the interfacial tension between the two immiscible liquids in that there has to be the capability to break droplets of the dispersed phase in the continuous phase and there has to be strong enough surface tension to drive coalescence at a rate that makes the extraction reasonably effective. In terms of energy, surface tension of a liquid is the ratio of the change in the energy of the liquid to the change in the surface area of the liquid where the surface area change led to the change in energy as seen in Equation 1-6.

Equation 1-6

$$\gamma = \frac{F}{2L} = \frac{A^H}{\Delta A}$$

As stated before, since mechanical systems desire to reach a state of minimum free energy, a free drop of liquid immersed in an immiscible liquid will assume a spherical shape, which has the minimum surface area for a given volume. Multiple droplets will coalesce into fewer, larger drops to reduce surface area and reduce free energy. This is because the molecules in the interfacial region are at a higher free energy than those in the corresponding bulk. Values of surface tension for various liquids can be found in literature where the measurement is that of the liquid surrounded by air. For liquid-liquid extraction, surface tension of the dispersed phase is dependent not only on the surface tension of the dispersed phase, but also of that of the continuous phase. Antonoff's rule provides a prediction of the interfacial tension between two liquids, the dispersed and continuous phases, as the difference in the surface tension of each liquid shown in Equation 1-7 [4].

Equation 1-7

$$\gamma_{Continuous \cdot Dispersed} = \left|\gamma_{Continuous} - \gamma_{Dispersed}\right|$$

So for a system where benzene is the continuous phase and water is the dispersed phase at 105°F with the surface tension for each independent liquid, the interfacial tension can be estimated as shown in Equation 1-8.

$$\gamma_{Benzene} = 26.21\frac{mN}{m}$$

$$\gamma_{Water} = 69.56\frac{mN}{m}$$

Equation 1-8

$$\gamma_{Continuous \cdot Dispersed} = \left|26.21\frac{mN}{m} - 69.56\frac{mN}{m}\right| = 43.35\frac{mN}{m}$$

This is also the value for the interfacial tension when benzene is the dispersed phase in water. A low interfacial tension between solvents means the drive to phase separate is reduced and the coalescing rate is reduced in comparison to a system with high interfacial tension between solvents. This is known as the surface tension case where the droplets of the dispersed phase remain so small that they stay suspended in the continuous phase with a significantly reduced rate of coalescence.

Solute Concentration Effects on Interfacial Tension

Surface tension can also be affected by solute concentration which is dependent on the structure of the solute. The interfacial tension tends to decrease considerably with increasing solute concentration in the system, and the transfer of solute retards drop coalescence due to the decrease in surface tension. The surface tension of a solute in a solvent can be calculated using the Gibbs adsorption isotherm Equation 1-9[5].

Equation 1-9

$$d\gamma = -\Gamma_1 d\mu_1 - \Gamma_2 d\mu_2$$

Where 1 is the solvent and 2 is the solute. Assuming the interface is ideal we can conclude that $\Gamma_1 = 0$ simplifying to Equation 1-10.

Equation 1-10

$$d\gamma = -\Gamma_2 d\mu_2$$

And the chemical potential of the solute can be obtained from Equation 1-11:

Equation 1-11

$$\mu_2 = \mu_2^o + RT \ln\left(\frac{a}{a_0}\right)$$

Which results in the Gibbs Isotherm shown in Equation 1-12:

Equation 1-12

$$\Gamma = -\frac{1}{RT}\left(\frac{\partial \gamma}{\partial C}\right)_{T,P}$$

Where C is the concentration of the solute in the bulk solution. The surface concentration, Γ, represents excess of solute per unit area of the surface with the assumption that the bulk concentration is equivalent all the way to the surface. Transfer of the solute out of the dispersed phase aids in coalescence whereas transfer from the continuous phase into the dispersed phase reduces the rate of coalescence.

The Szyzkowski isotherm can also be used to calculate the effects of solute concentration on the interfacial tension shown in Equation 1-13[6].

Equation 1-13

$$\gamma_{i,T} = \gamma_{0,T} \cdot \left[1 - B_{SZ} \ln\left(\frac{C_i}{A_{SZ}} + 1\right)\right]$$

Where A_{SZ} and B_{SZ} are Szyzkowski adsorption coefficients.

The temperature influence on the interfacial tension of a system without solute present can be determined by Equation 1-14, the Jasper correlation[7].

Equation 1-14

$$\gamma_{0,T} = \gamma_{0,293K} - A_J(T - 293)$$

Where A_J is the Jasper coefficient.

Interfacial Turbulence

Interfacial turbulence is the spontaneous agitation of the interface between two unequilibrated liquids. This is known as the Marangoni effect which involves the rapid movement at a liquid interface caused by local variations in surface tension[8, 9, 10, 11]. The gradient in surface tension causes a hydrodynamic drag which leads to movement of the liquid at the interface. Some extraction systems are stable with transfer of the solute from one solvent to another, but are unstable with transfer in the opposite direction. Interfacial turbulence is promoted by solute transfer out of the higher viscosity phase, out of the phase in which its diffusivity is lower, steep concentration gradients near the interface, low viscosities and diffusivities in both phases, interfacial tensions that are highly sensitive to solute concentration, interfaces of large extent, and large differences in kinematic viscosity and solute diffusivity between the two phases[9, 12]. Interfacial turbulence can increase coalescence rates in some cases and reduce coalescence rates in others.

Salt Concentration Effects on Interfacial Tension

Surface tension of water can be affected by salts. The surface tension tends to increase with increasing concentration of salt dissolved in water[13]. The increased surface tension of the water will increase the interfacial tension between water and another immiscible solvent.

The dissolved ions of a salt will be surrounded by water molecules with the oxygen atoms associated to the cations and the hydrogen atoms associated with the anions. This results in some ionic component interactions combined with the hydrogen bonding interactions which lead to increased surface tension. Figure 1-2 shows the increase in the surface tension of water based on the concentration of different salts.

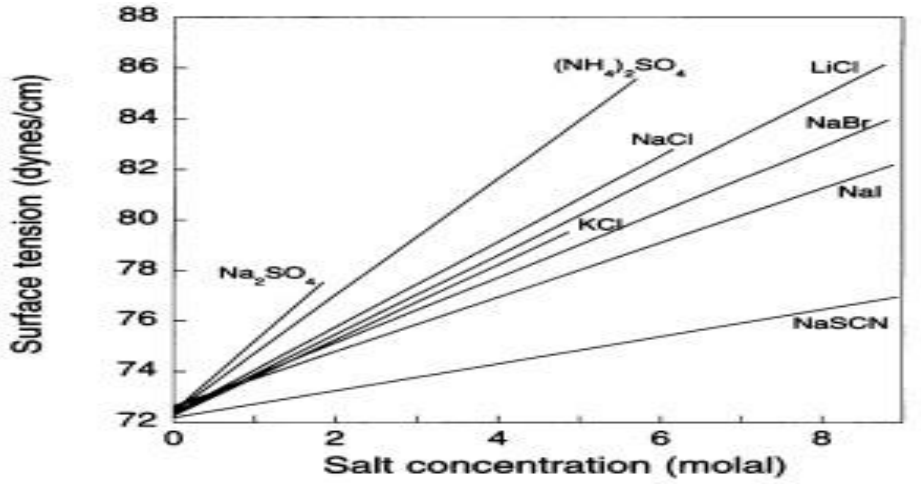

Figure 1-2 Water Surface Tension vs. Salt Concentration[14]

Effects on Surface Tension by pH, Surfactants and Solvent-Solvent Solubility

pH affects the surface tension of water in that lower pH slightly decreases the surface tension and a higher pH shows a slight increase in surface tension. Surface tension can also be affected by solvent-solvent solubility. The more soluble the dispersed phase is in the continuous phase, the lower the surface tension. That is, mutual solubility between the two solvents tends to decrease the interfacial tension[14]. Surfactants also act as additives that can reduce interfacial tension between two immiscible solvents[15].

Drop Coalescence

Coalescence rate is determined by interfacial tension and interfacial tension gradients[16]. Coalescence is promoted by solute transfer out of the dispersed phase but is stunted by solute transfer into the dispersed phase from the continuous phase[16, 17, 18, 19].

Coalescence of drops of the dispersed phase occur in 5 successive steps[16, 20, 21]. First the drop arrives at an interface where the drop and the interface undergo mutual deformation. The trapped film of continuous phase that separates the drop and the interface drains or reduces in thickness. The film continues the thinning process until it reaches a critical thickness threshold where it ruptures. Upon rupture of the film, the drop then deposits into the bulk of the combined drop phase. The predominant factor in the draining of the continuous phase film is the difference in the interfacial tension produced over the surface of the drops[14].

Extraction Columns

Extraction columns are utilized in a number of chemical and biochemical industries, and there are numerous types of extraction columns that are utilized for purification steps in chemical processes. A majority of solvent extractions in columns consist of two immiscible liquids that flow countercurrent to one another based on each solvent's relative density. The heavier liquid is fed at the top of the column and flows downward via gravitational forces through the lighter fluid which is fed at the bottom of the column. The solvents in the extraction column system are characterized as either the dispersed phase or the continuous phase. The dispersed phase is usually a fraction of the feed rate of the continuous phase, and the column usually contains internals that assists in droplet breakage of the dispersed phase to maximize interfacial area. The continuous phase envelops the droplets of the dispersed phase and smaller dispersed phase droplet size means more surface area for solute extraction. Some drawbacks to excessive droplet

breakage include carryover, flooding or emulsion formation in the extraction column. Solute extraction can occur in either direction from the dispersed to the continuous phase or from the continuous to the dispersed phase.

Types of Extraction Columns

There are various types of columns used in industry with varying internal components that assist in maintaining dispersion of the droplets. Some of these columns achieve this with static internals and other by inputting mechanical energy into the fluids in the extraction column.

Solvent Extraction Columns with Static Internals

Static solvent extraction columns have no internal moving parts to induce mixing or internal droplet formation of the solvents. The surface area of the dispersed phase and thereby the transfer of the solute from one solvent to the other is controlled by the flow past immobile column internals.

The most elementary of this type of column is the spray column where the dispersed phase is fed through a dispersion ring of nozzles either from the top or bottom of the column. The drops formed by each nozzle flow up/down the column and have the ability to coalesce without internal resistance other than distance between the drops of the dispersed phase in the continuous phase. Therefore the spray column is the least efficient of the solvent extraction columns.

Additional internals that hinder coalescense of the dispersed phase to assist in maintaining increased surface area between the two solvents include packed beds and sieve trays. Packed bed extraction columns can have either random or structured packing and sieve tray extraction columns have several perforated trays. The packing assists in droplet formation and the trays allow coalescence of the dispersed phase followed by redistribution through the

perforations into the continuous phase[22]. An illustration of these three types of extraction columns is shown in Figure 1-3.

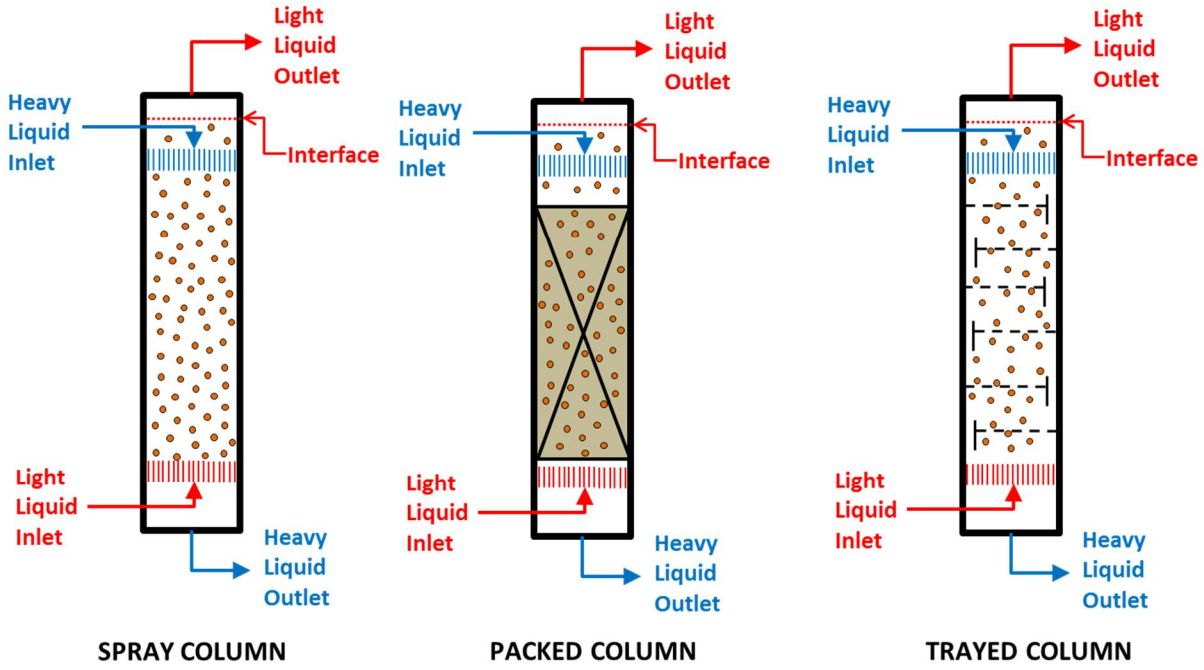

Figure 1-3 Solvent Extraction Columns with Static Internals

Agitated Solvent Extraction Columns

Agitated solvent extraction columns incorporate a mechanically driven apparatus within the column that agitates the liquids as they flow through the column. The purpose of the agitation is to apply the necessary force to the dispersed phase causing breakage of droplets thereby increasing interfacial surface area.

Pulse-packed columns are structure packed extraction columns that incorporate a pulse of pressure in the liquid from the bottom of the column typically by utilizing a pump with wing vessels and a rotary valve located in the bottom of the column. As the rotary valve opens and closes the flow path into the column from the pump, the pulsation that occurs in the liquid assists in droplet breakage of the dispersed phase within the packing.

Rotating disk contactor (RDC) extraction columns have a rotor shaft with mounted disks that penetrate down the center of the column. Rotation of the shaft and disks serve to agitate the liquid and thereby maintain droplet dispersion[23]. These RDC columns also contain baffles called stators that allow regions along the walls of the column for phase separation between each rotating disk contactor. Some major advantages to RDC extraction columns are the minimization of axial mixing compared to non-agitated columns and these columns are less prone to fouling and solids plugging the flow path.

More advanced agitated columns include the Scheibel column and the Karr column. The Scheibel column incorporates a rotating shaft with agitation paddles on the disks that mix the liquids between two inner baffles and separation occurs in compartments with outer baffles and in the screen mesh settling regions between the outer baffle sections[24]. A depiction of a section of the Scheibel column between two of the horizontal outer baffles is shown in Figure 1-4. The Oldshue-Rushton column is very similar to the Scheibel column with the exception that the Oldshue-Rushton column does not have the inner baffles or the screen mesh settling region[74].

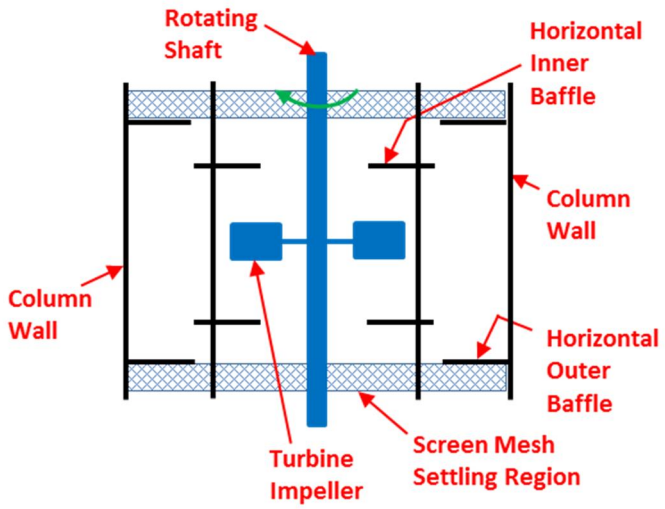

Figure 1-4 Scheibel Column[24]

The Karr column incorporates a set of perforated plates and baffles mounted to a shaft in the column that moves up and down in a piston-like motion within the column[25, 26]. Further modifications to the original RDC column include the Kuhni, Modified RDC and Asymmetric RDC columns. The Kuhni column

incorporates rotary disk contactors that have perforations in the disks with agitation disks spaced and located between each contactor disk[27]. There are also modified RDC columns where only a fraction of the disks in the RDC are perforated[28]. Asymmetrical RDC columns have the shaft with the disk contactors asymmetric to the column and the column has a stator section typically on the side of the column farthest from the shaft location. The stators are only located on approximately a third of the column diameter[29, 30].

Each type of extraction column has its advantages and disadvantages[31]. The spray columns are the least expensive option but they also provide the lowest efficiency extraction capabilities. The packed bed columns are highly efficient however they are prone to fouling and plugging caused by solids. The packing also reduces throughput and there is a potential for channeling of the dispersed liquid through the column. Sieve tray columns allow for a sizeable throughput, but similarly to the packed columns, they are prone to solids plugging the perforations of the trays and potential for channeling flow. The pulse packed columns provide good dispersion, improve efficiency two-fold, and have no internal mechanical parts. However the pulse packed columns provide lower throughput and are more expensive than the non-agitated columns. The rotating disk contactor columns deliver good dispersion with little axial mixing, however any maintenance on the interior mechanical parts can require significant process downtime.

RDC Extraction Columns

The rotating disk contactor columns were originally developed by the Royal Dutch/Shell group in Amsterdam Laboratories in the 1950's[32]. It is a mechanically driven extraction column that is widely used in industry due to its efficiency in liquid-liquid systems with low interfacial tension. The RDC column has a shaft that protrudes down the center of the column,

and the agitation is motor driven from the top of the column. The shaft contains a number of circular disk contactors which are what agitates the liquids to maintain dispersion. Maintaining a dispersed droplet size along the length of the column sustains the needed interfacial surface area which is essential for efficient column performance. This column also has annulus shaped stators that encircle the inside of the column with an inner diameter that is larger than the diameter of the disk contactors. The reason for the larger diameter annulus in comparison to the disk contactors is to allow for removal of the rotor shaft and disks for maintenance. The purpose of the stators are to provide sections along the wall of the column for each disk contactor that allows for coalescence of the dispersed phase. As the dispersed phase coalesces between a pair of stators, it is allowed to travel past the stator through the annulus opening to the next rotating disk contactor and the process is repeated for as many stator sections and disk contactors that are in the extraction column. A section of a RDC extraction column is portrayed in Figure 1-5.

As the liquids flow countercurrent based on densities, there is a complex mixing regime within each stator compartment. First as the liquids contact the rotating disk where the shear force breaks droplets and force the dispersed phase to rotate the same direction as the disk due to the no slip condition on the surface of the disk[33, 34, 35]. There are also horizontal vortices that occur as shown by the red arrows in Figure 1-6 where the vortex starts at the tip of the rotating

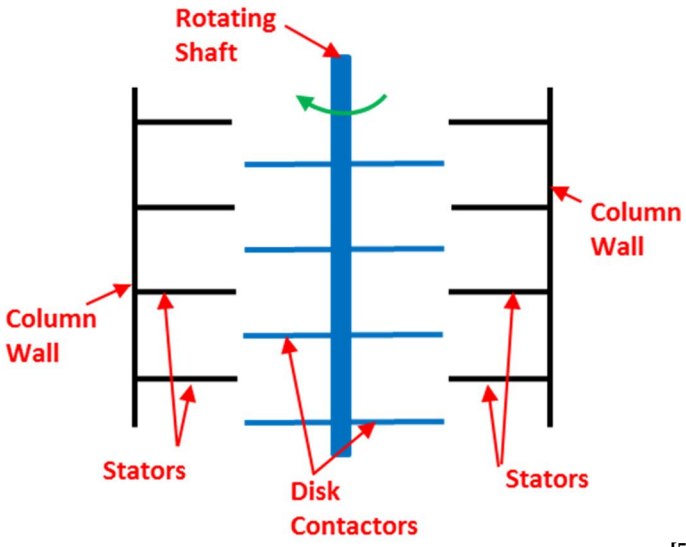

Figure 1-5 Section of a RDC Extraction Column[55]

disk and moves outward to the wall where it is deflected up or down to the stator then back towards the rotating shaft[36]. The combination of the horizontal rotation of the fluid and the vortex flow results in toroidal vortices in each compartment creating turbulence in the liquid which leads to droplet breakage of the dispersed phase.

Separation occurs at sections called settling zones located at either the top or the bottom of the RDC extraction column depending upon which liquid is the dispersed phase and which is the continuous phase. If the heavier liquid is the continuous phase, then the interfacial separation will occur at the top of the column where the lighter dispersed phase coalesces then is allowed to gravity overflow out of the column. If the less dense liquid is the continuous phase, then the interfacial separation will occur at the bottom of the column and the heavier liquid is pumped out of the compartment via a control loop including an interface level controller with an interface level control valve. Settling compartments are located above the top stator and below the bottom stator to break the agitation of the liquids.

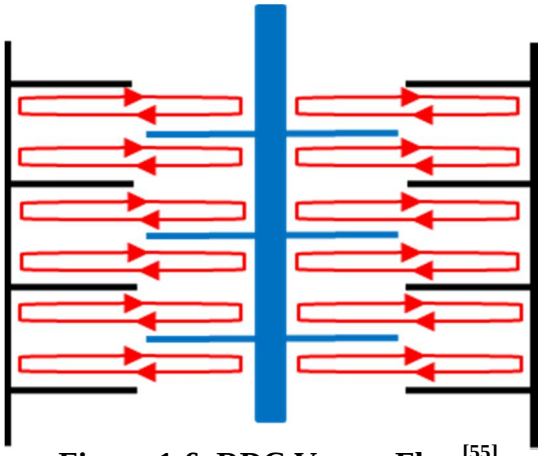

Figure 1-6 RDC Vortex Flow[55]

The rotary disk contactors of the RDC extraction column act to break the dispersed phase droplets thereby increasing the interfacial area. The high velocity of the outermost portion of the rotating disk produces turbulent zones of intense flow between the continuous and dispersed phases. Three quarters of the kinetic energy of the rotation is applied within the turbulent zone which is estimated to be within 2-3 inches of the disk diameter. The shear forces produce very small droplets of the dispersed phase and maintenance of the fine dispersion is important for

providing large interfacial area for solute diffusion. The rotating disks provide enough energy to the dispersed phase to break the droplets into smaller droplets thereby increasing surface area and increasing the free energy of the system.

Rotor Speed

An important factor to consider for solvent extraction for rotating disk contactor extraction columns is the range of agitation at which solute transfer is maximized while carryover, holdup and axial mixing are minimized. If the droplets are broken into such small droplets by the agitation and the flowrate does not allow the residence time required for full coalescence of the dispersed phase, then carryover of the dispersed phase in the continuous phase can occur. This can be very problematic if the next step in the purification train after the RDC extraction column is negatively affected by the liquid carried over. These problems can include reduced extraction efficiency in another extraction column in series, fouling of the internals of the equipment in the next process step, or even formation of an extremely slow separating emulsion in the next purification step.

For RDC extraction columns, energy is input into the liquids via the rotating disks, and rotor speed is proportional to the energy delivered to the extraction column media. Each flowrate in an RDC extraction column has a characteristic rotor speed that produces the highest extraction efficiency while exceeding or undershooting this rotor speed can result in one or more complications with the extraction. Axial mixing is back mixing of either the continuous or dispersed phases in the extraction column which reduces the driving force of mass transfer and therefore reduces extraction efficiency. Hold up, flooding and axial mixing in an extraction column are where the dispersed phase stays dispersed in the column to a point where it remains in the column much longer than expected and there is potential for two different interfacial

separations to occur in the separation compartments at the top and the bottom of the column. Carryover, axial mixing and holdup are typical problems incurred when the rotor speed is too high[37]. Poor extraction efficiency is prominent when the rotor speed is too low, therefore rotor speed is very important for efficient extraction of the solute.

The upper and lower critical rotor speeds are generated based on the probability of droplet breakage of the dispersed phase. The upper critical rotor speed correlates to a droplet breakage probability of 1 and the lower critical rotor speed is for a probability of 0. Equation 1-15 was developed to determine the lower critical speed for any liquid-liquid system and for any column geometry[38].

Equation 1-15

$$N_{cr_1}^2 = \frac{g}{25\, D_R}\left[\left(\frac{\gamma^3 \rho_c}{\mu_c^4 g}\right)^{\frac{1}{4}}\left(\frac{\Delta\rho}{\rho_c}\right)^{\frac{3}{5}}\right]^{0.5}$$

This equation was further modified to obtain the relationship shown in Equation 1-16 for the upper critical rotor speed[39].

Equation 1-16

$$N_{cr_2}^2 = \frac{g}{9\, D_R}\left[\left(\frac{\gamma^3 \rho_c}{\mu_c^4 g}\right)^{\frac{1}{4}}\left(\frac{\Delta\rho}{\rho_c}\right)^{\frac{3}{5}}\right]^{0.5}$$

The lower critical rotor speed represents the rotor speed where drop breakage begins to occur, and any rotor speed lower than this critical speed has a probability of zero for breaking droplets of a specific size. The upper critical rotor speed is the point where the probability for breaking droplets of a specific size equals 1. It can be expected that running the rotor speed below the lower critical speed, extraction efficiency will be poor.

Bahmanyar and Slater proposed the correlation in Equation 1-17 where drop size was introduced into the rotor speed equation[40]. They utilized a simplified balance of shear force arising from a generalized velocity gradient and the resisting force due to interfacial tension.

Equation 1-17

$$\frac{d_{cr}}{D_R} = (3.856 \times 10^{-3})\left(\frac{\rho_c N^2 D_R^3}{\gamma}\right)^{-0.8}\left(\frac{\rho_c N D_R^2}{\mu_c}\right)^{0.7} = (3.856 \times 10^{-3})(We_D)^{-0.8}(Re_D)^{0.7}$$

The characteristic velocity of the dispersed phase droplets remains constant up to a certain rotor speed, and it then decreased with further increases in rotor speed as seen in Equation 1-18[41, 42].

Equation 1-18

$$\bar{u}_0 = \frac{\beta}{G_f}\left[\left(\frac{g}{d_R N^2}\right)\left(\frac{\gamma^3 \rho_c}{\mu_c^4 g}\right)^{0.25}\left(\frac{\Delta\rho}{\rho_c}\right)^{0.6}\right]^p \left(\frac{\gamma \Delta\rho g}{\rho_c^2}\right)^{0.25}$$

The speed of the rotor, which is related to the energy input into the system, provides the means for managing the drop size and is considered one of the key operating variables for RDC extraction columns. Dialing in the proper rotor speed for a specific flow range can lead to optimum performance of the extraction. The correlation for the power input is given by Equation 1-19[55].

Equation 1-19

$$\frac{P_w}{\rho N^3 R^5} = f\left(\frac{\rho N R^2}{\mu}\right)$$

From the calculated result for the bracketed fraction on the right hand side of the equation, the graph shown in Figure 1.7 will provide the result for the left hand side of the equation which will allow for determination of the power input.

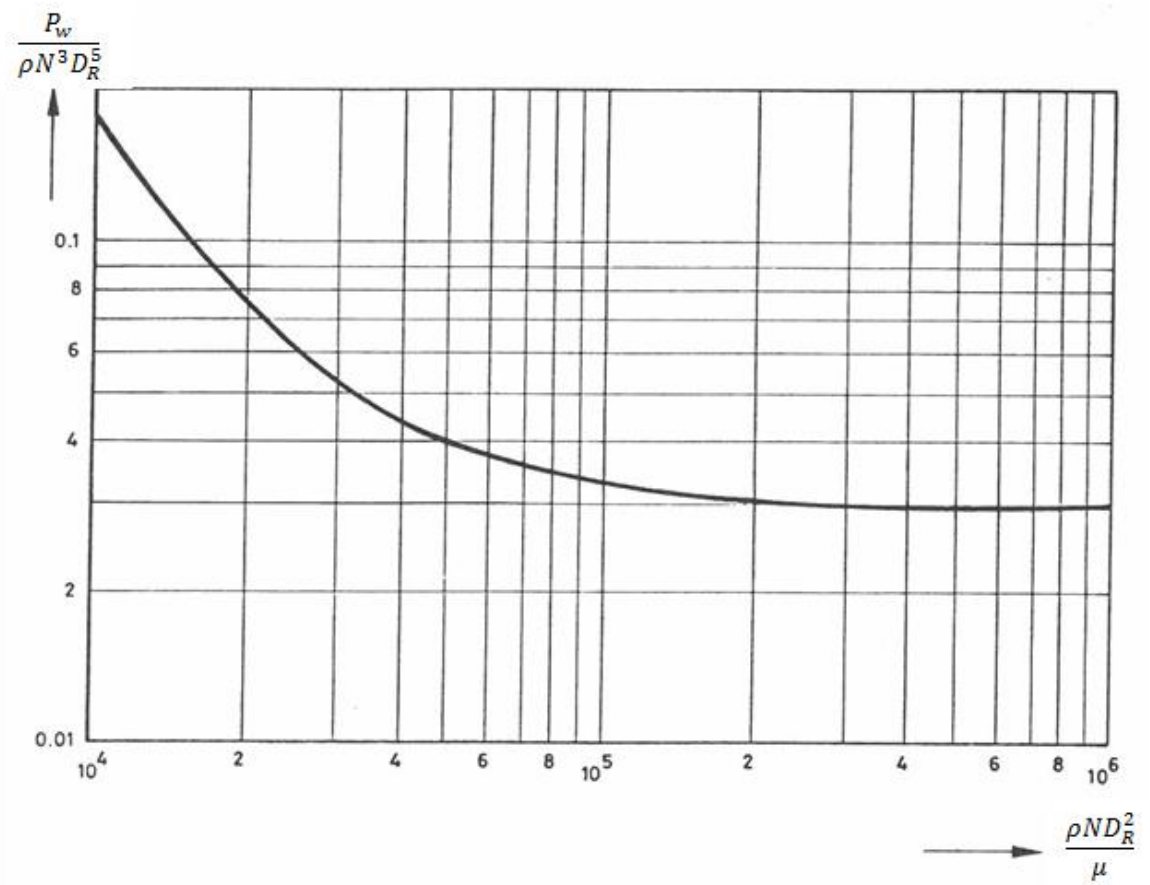

Figure 1-7 Power Input per Rotor Disk[55]

Typically RDC extraction columns are operated at ranges above 2×10^5 for the bracketed fraction on the right hand side of the equation because in this region, the left hand side of the equation becomes constant. The power input per unit mass is proportional to the specific power input shown in Equation 1-20 which is typically used to correlate RDC extraction column performance.

Equation 1-20

$$specific\ power\ input\ group \equiv \frac{N^3 D_R^5}{H{D_C}^2}$$

Rotor Speed Curves

Developing rotor speed curves for an RDC extraction column is dependent upon the dispersed phase holdup in the column. The amount of dispersed phase holdup is a function of the superficial velocities of the continuous and dispersed phases within the column. Dispersed phase holdup is a phenomena where the velocity of the continuous phase impedes the counter-current flow of the dispersed phase and thereby increases the residence time and overall volume fraction of the dispersed phase in the column. Phase inversion can occur when the volume of the dispersed phase exceeds the volume of the continuous phase thereby reversing the roles where the continuous phase becomes a pseudo-dispersed phase and vice versa. This typically occurs at what is known as the flooding point. Rotor speed curves are generated by determining the rotor speed at a given feed and solvent flowrate that affords a percentage of the holdup at flooding of the dispersed phase. Typically the ideal operating range of rotor speeds fall within 75% to 85% of the dispersed phase holdup at flooding.

Theoretical Stages of Extraction for RDC extractors

The height of a theoretical stage for extraction columns is dependent on the type of extraction column. The height of a theoretical stage of an RDC extraction column depends on phase velocities, droplet size, axial mixing and rotor speed. The theoretical stages are also dependent upon fluid characteristics such as interfacial tension and the partition coefficient of the solute. Higher rotor speeds afford more achieved equilibrium stages and therefore running closer to the holdup at flooding curve achieves more actual equilibrium stages and hence more efficient extraction.

RDC Extraction Columns Under Investigation

Process Flow Diagram

The process to be considered in this work includes 3 RDC extraction columns in series as depicted in Figure 1.8 which is a process that is widely found in literature[45, 46].

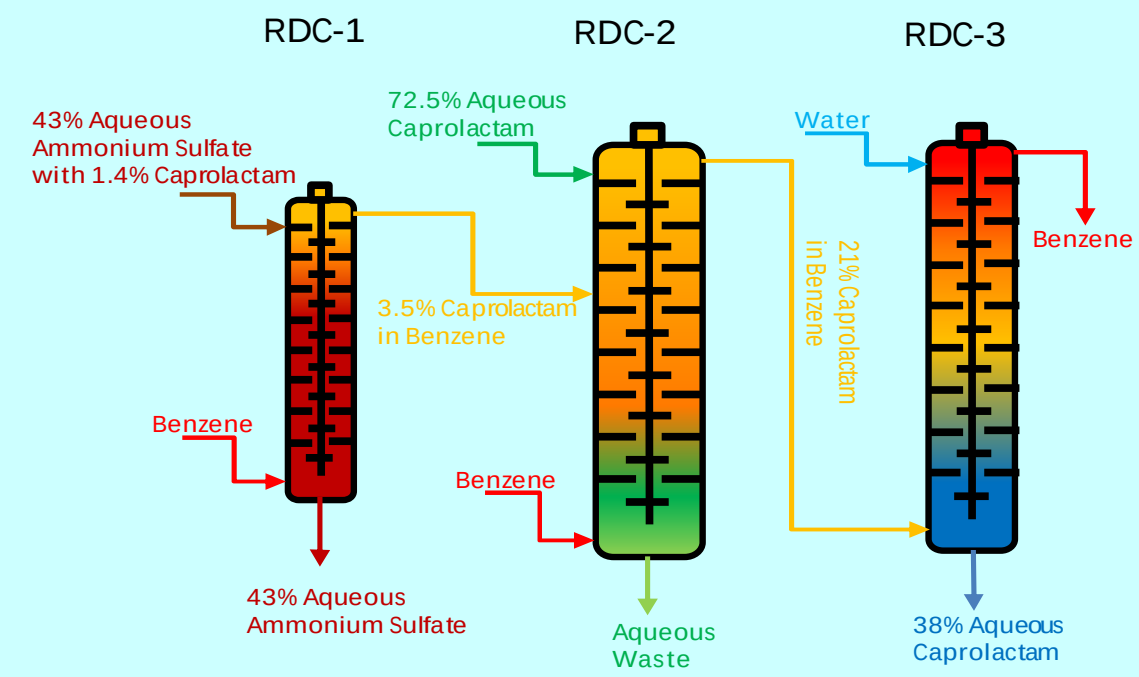

Figure 1-8 RDC Extraction Columns for Caprolactam Purification

RDC-1

The first column in the series serves to extract residual caprolactam from the 43% aqueous ammonium sulfate solution that is separated after the Beckmann Rearrangement of cyclohexane oxime to caprolactam. Benzene and aqueous ammonium sulfate are fed to RDC-1 at a ratio of 0.36 to 1; therefore the benzene is the dispersed phase and the aqueous ammonium sulfate is the continuous phase in this system. Caprolactam is soluble in both benzene and water, but it has a greater affinity for water and therefore is more soluble in water. The driving force of the extraction of caprolactam from the aqueous ammonium sulfate into the benzene occurs

because the water is nearly saturated with ammonium sulfate and the ammonium sulfate is not soluble in benzene. If the concentration of ammonium sulfate in the aqueous phase drops, then more caprolactam will exit the column in the aqueous stream. The separation interface for this column is located at the top section of the column. The resulting 3.7% caprolactam in benzene overflows from RDC-1 into the top third of RDC-2.

RDC-2

The second column in the series functions to extract caprolactam from the crude Beckmann Rearrangement 72.5% caprolactam in water solution into benzene. Most aqueous soluble impurities remain in the waste water stream exiting the bottom of the extraction column, however some caprolactam, approximately 0.5%, remains in the stream as well. The feed to RDC-2 consists of 72.5% caprolactam in water at a 1:2.3 ratio to benzene. The column also has 3.7% caprolactam in benzene entering the top third of the column from the overflow of RDC-1. In RDC-2 the benzene is the continuous phase and the aqueous stream is the dispersed phase. The interface is controlled at the bottom section of the column. The driving force to extract the caprolactam is the excessive amount of benzene to water which is roughly 10:1 considering the amount of water in the aqueous caprolactam feed and the incoming caprolactam/benzene solution from the first column. Therefore the benzene is the continuous phase and the aqueous stream is the dispersed phase.

RDC-3

The third column in the series is considered a back-extraction. RDC-3 uses the higher affinity between caprolactam and water to extract the caprolactam back into an aqueous stream from the organic, benzene stream. Water is fed to RDC-3 at a 0.4:1 ratio to the 21% caprolactam in benzene. The benzene exiting this column is in a loop that feeds RDC-1 and RDC-2 so if the

caprolactam concentration in the benzene exiting RDC-3 increases, the extraction efficiency of the first two columns suffers. The amount of caprolactam in the benzene overflow from RDC-3 is typically less than 0.1%. Water feed temperature has an effect on extraction efficiency in RDC-3. As the temperature increases, more caprolactam is carried over in the benzene as higher temperatures tend to reduce the hydrogen bonding capabilities of the caprolactam and water molecules. The benzene serves to remove organic impurities that have less solubility in water from the caprolactam, and the benzene loop has a "kidney loop" stripper to help maintain purity of the benzene. In RDC-3, the benzene is the continuous phase and the aqueous stream is the dispersed phase. The interface in RDC-3 is controlled at the bottom of the column.

Proposed Work

The purpose of this work is to first determine the rotor speed curves for each of the RDC extraction columns for 100%, 85% and 75% of dispersed phase holdup at flooding. Then to calculate the number of theoretical stages achieved in each of the RDC extraction columns. The resulting rotor speeds will then be compared to the correlations discussed above concerning the upper and lower critical rotor speeds for comparison to droplet breakage probability.

The number of theoretical stages achieved at each rotor speed up to the rotor speed at 85% of dispersed phase holdup at flooding will be calculated. This will provide a better understanding of the effect on extraction of slower rotor speeds.

This work will include a literature and research review on the numerous solvent alternatives to benzene in caprolactam purification as well as potential drawbacks for each alternative solvent.

Chapter 2 - Rotor Speed

Effect of Rotor Speed

As the disks on the shaft of an RDC extraction column rotate, toroidal vortices within each stator compartment causes turbulence which in effect breaks up droplets of the dispersed phase. Increased breakage of droplets leads to increased surface area which in turn improves the efficiency of the solute transfer between solvents. RDC performance is highly dependent upon the geometry of the column and the speed at which the disks rotate. The rotor speed is proportional to the energy that is input into the system, however a disproportionate energy input can lead to excessive droplet breakage that in turn causes dispersed phase flooding in the extraction column.

Development of rotor speed curves for RDC extraction columns is based on the characteristic flooding curves. The flooding curves provide a theoretical correlation of desired rotor speeds as a function of the extraction column loading. These desired rotor speeds fall within a range that are based on a percentage of the amount of dispersed phase holdup that occurs at the point of flooding. The maximum throughput of an RDC extraction column is calculated by estimating the mean droplet size and the maximum superficial velocity of the continuous phase subsequently. The resulting curves estimate theoretical rotor speeds that should be evaluated with plant testing to ensure validity. The range from 75% to 85% of the holdup that is achieved at flooding for each rotor speed is the target range for ideal rotor speeds to maximize extraction efficiency while minimizing the potential for column flooding.

Mean Droplet Diameter

Correlations for predicting the average drop size of the dispersed phase in RDC extraction columns were generated by Kumar and Hartland[47]. The mean droplet diameter is

necessary for determining the maximum possible throughput of the RDC extraction column. The rotor Reynolds number based on the rotor diameter can be calculated using Equation 2-1.

Equation 2-1

$$Re_R = \frac{N \cdot D_R^2 \cdot \rho_c}{\mu_c}$$

The resulting Reynolds number is then used in Equation 2-2 to calculate the dimensionless power number of the rotor[47, 48].

Equation 2-2

$$N_P = \frac{109.4}{Re_R} + 0.74\left[\frac{1000 + 1.2 \cdot Re_R^{0.72}}{1000 + 3.2 \cdot Re_R^{0.72}}\right]^{3.3}$$

This power number of the rotor is used to estimate the power dissipation in the compartment via Equation 2-3[49].

Equation 2-3

$$P_w = N_P \cdot N^3 \cdot D_R^5 \cdot \rho_c$$

The mechanical power dissipation per unit mass is calculated by the following equation using the power dissipation in the compartment. The mechanical power dissipation per unit mass is the correlation shown in Equation 2-4 that incorporates the impact of the rotor speed on the mean droplet diameter of the dispersed phase in the extraction column[48, 49].

Equation 2-4

$$\varepsilon = \frac{4 \cdot P_w}{\pi \cdot D_C^2 \cdot H \cdot \rho_c}$$

The mean droplet diameter is then calculated by Equation 2-5 where $C_\Psi = 1.0$ if the mass is transferred from the continuous phase to the dispersed phase and $C_\Psi = 1.29$ if the mass is transferred from the dispersed phase to the continuous phase[47].

Equation 2-5

$$d_{32} = H\left[\frac{C_\psi \cdot \left(\left(\frac{D_S}{D_C}\right)^2\right)^{0.64}}{\frac{1}{2.54 \cdot \left(\frac{\gamma}{\Delta\rho \cdot g \cdot H^2}\right)^{\frac{1}{2}}} + \frac{1}{0.97 \cdot \left[\left(\frac{\varepsilon}{g}\right) \cdot \left(\frac{\rho_c}{g \cdot \gamma}\right)^{\frac{1}{4}}\right]^{-0.45} \cdot \left[H \cdot \left(\frac{\rho_c \cdot g}{\gamma}\right)^{\frac{1}{2}}\right]^{-1.12}}}\right]$$

Maximum RDC Extraction Column Throughput and Holdup at Flooding

The superficial velocity of the continuous phase at the point of flooding in an RDC extraction column is considered the maximum throughput of the column. Kumar and Hartland devised Equation 2-6 to determine the superficial velocity of the continuous phase at flooding[50, 51].

Equation 2-6

$$V_{c,f} = C_R \cdot \left(-C_1 + \sqrt{C_1^2 + \frac{4 \cdot C_2\left(1-\phi_f\right)}{1 + 4.56 \cdot {\phi_f}^{0.73}}}\right) \cdot \frac{\phi_f \cdot \left(1-\phi_f\right)}{2 \cdot \left(\phi_f + \check{R} \cdot \left(1-\phi_f\right)\right)}$$

A separate iterative loop is required to determine the dispersed phase holdup with Equation 2-7.

Equation 2-7

$$\left[\left(\left(C_3 - C_1\right) \cdot \left(1 - 2\phi_f\right)\right) - \left(\frac{2C_2\phi_f\left(1-\phi_f\right)}{C_3 \cdot \left(1 + 4.56 \cdot {\phi_f}^{0.73}\right)^2}\right) \cdot \left(1 + 4.56 \cdot {\phi_f}^{0.73} + 0.33 \cdot {\phi_f}^{-0.27} \cdot \left(1 + \phi_f\right)\right)\right] \cdot \left(\phi_f + \check{R} \cdot \left(1-\phi_f\right)\right) + \left(C_3 - C_1\right) \cdot \phi_f \cdot \left(1-\phi_f\right) \cdot \left(\check{R} - 1\right) = 0$$

The three constants in Equation 2-7 are defined by Equations 2-8, 2-9 and 2-10..

Equation 2-8

$$C_1 = \frac{24 \cdot \mu_c}{0.53 \cdot d_{32} \cdot \rho_c}$$

Equation 2-9

$$C_2 = \frac{4 \cdot d_{32} \cdot g \cdot \Delta\rho}{1.59 \cdot \rho_c}$$

Equation 2-10

$$C_3 = \sqrt{{C_1}^2 + \frac{4 \cdot C_2 \cdot \left(1 - \phi_f\right)}{1 + 4.56 \cdot {\phi_f}^{0.73}}}$$

The volumetric phase ratio and the constriction factor are given by Equations 2-11 and 2-12.

Equation 2-11

$$\check{R} = \frac{Q_d}{Q_c}$$

Equation 2-12

$$C_R = \left(\frac{D_s}{D_c}\right)^2$$

Calculation of the maximum superficial velocity of the continuous phase which is a function of average droplet diameter provides the point at which flooding occurs in the column. The average droplet diameter is a function of rotor speed. Therefore rotor speed curves can be developed for RDC extraction columns based on percentage of holdup up to the point of flooding.

RDC Extraction Column Dispersed Phase Holdup

Kumar and Hartland further developed a correlation to approximate the fraction of dispersed phase holdup in the column that is a single, unified equation for any type of extraction column and is shown as Equation 2-13[48].

Equation 2-13

$$h = \left[0.27 + \left\{\frac{\epsilon}{g}\left(\frac{\rho_c}{g\,\gamma}\right)^{\frac{1}{4}}\right\}^{0.78}\right]\left[V_d\left(\frac{\rho_c}{g\,\gamma}\right)^{\frac{1}{4}}\right]^{0.87} exp\left[3.34V_c\left(\frac{\rho_c}{g\,\gamma}\right)^{\frac{1}{4}}\right]\left(\frac{\Delta\rho}{\rho_c}\right)^{-0.58}\left(\frac{\mu_d}{\mu_w}\right)^{0.18}$$

$$\times\left(\frac{D_R}{H}\right)^{0.62}\left(\left(\frac{D_S}{D_C}\right)^2\right)^{-0.26}\left[H\left(\frac{\rho_c g}{\gamma}\right)^{\frac{1}{2}}\right]^{-0.39}$$

For each set of flows to an extraction column, an iterative set of steps can be completed to determine the rotor speed that will achieve a determined amount of fractional holdup. First, the holdup at flooding for a specific rotor speed, feed rate and solvent flow is calculated based on the iterative loop shown earlier for calculating the superficial velocity of the continuous phase at the flooding point of the dispersed phase. The unified correlation developed by Kumar and Hartland is then used to calculate the holdup based on rotor speed. The rotor speed is adjusted until said holdup calculation approaches the targeted percentage of dispersed phase holdup at flooding.

The superficial velocities of the continuous and dispersed phases are calculated based on the resulting holdup which is adjusted for each iteration until the associated holdup at flooding, percent of holdup targeted, and the rotor speed all relate. This process is repeated for each set of flow rates and for 75%, 85% and 100% of the holdup at flooding, and a set of curves are generated which present the most efficient range of rotor speeds at which the column will be most efficient between 75% and 85% of the holdup at flooding. The parameters used for all calculations are shown in Table 2-1.

	RDC-1	RDC-2 TOP	RDC-2 BOTTOM	RDC-3	
ρ_c	1230	895	858	858	kg/m^3
μ_c	0.00253	0.00077	0.00049	0.0007	Pa sec
ρ_d	858	1038	994	1028	kg/m^3
μ_d	0.00049	0.00553	0.00073	0.0022	Pa sec
$\Delta\rho$	372	143	136	162	kg/m^3
g	9.81	9.81	9.81	9.81	m/sec^2
Υ_{top}	0.065	0.0022	0.03	0.0035	N/m
L	15.74	4.09	11.65	15.32	m
H	0.157	0.2003	0.2003	0.167	m
D_{rotor}	0.951	1.346	1.346	1.0004	m
D_{stator}	0.9784	1.4	1.4	1.14	m
D_{column}	1.6	2.012	2.012	1.7	m
A_{stator}	0.7518	1.5393	1.5393	1.0207	m^2

Table 2-1 RDC Extraction Column Parameters

Critical Rotor Speeds

Critical rotor speeds are based on the probability of droplet breakage. Kannappan et al. proposed Equation 1-15 to predict the first critical rotor speed for any given liquid system and column geometry[38]. This is an estimate of the rotor speed at which droplet breakage begins to occur.

Equation 1-15

$$N_{cr_1}^2 = \frac{g}{25\, D_R}\left[\left(\frac{\gamma^3 \rho_c}{\mu_c^4 g}\right)^{\frac{1}{4}}\left(\frac{\Delta\rho}{\rho_c}\right)^{\frac{3}{5}}\right]^{0.5}$$

Khadivparsi et al. further modified Equation 1-15 to afford Equation 1-16 to estimate the second critical rotor speed[39]. The second critical rotor speed estimates at which rotor speed the droplet breakage probability is at a maximum.

Equation 1-16

$$N_{cr_2}^2 = \frac{g}{9\,D_R}\left[\left(\frac{\gamma^3\rho_c}{\mu_c^4 g}\right)^{\frac{1}{4}}\left(\frac{\Delta\rho}{\rho_c}\right)^{\frac{3}{5}}\right]^{0.5}$$

Niasar and Bahmanyar have further modified Equations 1-15 and 1-16 for the first and second critical rotor speeds with accountancy for the critical droplet size and the continuous phase height to afford Equation 2-14 and 2-15[52].

Equation 2-14

$$N_{cr_1} = 0.56 \times \frac{\gamma^{0.7}}{2\pi\rho_c^{0.3}\mu_c^{0.4}d_{cr}^{0.59}D_R^{0.71}} \times {h_c}^{-0.15}$$

Equation 2-15

$$N_{cr_2} = 1.05 \times \frac{\gamma^{0.7}}{2\pi\rho_c^{0.3}\mu_c^{0.4}d_{cr}^{0.59}D_R^{0.71}} \times {h_c}^{-0.15} + 4.23$$

Calculations of the critical rotor speeds for each of the extraction columns are completed for comparison to the rotor speed curves generated based on dispersed phase holdup.

RDC-1

Mean Droplet Diameter, Reynolds Number and Power Dissipation for RDC-1

The agitation Reynolds number is calculated for RDC-1 with the 42.5 weight percent aqueous ammonium sulfate as the continuous phase in benzene. A plot of the Reynolds number versus rotor speed is shown in Figure 2-1 which shows a linear relationship. From the Reynolds number, the power number is calculated and plotted versus rotor speed in Figure 2-2. The power dissipation within a compartment is estimated using the power number. This power dissipation within a compartment versus rotor speed is shown in Figure 2-3. As rotor speed increases, the power number decreases and the power dissipation in compartment increases. Finally the mechanical power dissipation is calculated and plotted versus rotor speed shown in Figure 2-4.

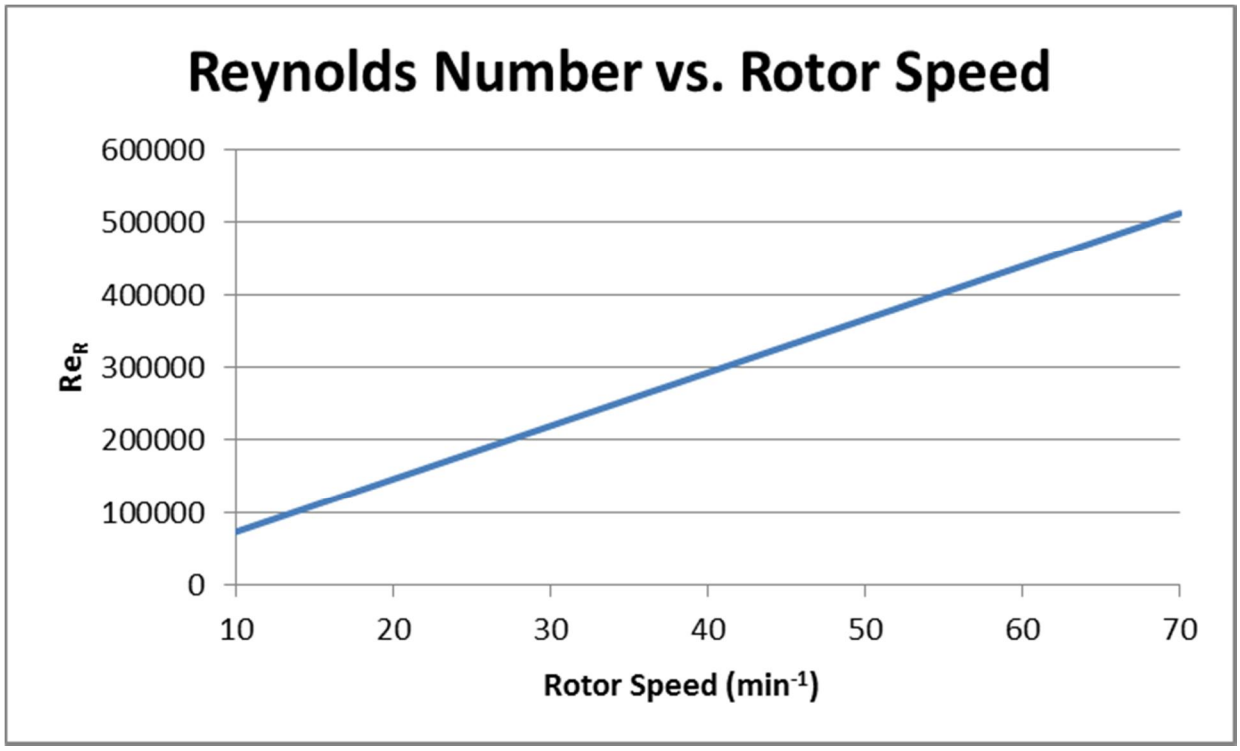

Figure 2-1 RDC-1 Reynolds Number vs. Rotor Speed

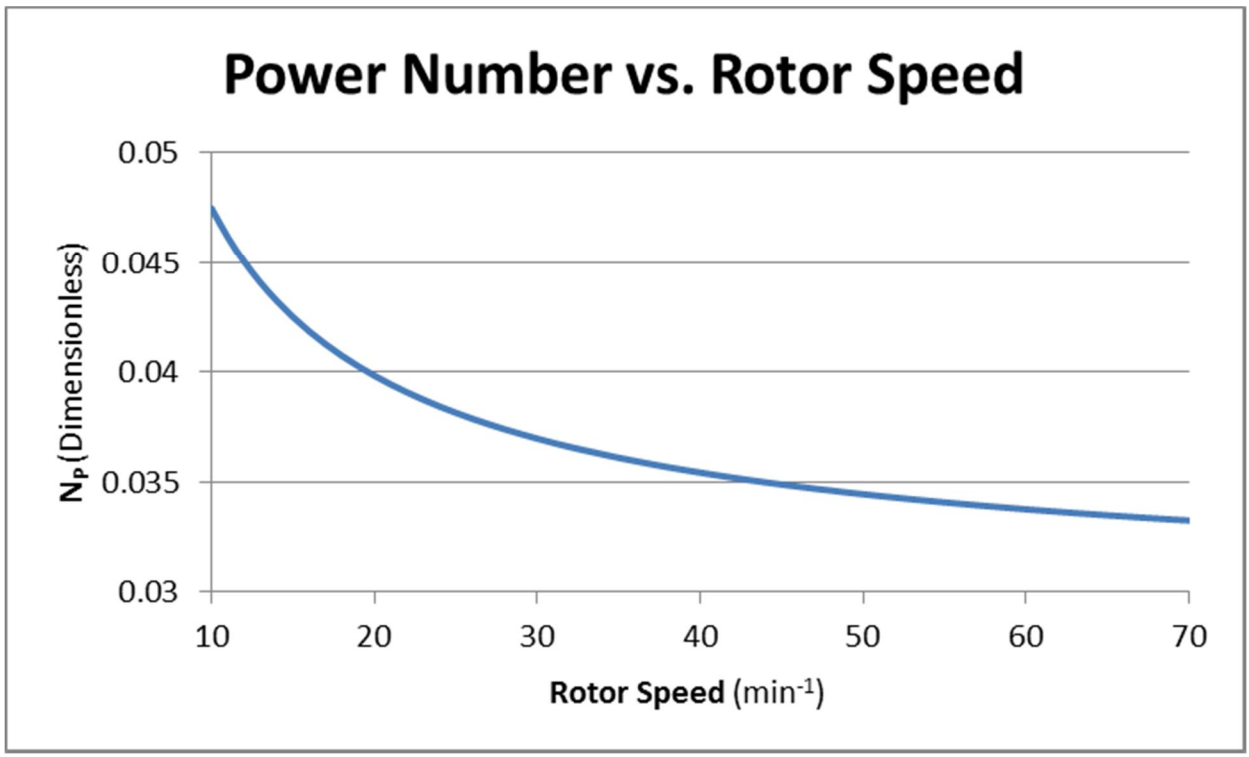

Figure 2-2 RDC-1 Power Number vs. Rotor Speed

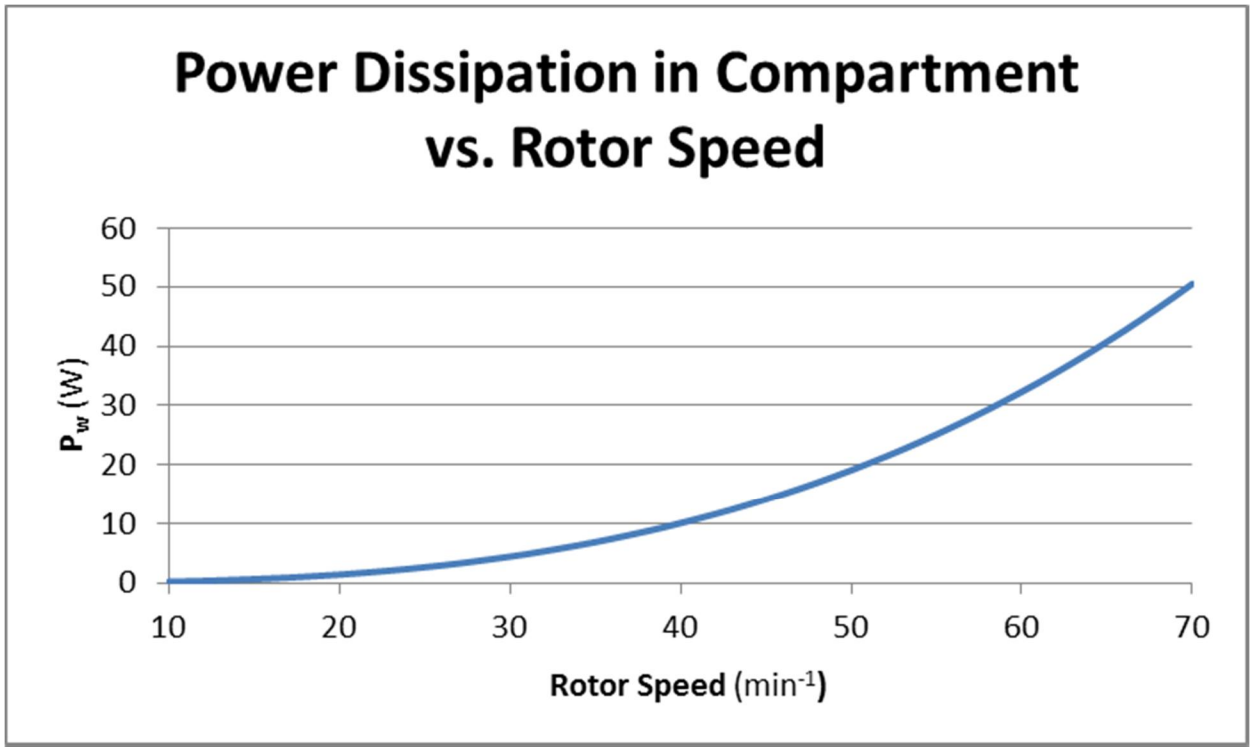

Figure 2-3 RDC-1 Power Dissipation in Compartment vs. Rotor Speed

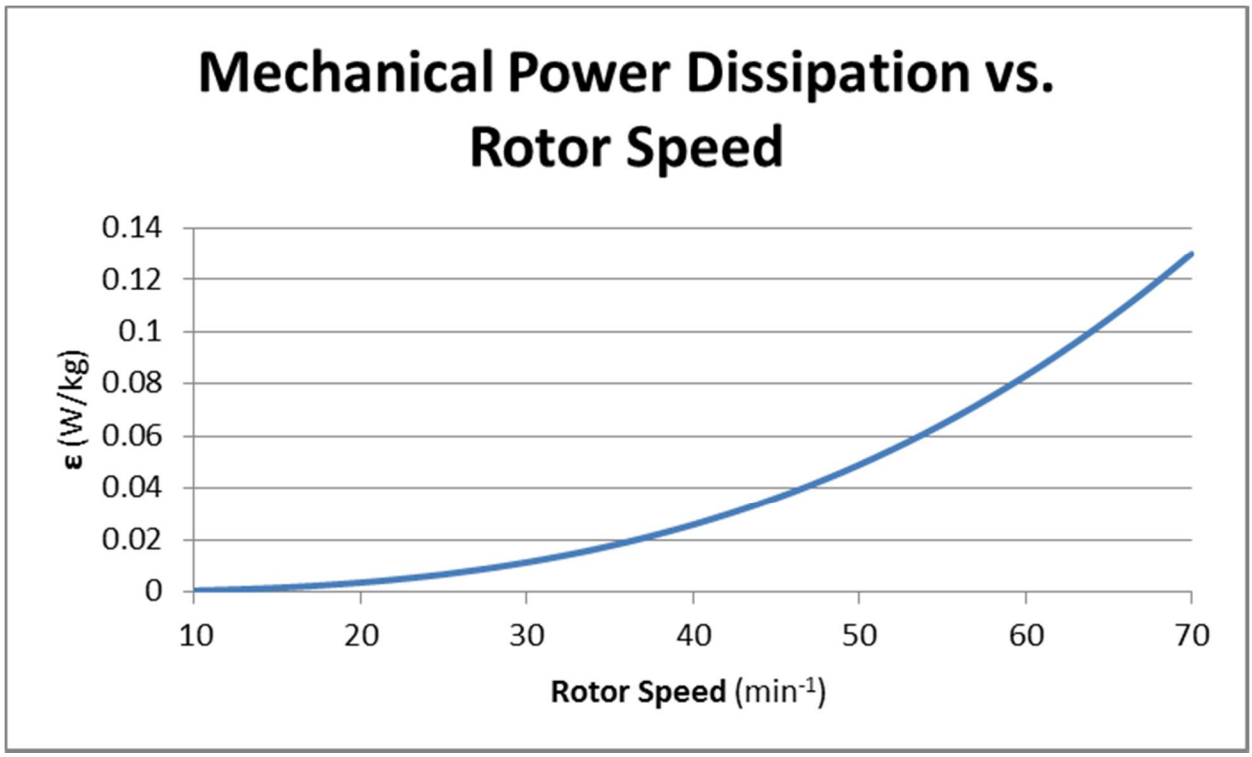

Figure 2-4 RDC-1 Mechanical Power Dissipation vs. Rotor Speed

The mean droplet diameter is calculated for the corresponding rotor speed based on the correlation proposed by Kumar and Hartland. The mass transfer direction constant for this calculation is 1.0 since the mass transfer is occurring from the aqueous ammonium sulfate continuous phase into the dispersed benzene solvent phase. With the increased surface tension of water due to the ammonium sulfate and the low concentration profile of caprolactam throughout the extraction column, a conservative estimate of interfacial tension of 0.9 mN/m is used in the calculation of the mean droplet diameter. This mean droplet diameter is plotted for the range of rotor speeds in Figure 2-5.

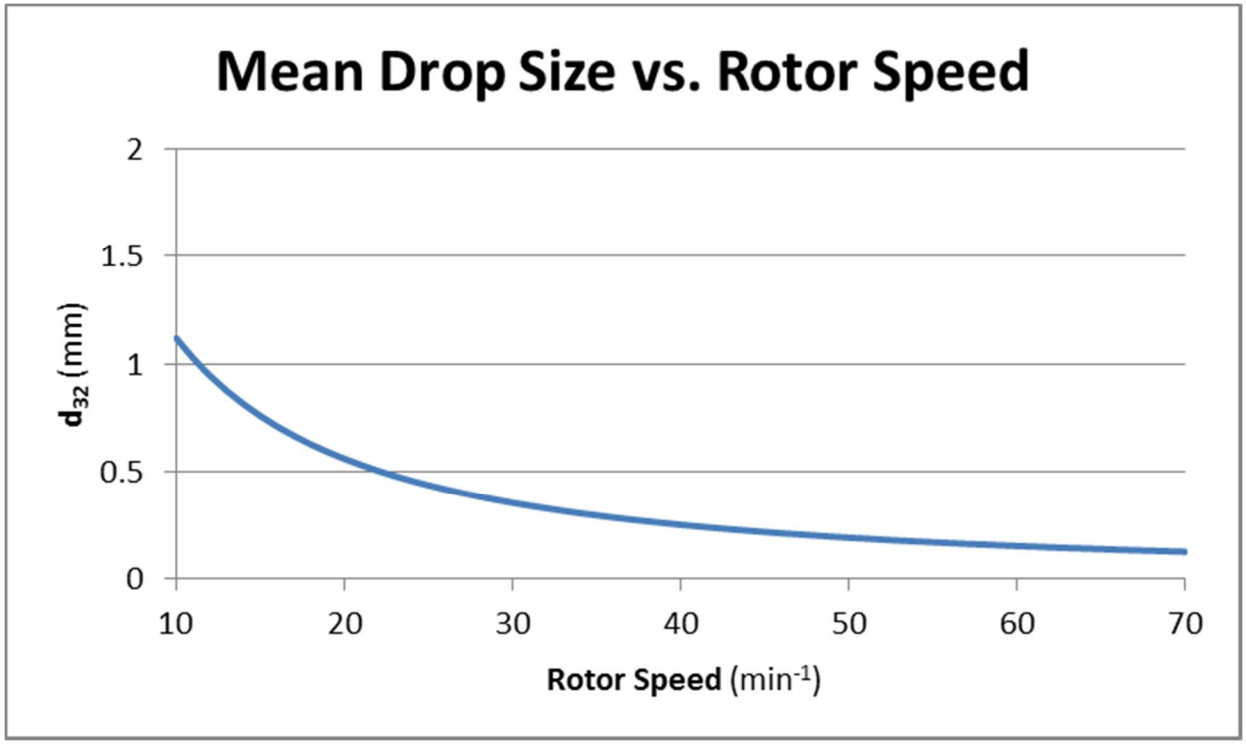

Figure 2-5 RDC-1 Mean Droplet Diameter vs. Rotor Speed

Rotor Speed Curves for RDC-1

The iterative process for calculating the rotor speed was performed to develop rotor speed curves for RDC-1 at various flow rates and for flooding conditions as well as for 75% and 85% of the holdup at flooding. The resulting curves are shown in Figures 2-6 and 2-7. The proposed

range of operating rotor speeds to target for production fall within the curves for 75% and 85% of dispersed phase holdup.

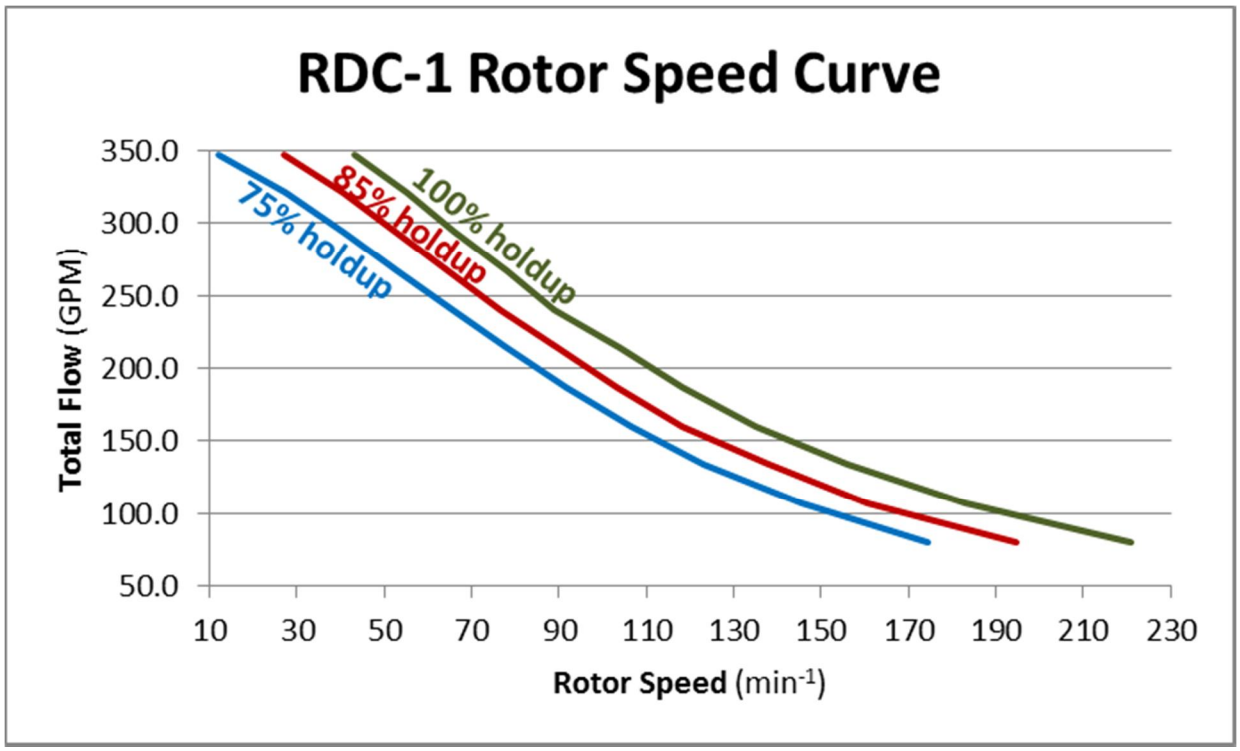

Figure 2-6 RDC-1 Rotor Speed Curve - Total Flow

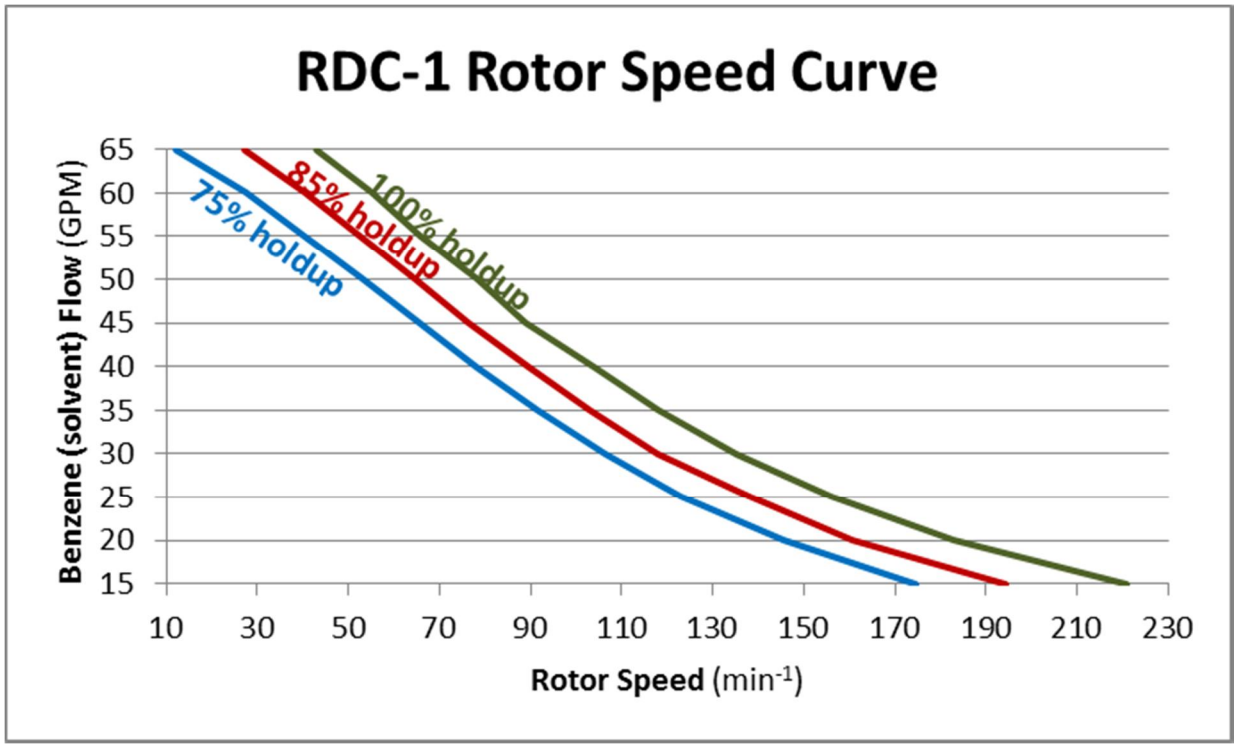

Figure 2-7 RDC-1 Rotor Speed Curve - Solvent Flow

RDC-2

Mean Droplet Diameter, Reynolds Number and Power Dissipation for RDC-2

The top and bottom of RDC-2 was treated as two separate RDC extraction columns. The Reynolds number is calculated for the top 4.1 meters and the bottom 11.7 meters of RDC-2 separately since a majority of the extraction occurs in the top portion of the column and because the additional flow from the overflow of RDC-1 to RDC-2 only impacts the top portion of the column. The interfacial tension between the feed and the solvent also differ significantly between the top and bottom portions of RDC-2. A plot of the agitator Reynolds number versus rotor speed for the top section of the column is shown in Figure 2-8 and for the bottom section of the column is shown in Figure 2-9. The power number, power dissipation and mechanical power

dissipation for the top and bottom portions of RDC-2 are plotted together versus rotor speed for comparison in Figures 2-10, 2-11 and 2-12, respectively.

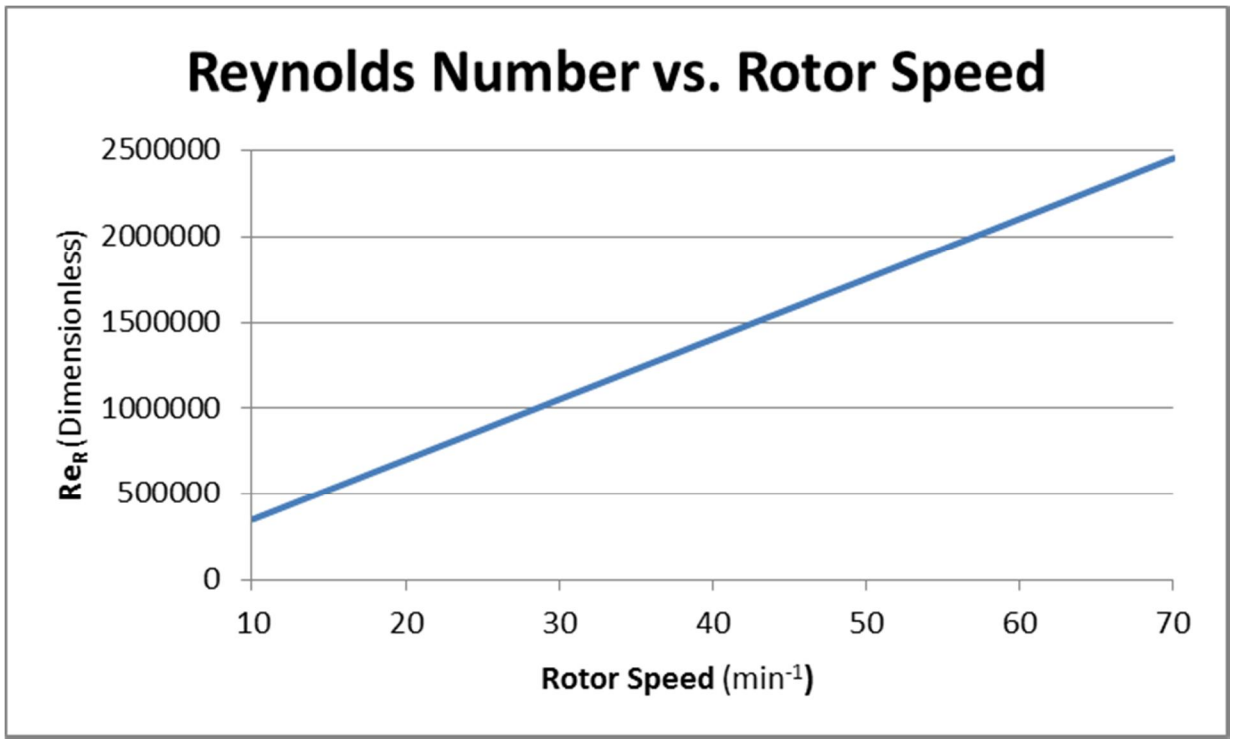

Figure 2-8 Reynolds Number vs. Rotor Speed for the Top Section of RDC-2

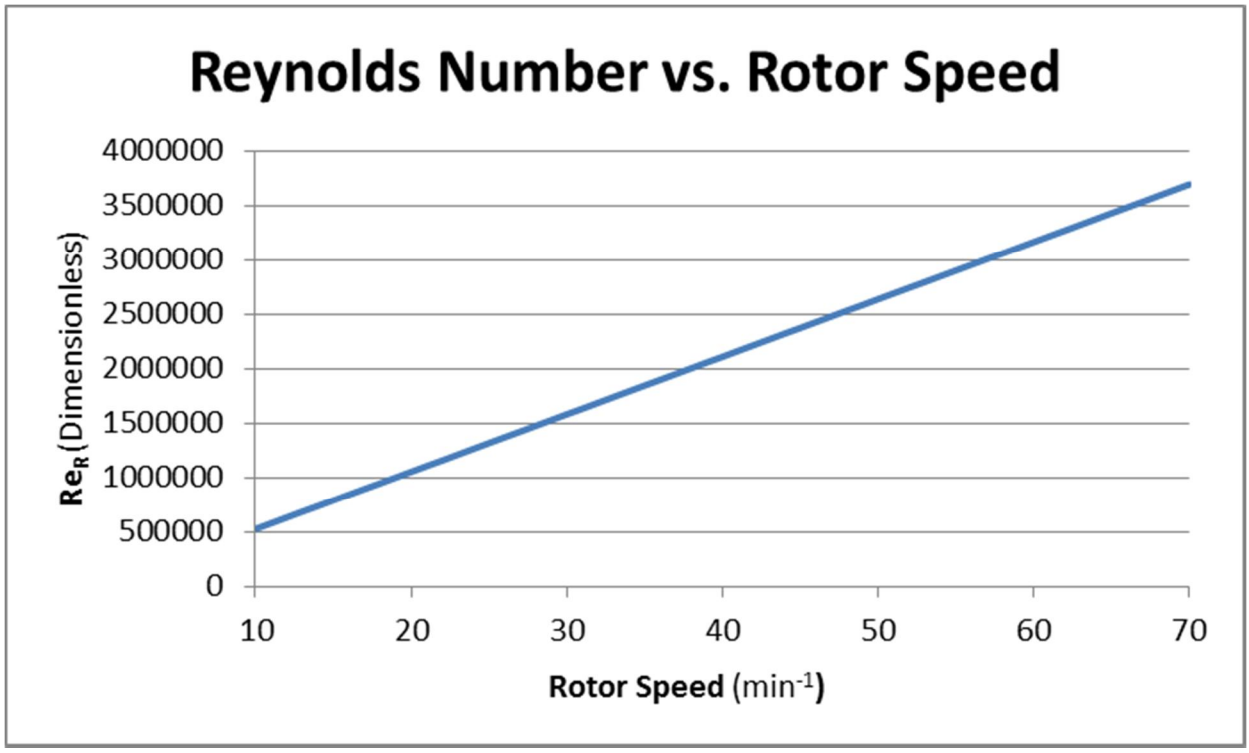

Figure 2-9 Reynolds Number vs. Rotor Speed for the Bottom Section of RDC-2

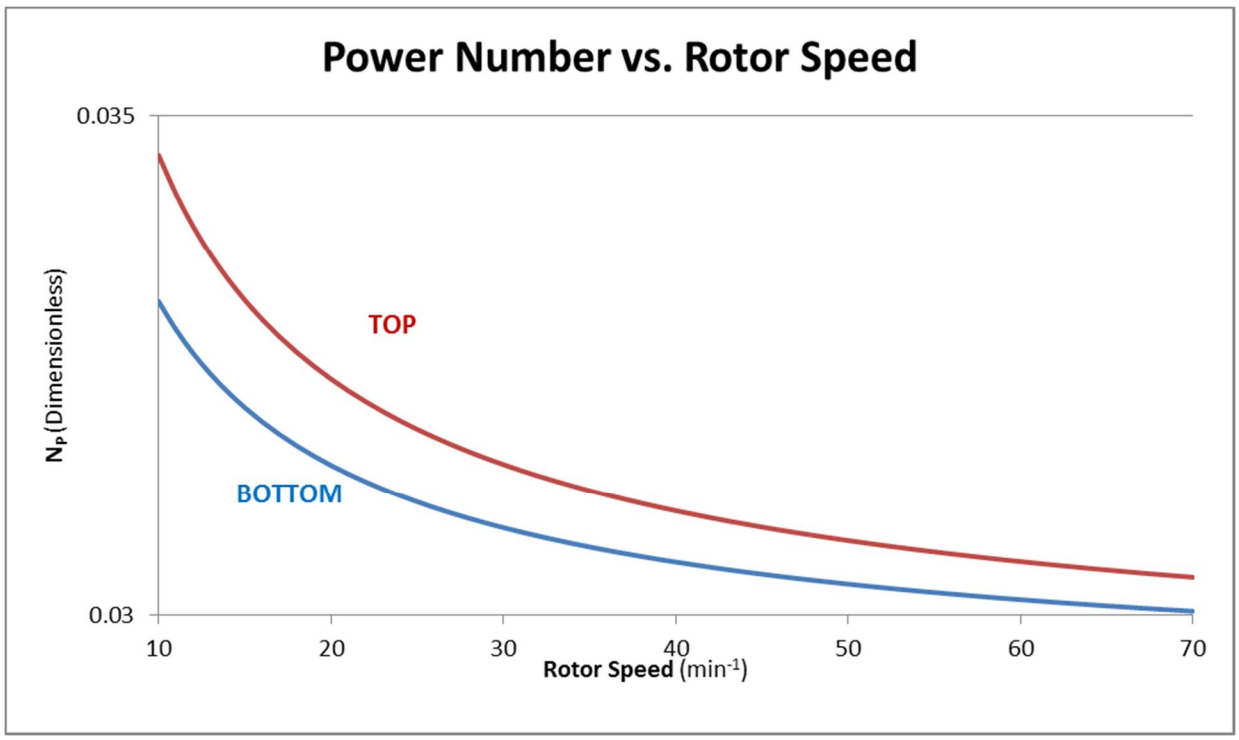

Figure 2-10 RDC-2 Power Number vs. Rotor Speed

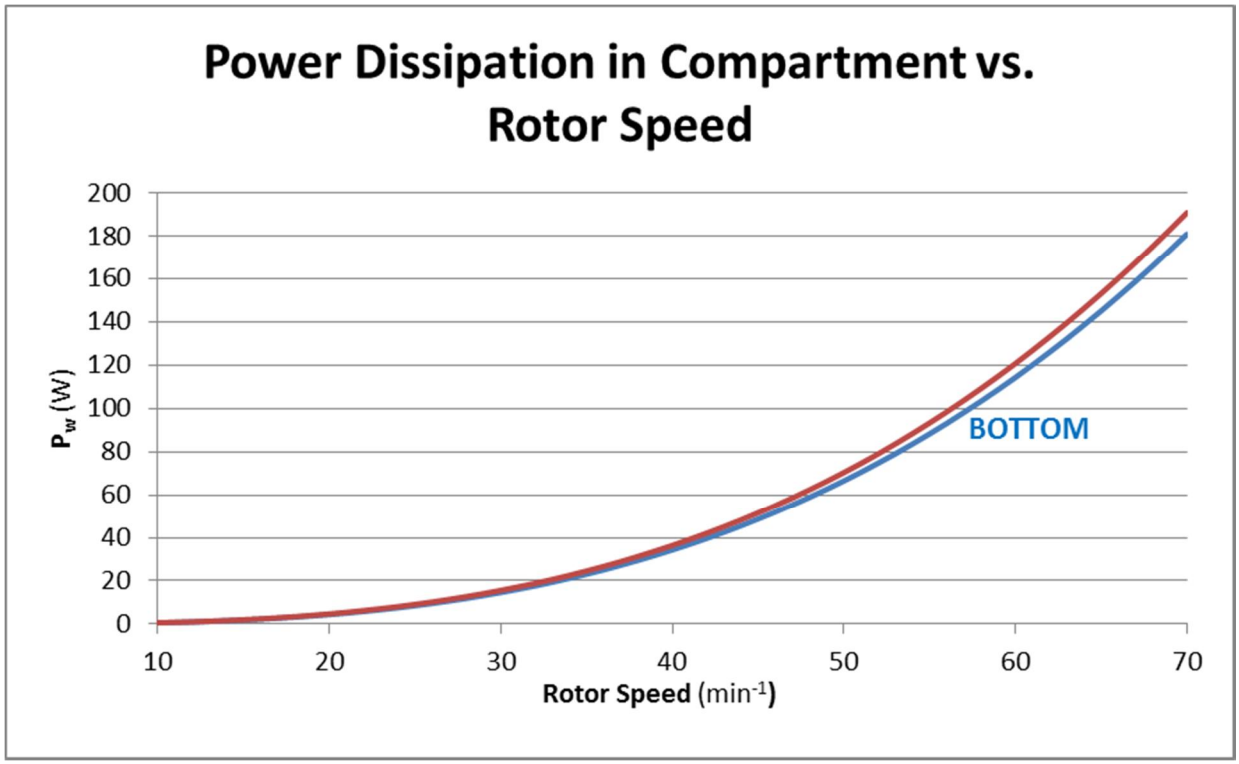

Figure 2-11 RDC-2 Power Dissipation vs. Rotor Speed

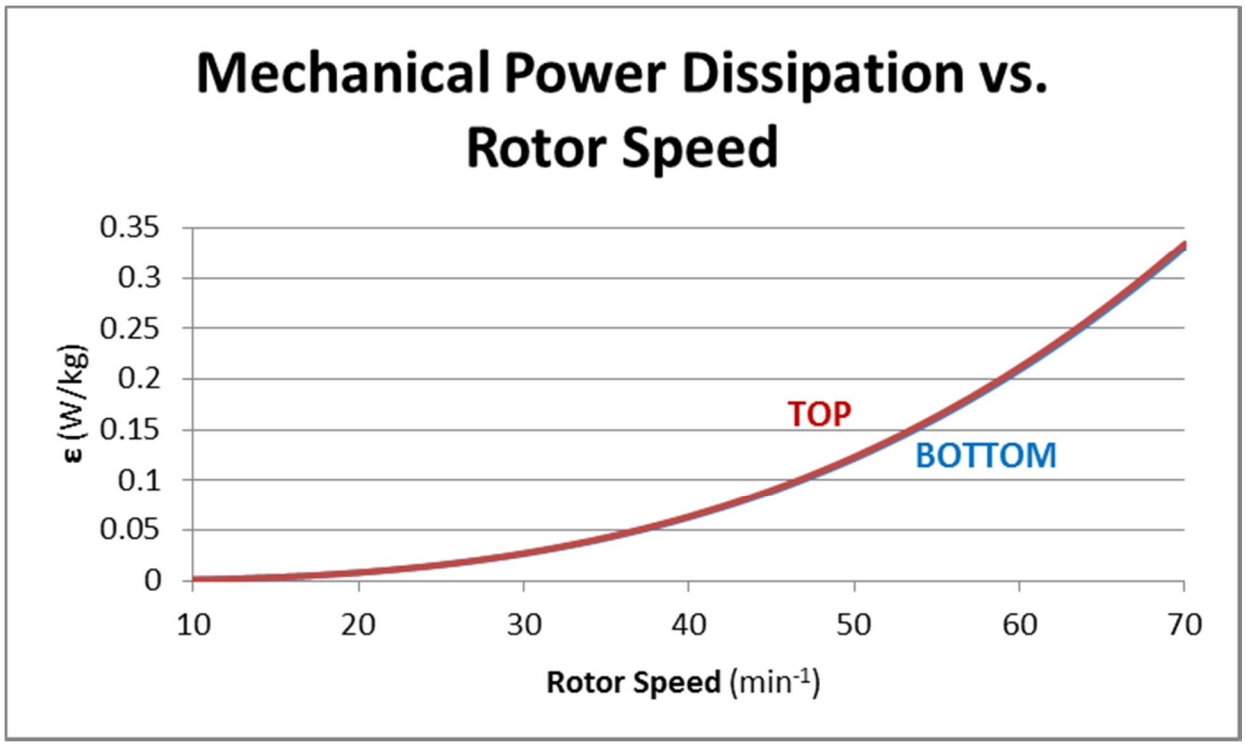

Figure 2-12 RDC-2 Mechanical Power Dissipation vs. Rotor Speed

The mean droplet diameter is calculated for the corresponding rotor speed based on the correlation proposed by Kumar and Hartland[47] for the bottom and top sections of RDC-2. The mass transfer direction constant for this calculation is 1.29 since the mass transfer is occurring from the aqueous caprolactam oil dispersed phase into the continuous benzene solvent phase. This mean droplet diameter for the top and bottom sections of the column are plotted together for the range of rotor speeds in Figure 2-13. Clearly the reduced interfacial tension in the top portion of the RDC extraction column due to higher solute concentrations reduces the average size of the droplets.

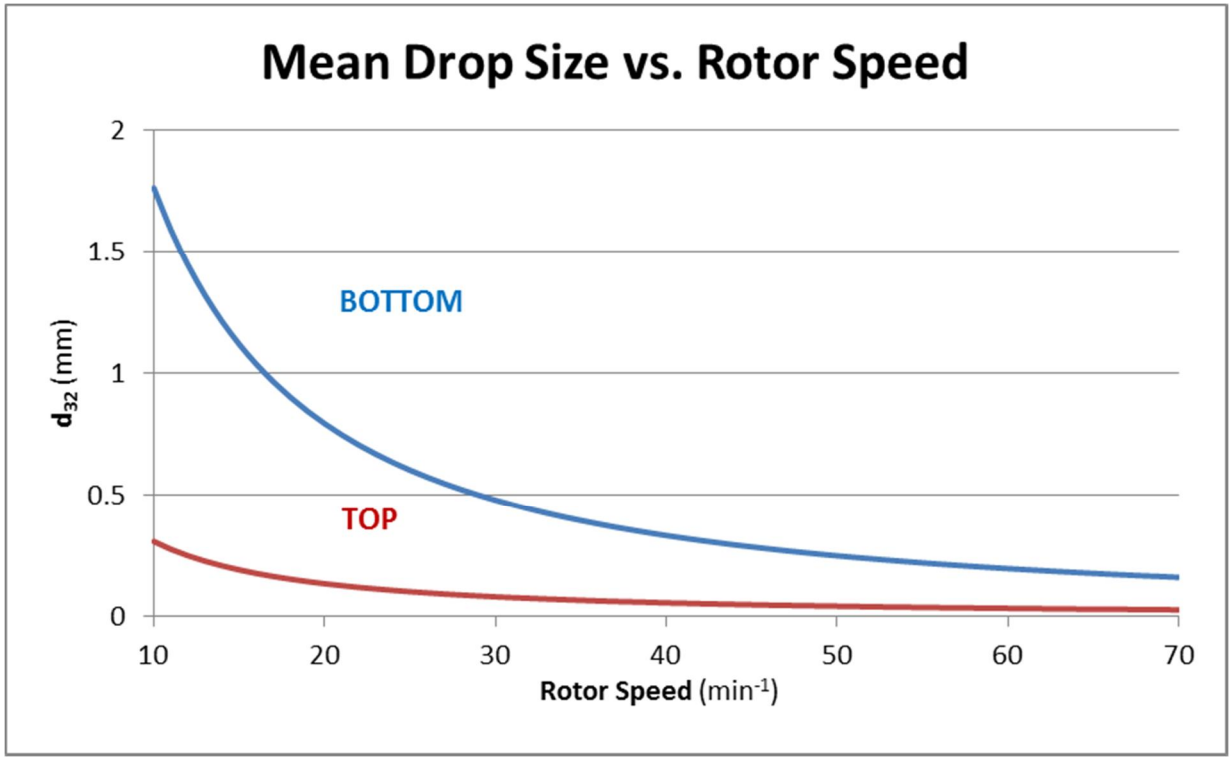

Figure 2-13 RDC-2 Mean Drop Size vs. Rotor Speed

Rotor Speed Curves for RDC-2

The iterative process for calculating the rotor speed was performed to develop rotor speed curves for RDC-2 at various flow rates and for flooding conditions as well as for 75% and 85%

of the holdup at flooding. The resulting curves are shown in Figures 2-14, 2-15, 2-16 and 2-17. Since the top section of RDC-2 has more flow and hence higher continuous phase velocity as well as reduced interfacial tension in comparison to the bottom section of RDC-2, then it is anticipated that the rotor speed curve prediction would be lower for the top section. This is clearly shown in the plotted curves and the range for ideal operating rotor speeds that should be targeted is that of the top section of RDC-2. The plots in Figures 2-14 and 2-16 show the rotor speed curves versus total flowrate, whereas the plots in Figures 2-15 and 2-17 show the rotor speed curves versus the solvent flowrate coming into the column. The proposed range of operating rotor speeds to target for production fall within the curves for 75% and 85% of dispersed phase holdup.

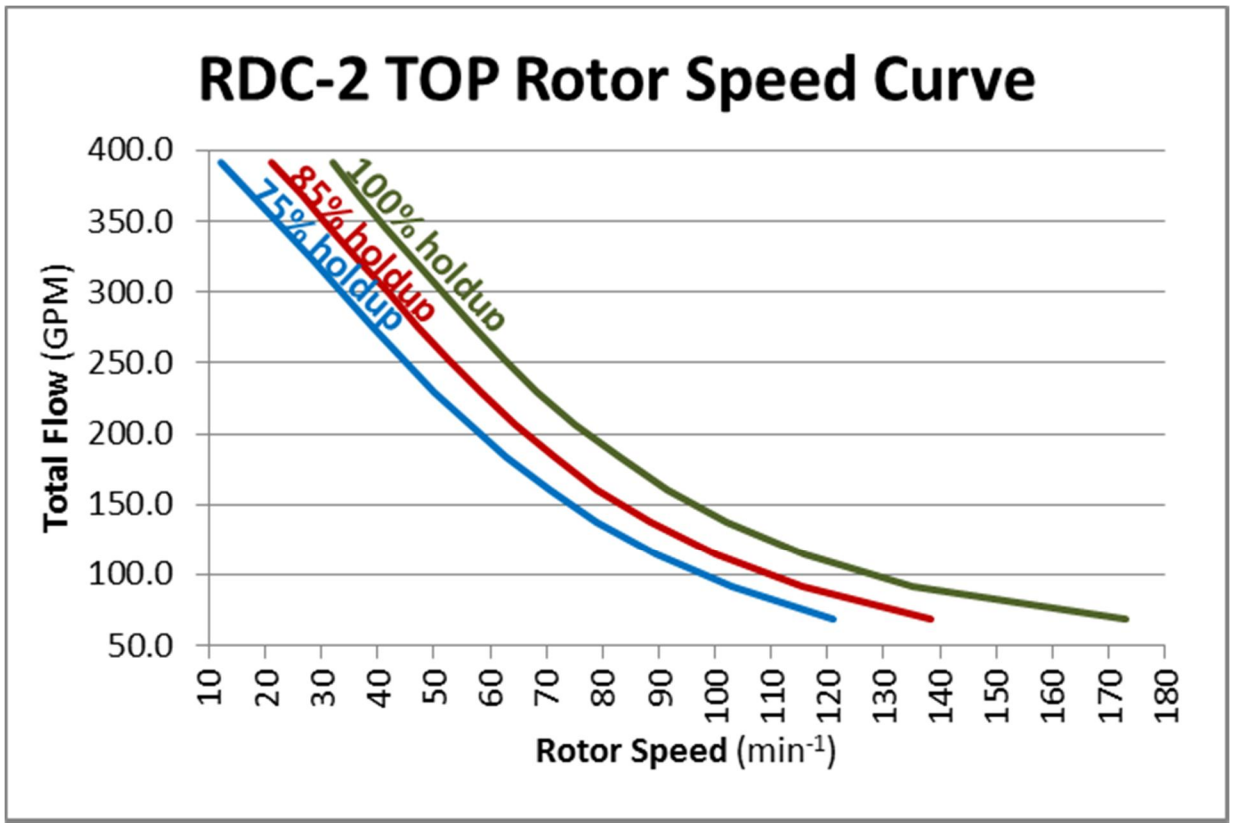

Figure 2-14 Rotor Speed Curve vs. Total Flow for the Top Section of RDC-2

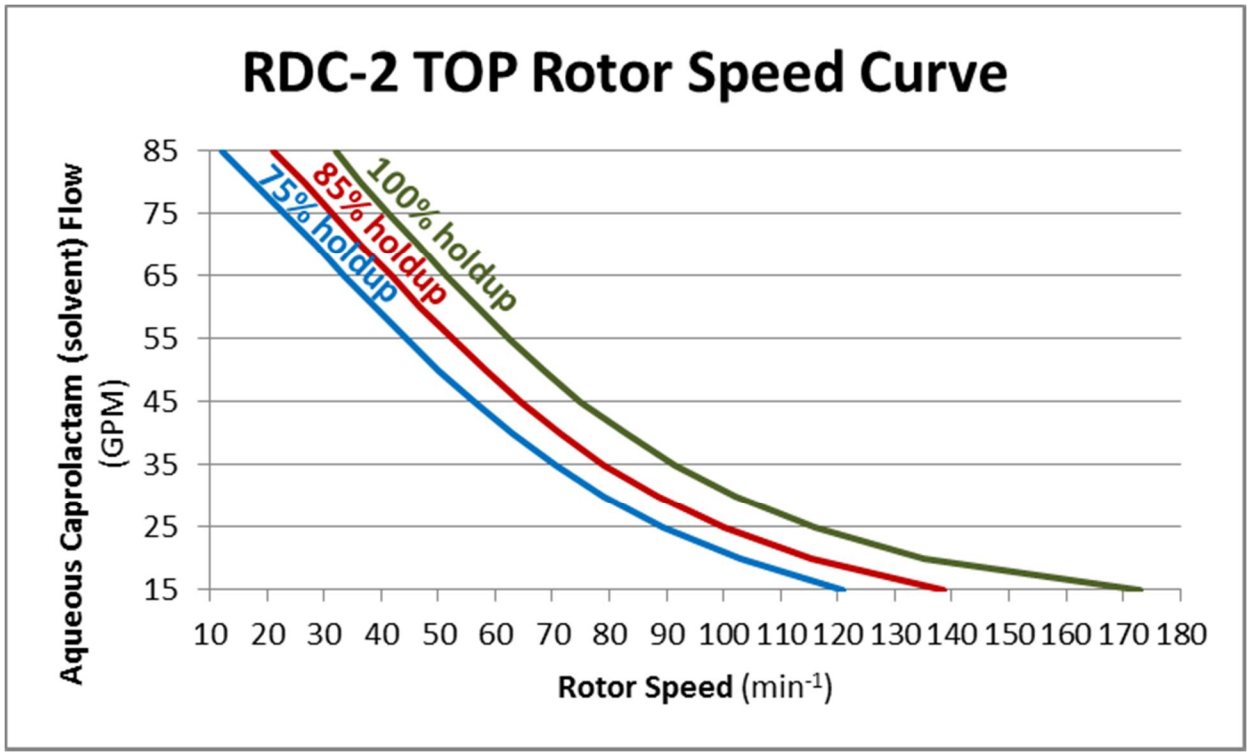

Figure 2-15 Rotor Speed Curve vs. Solvent Flow for the Top Section of RDC-2

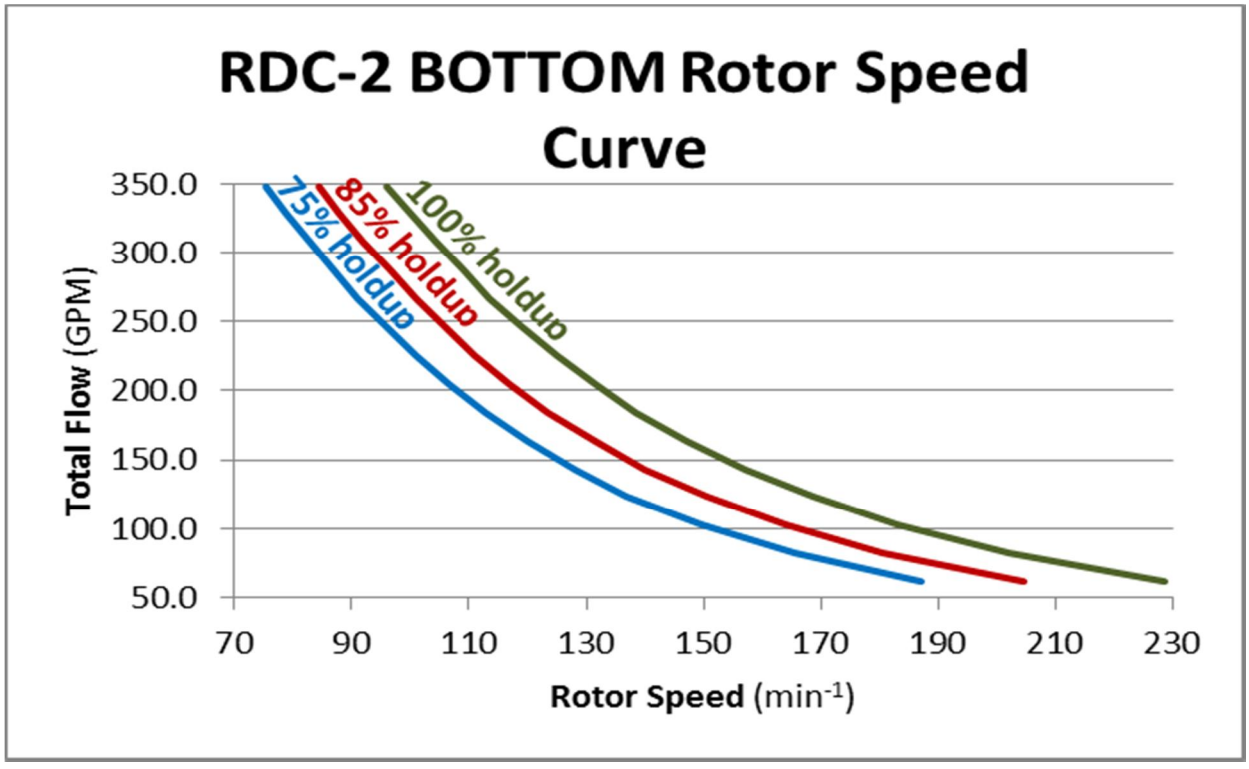

Figure 2-16 Rotor Speed Curve vs. Total Flow for the Bottom Section of RDC-2

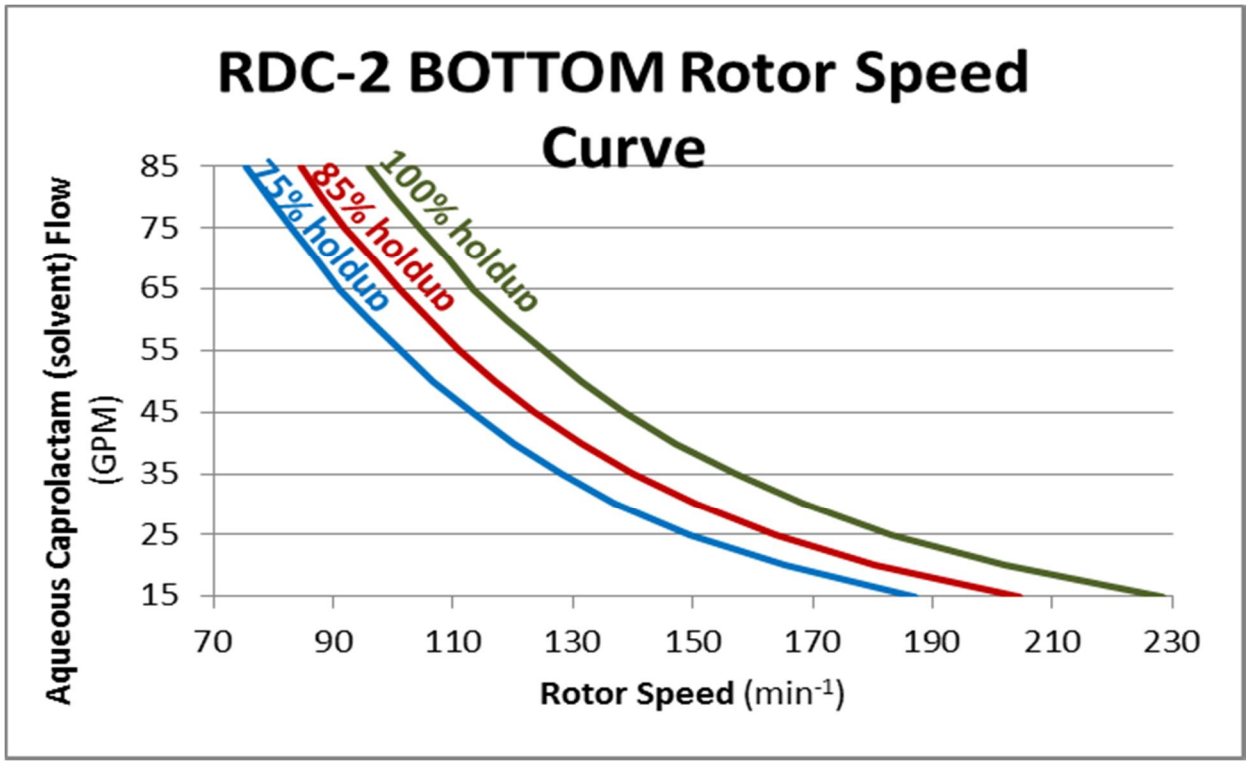

Figure 2-17 Rotor Speed Curve vs. Solvent Flow for the Bottom Section of RDC-2

RDC-3

Mean Droplet Diameter, Reynolds Number and Power Dissipation for RDC-3

The agitation Reynolds number versus rotor speed is calculated for RDC-3 and plotted in Figure 2-18. The power number, power dissipation for compartment and mechanical power dissipation at each rotor speed are plotted in Figures 2-19, 2-20 and 2-21, respectively. The average drop size versus rotor speed is shown in Figure 2-22 and is very similar to the plot of the top section of RDC-2.

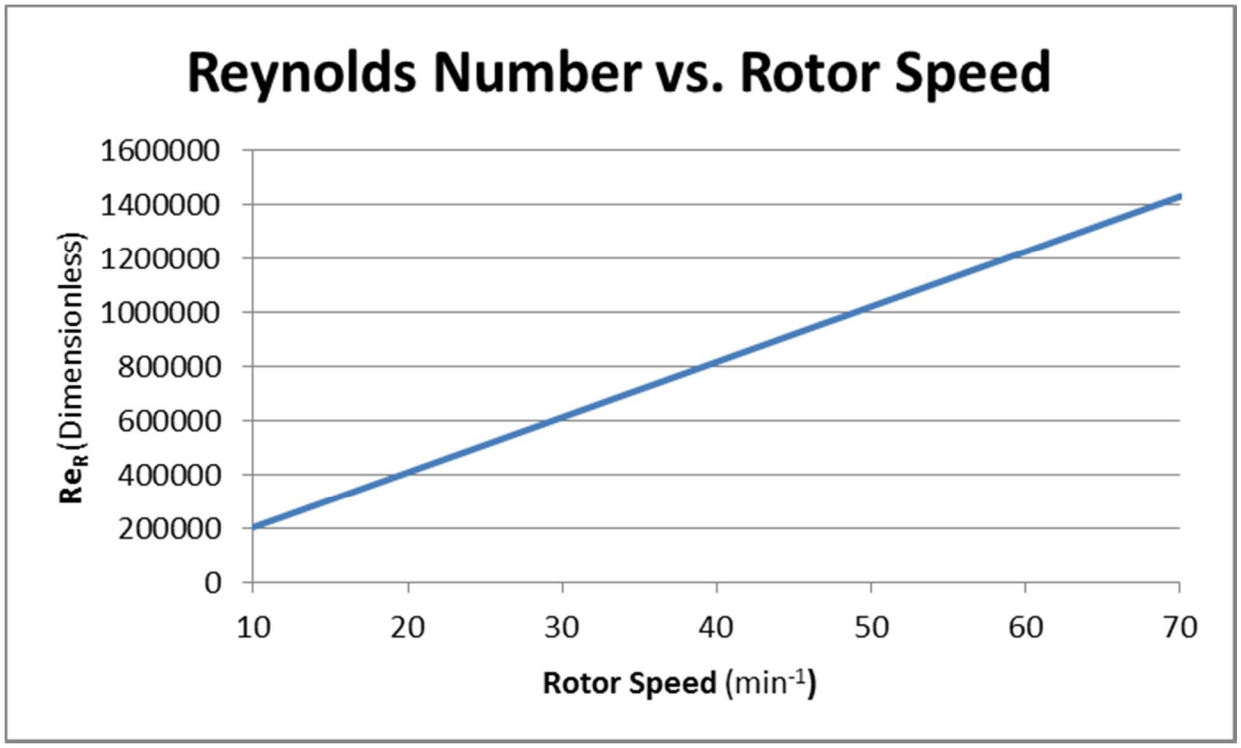

Figure 2-18 RDC-3 Reynolds Number vs. Rotor Speed

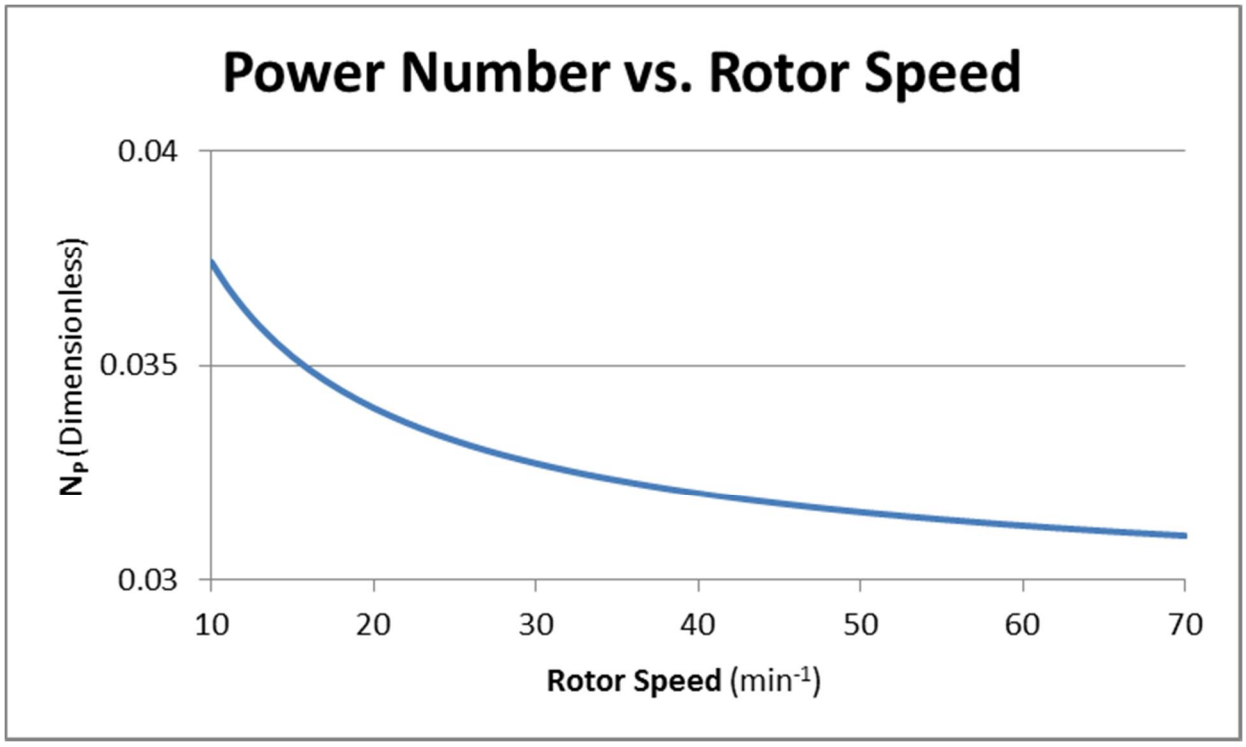

Figure 2-19 RDC-3 Power Number vs. Rotor Speed

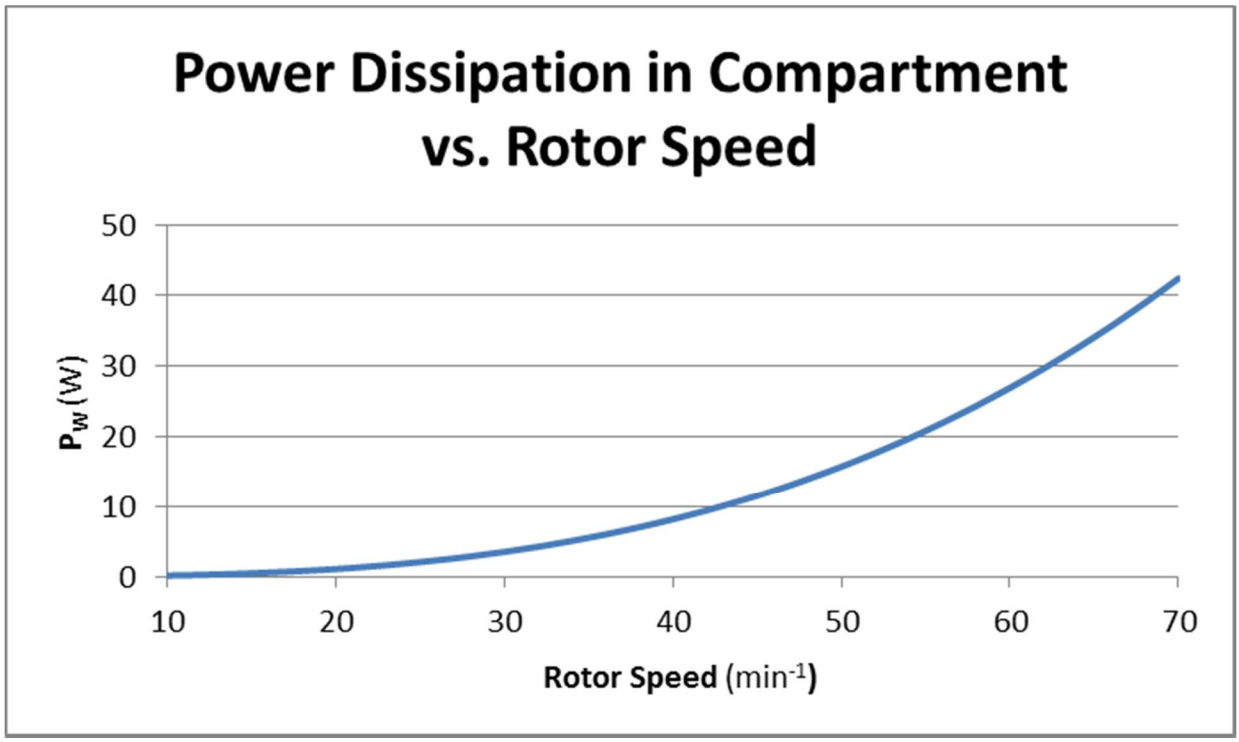

Figure 2-20 RDC-3 Power Dissipation in Compartment vs. Rotor Speed

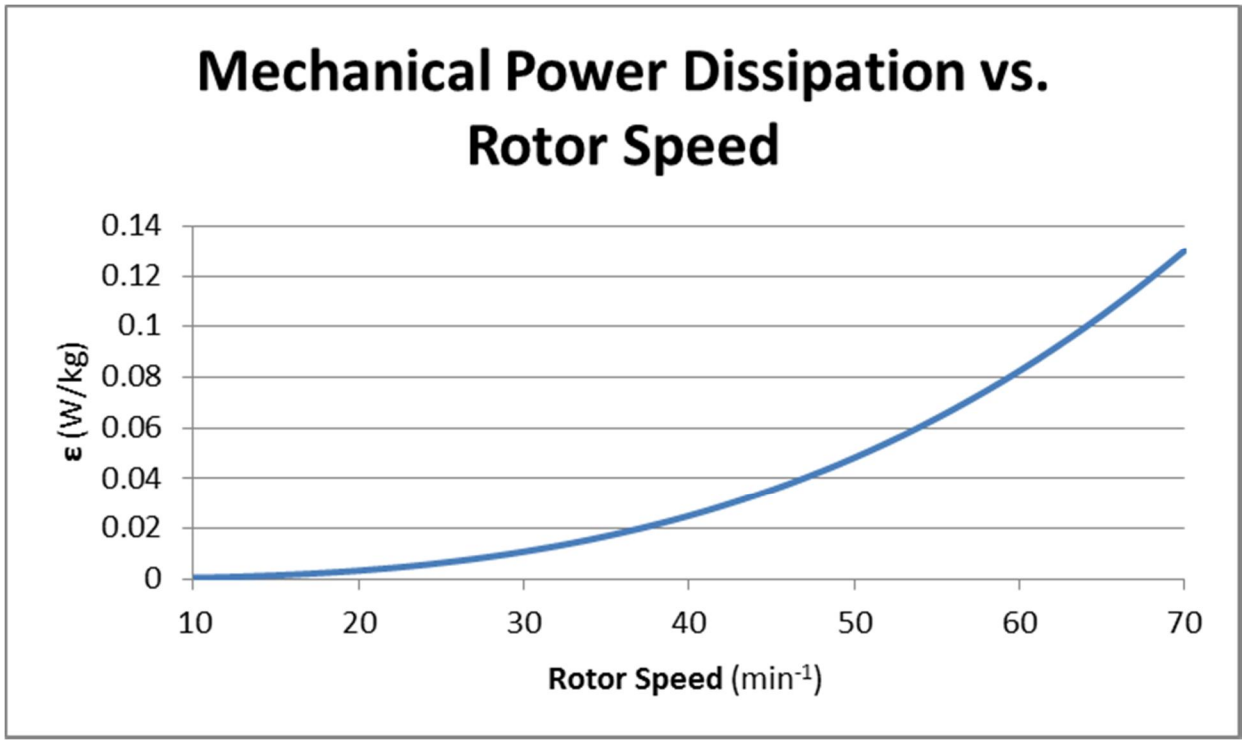

Figure 2-21 RDC-3 Mechanical Power Dissipation vs. Rotor Speed

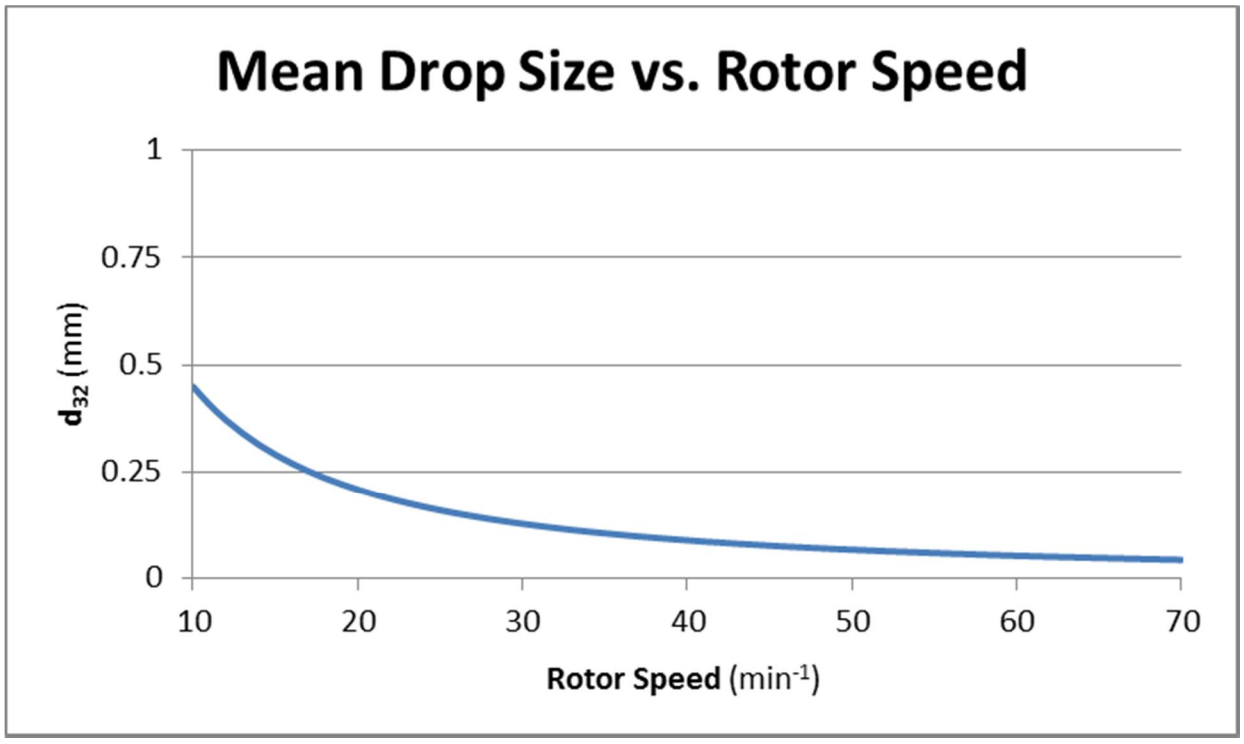

Figure 2-22 RDC-3 Mean Drop Size vs. Rotor Speed

Rotor Speed Curves for RDC-3

The iterative process for calculating the rotor speed was performed to develop rotor speed curves for RDC-3 at various flow rates and for flooding conditions as well as for 75% and 85% of the holdup at flooding as it was for RDC-1 and RDC-2. The resulting curves are shown in Figures 2-23 and 2-24. And as for the first two columns, the proposed range of operating rotor speeds to target for production fall within the curves for 75% and 85% of dispersed phase holdup. Figure 2-23 shows a plot of the rotor speed versus the total flow rate to the column and Figure 2-24 shows a plot of the rotor speed versus the solvent flow coming into the column.

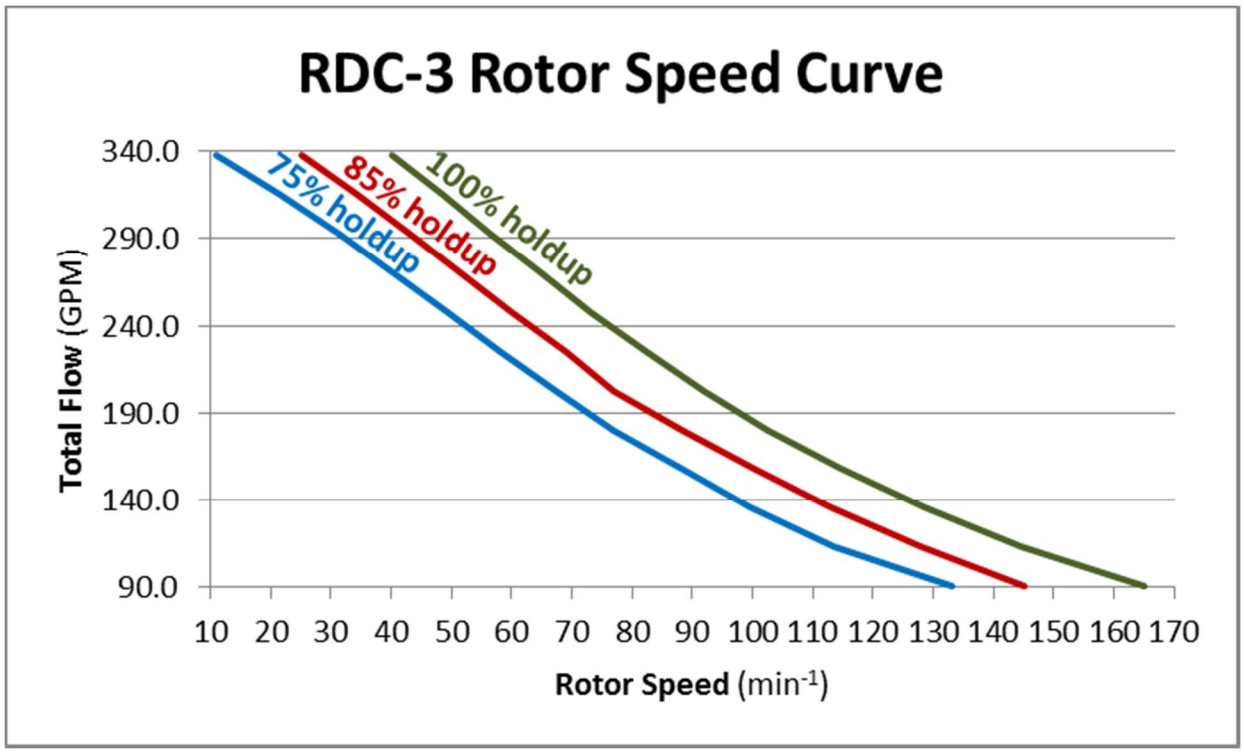

Figure 2-23 RDC-3 Rotor Speed Curve vs. Total Flow

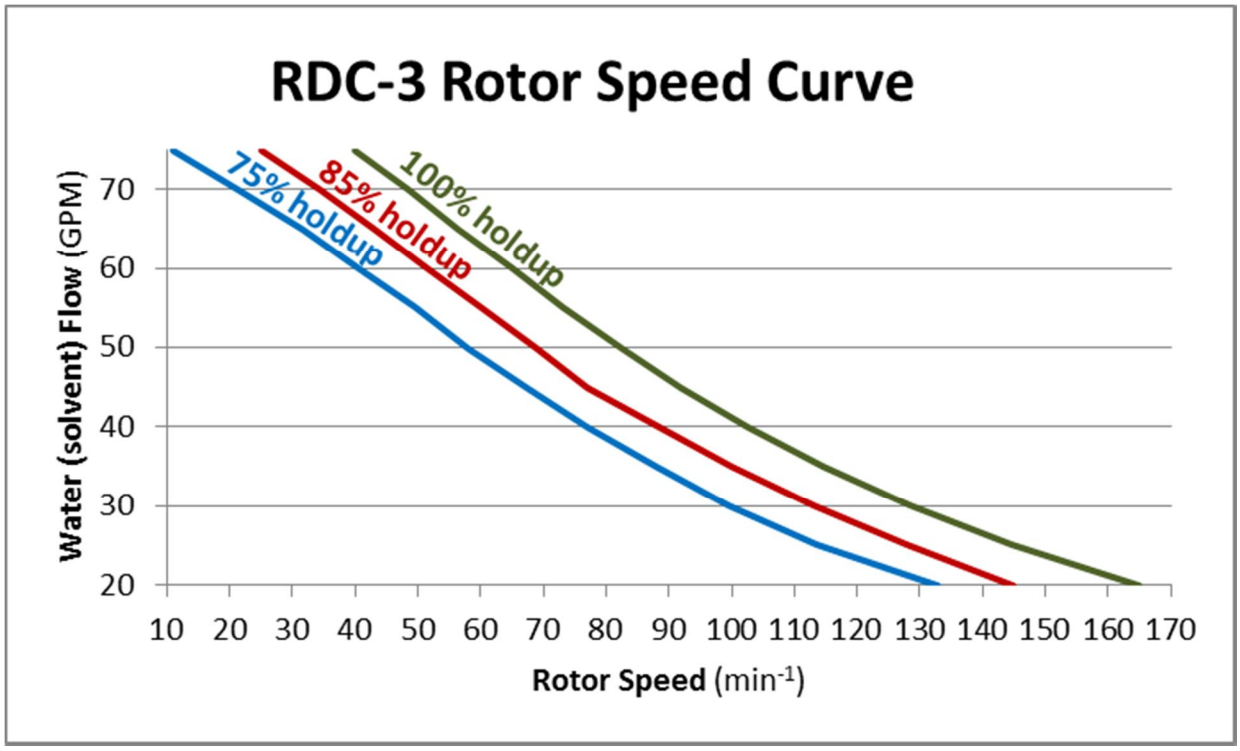

Figure 2-24 RDC-3 Rotor Speed Curve vs. Solvent Flow

Critical Rotor Speeds

First Critical Rotor Speed

The values for the first critical rotor speed based on the correlation proposed by Kannappan et al. are calculated for the three RDC extraction columns including the top and bottom sections of RDC-2[38]. The values for the first critical rotor speed based on the correlation proposed by Niasar and Bahmanyar are also calculated for each of the RDC extraction columns[40]. The results are shown in Table 2-2 with the units of number of revolutions per minute.

	Kannappan N_{Cr1}	**Niasar and Bahmanyar** N_{Cr1*}
RDC-1	80.3	74.4
RDC-2 TOP	62.2	70.0
RDC-2 BOTTOM	115.0	190.0
RDC-3	82.3	92.6

Table 2-2 Values of the First Critical Rotor Speed

Second Critical Rotor Speed

Values for the second critical rotor speed based on the correlation proposed by Khadivparsi et al. are calculated for the three RDC extraction columns including the top and bottom sections of RDC-2[39]. The values for the second critical rotor speed based on the correlation proposed by Niasar and Bahmanyar are also calculated for each of the RDC extraction columns. The results are shown in Table 2-3 with the units of number of revolutions per minute.

	Khadivparsi N_{Cr2}	**Niasar and Bahmanyar** N_{Cr2*}
RDC-1	133.9	393.4
RDC-2 TOP	103.6	385.0
RDC-2 BOTTOM	191.6	610.0
RDC-3	137.1	427.3

Table 2-3 Values of the Second Critical Rotor Speed

Conclusion on Critical Rotor Speeds

The critical rotor speeds calculated by the correlations from literature relate to the probability of droplet breakage. The first critical rotor speed is the speed required to start droplet breakage and the second critical rotor speed is that at which droplet breakage probability is 1. The RDC extraction columns under investigation in this report typically run at a fraction of the calculated values of the first critical rotor speed, which would mean that there is a 0 probability of droplet breakage, however these extractions are carried out efficiently at the lower rotor speed. Therefore, the critical rotor speeds determined by these equations do not seem to be in agreement with the efficiency of the extraction.

The disagreement in these correlations versus the method for developing the rotor speed curves may be in the fact that the critical speed correlations do not account for continuous and

dispersed phase velocities as they were developed with non-flowing continuous phase. The disagreement between the correlations and experimental data with the extraction columns under investigation could also be caused by the variations in physical properties such as interfacial tension that can be caused by impurities that are not accounted for in the correlations.

Chapter 3 - Theoretical Stages of the RDC Extraction Columns

Number of Stages in an Extraction Column

The number of theoretical stages achieved can be calculated for a lot of extractions with the Kremser Equation 3-1[53] incorporating actual data of the solute weight fractions in the feed, raffinate and solvent and the solvent flow ratio. However, this equation alone does not account for axial mixing within an extraction column. This equation also accounts for the partition coefficient K_D of the solute in the two solvents of the system.

Equation 3-1

$$N_S = \frac{\ln\left[\left(\frac{X_F - \frac{Y_S}{K_D}}{X_R - \frac{Y_S}{K_D}}\right)\left(1 - \frac{1}{\left(K_D \frac{Q_S}{Q_F}\right)}\right) + \frac{1}{\left(K_D \frac{Q_S}{Q_F}\right)}\right]}{\ln\left(K_D \frac{Q_S}{Q_F}\right)}$$

In some cases the partition coefficient remains reasonably constant for a given solute in the solvent system, however in many cases it can vary significantly with variances in the weight fraction of solute in either phase. The partition coefficient for a system can be calculated with Equation 3-2 where it is the ratio of weight percent solute in the organic phase to weight percent solute in the aqueous phase.

Equation 3-2

$$K_D = \frac{wt.\%\, Solute_{Organic}}{wt.\%\, Solute_{Aqueous}}$$

If there is a variation in the partition coefficient with the change in the concentration, then an average of the partition coefficient can be used in the Kremser Equation.

Once the number of stages has been determined, the height equivalent to a theoretical stage (HETS) can be calculated by using Equation 3-3 with a basis on proven results from an extraction column and using the height of the agitated portion of the column.

Equation 3-3

$$HETS = \frac{H_C}{N_S}$$

Another way to calculate the number of theoretical stages achieved is to approach the column as a set of mixer-settlers in series where stage equilibrium is reached in each stage. This requires knowledge of the partition coefficient (K_d) based on solute concentrations in both the organic and aqueous phases entering each stage.

Rotating Disk Contactor Extraction Column Stages

Since an RDC extraction column does not really follow the concept of stage-wise mixing and settling but more as a continuously operating extractor, then the solute concentration profile will vary continuously. For RDC extraction columns, there are more variables that have to be considered in determining the number and height of theoretical stages due to axial mixing, dispersed phase holdup and power input by the rotor.

Phase Velocities and Dispersed Phase Holdup

The first set of variables that have to be considered are the phase and slip velocities. The superficial velocities for the dispersed and continuous phases are calculated based on the smallest area in the column internals which is the annular opening of the stator ring as shown in Equations 3-4 and 3-5.

Equation 3-4

$$\bar{V}_d = \frac{Q_d}{\pi\left(\frac{D_S}{2}\right)^2}$$

Equation 3-5

$$\bar{V}_c = \frac{Q_c}{\pi\left(\frac{D_S}{2}\right)^2}$$

The volume fraction of holdup of the dispersed phase in the extraction column is calculated by Equation 3-6[48].

Equation 3-6

$$h = \left[0.27 + \left\{\frac{\epsilon}{g}\left(\frac{\rho_c}{g\,\gamma}\right)^{\frac{1}{4}}\right\}^{0.78}\right]\left[V_d\left(\frac{\rho_c}{g\,\gamma}\right)^{\frac{1}{4}}\right]^{0.87} exp\left[3.34V_c\left(\frac{\rho_c}{g\,\gamma}\right)^{\frac{1}{4}}\right]\left(\frac{\Delta\rho}{\rho_c}\right)^{-0.58}\left(\frac{\mu_d}{\mu_w}\right)^{0.18}$$

$$\times\left(\frac{D_R}{H}\right)^{0.62}\left(\left(\frac{D_S}{D_C}\right)^2\right)^{-0.26}\left[H\left(\frac{\rho_c g}{\gamma}\right)^{\frac{1}{2}}\right]^{-0.39}$$

After calculation of the dispersed phase holdup (h), the actual average continuous and dispersed phase velocities can be calculated by Equations 3-7 and 3-8. Incorporation of the holdup factor accounts for the fraction of space taken up by the opposite phase in the flow path.

Equation 3-7

$$V_d = \frac{\bar{V}_d}{h}$$

Equation 3-8

$$V_c = \frac{\bar{V}_c}{(1-h)}$$

From these velocities, the second iteration of the dispersed phase holdup and the phase velocities is executed. This iterative process is repeated until the change in either the holdup or the velocities is insignificant from one iteration to the next.

The ratio of dispersed phase velocity to continuous phase velocity provides the dispersed phase holdup factor at flooding which can be determined from Figure 3-1, or the dispersed phase

holdup at flooding can be calculated with the correlation shown in Equation 3-9 developed by Kumar and Hartland[51].

Equation 3-9

$$\left[\left((C_3 - C_1)\cdot(1-2\phi_f)\right) - \left(\frac{2C_2\phi_f(1-\phi_f)}{C_3\cdot\left(1+4.56\cdot{\phi_f}^{0.73}\right)^2}\right)\right.$$

$$\left.\cdot\left(1+4.56\cdot{\phi_f}^{0.73}+0.33\cdot{\phi_f}^{-0.27}\cdot(1+\phi_f)\right)\right]\cdot\left(\phi_f+\check{R}\cdot(1-\phi_f)\right)$$

$$+(C_3-C_1)\cdot\phi_f\cdot(1-\phi_f)\cdot(\check{R}-1)=0$$

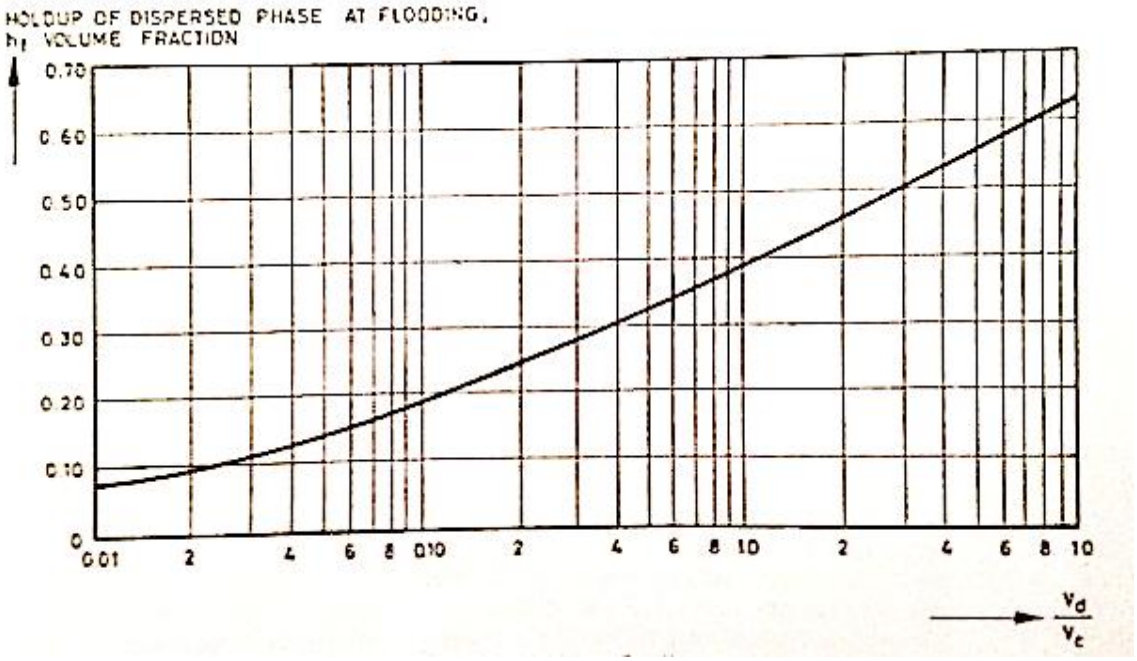

Figure 3-1 Dispersed Phase Holdup at Flooding[55]

The slip velocity is calculated as the sum of the relative velocities of the two phases shown in Equation 3-10[54].

Equation 3-10

$$\bar{V}_s = \frac{\bar{V}_d}{h} + \frac{\bar{V}_c}{1-h}$$

The effective slip velocity is calculated via Equation 3-11 to account for the fractional holdup.

Equation 3-11

$$\bar{V}_e = \bar{V}_s exp(-h)$$

The velocity of the continuous phase adjusted for the slip velocity is then correlated by Equation 3-12 where α is the ratio of $\bar{V}_d$ to $\bar{V}_c$.

Equation 3-12

$$\bar{V}_c = \frac{\bar{V}_e}{\frac{\alpha}{h} + \frac{1}{(1-h)}}$$

Plotting the relationship of $\bar{V}_c$ to h in the correlation above will afford a curve that will pass through a maximum which is the dispersed phase holdup at flooding.

HETS, HTU and HDU

To calculate the HETS for an RDC extraction column as shown in Equation 3-13, the effective height of a transfer unit (HTU_{eff}) must be considered[55].

Equation 3-13

$$HETS = \left[\frac{\ln\left(\frac{1}{K_d}\frac{Q_{feed}}{Q_{solvent}}\right)}{\left(\frac{1}{K_d}\frac{Q_{feed}}{Q_{solvent}}\right) - 1}\right] \cdot HTU_{eff}$$

The effective height of a transfer unit is the sum of the height of a transfer unit (HTU) and the height of a diffusion unit (HDU) as seen in Equation 3-14.

Equation 3-14

$$HTU_{eff} = HTU + HDU$$

The height of a transfer unit (HTU) is determined via Equation 3-15 by estimating the number of theoretical equilibrium stages required to achieve efficient extraction and dividing the height of the agitated section of the extraction column by this number of equilibrium stages.

Equation 3-15

$$HTU = \frac{L}{N_{eq}}$$

The height of a diffusion unit accounts for the axial mixing that occurs in the column and is correlated by Equation 3-16.

Equation 3-16

$$HDU = \frac{1}{\frac{Pe_0}{H} + \frac{0.8}{L} \cdot \frac{\ln\left(\frac{1}{K_d}\frac{Q_{feed}}{Q_{solvent}}\right)}{\left(\frac{1}{K_d}\frac{Q_{feed}}{Q_{solvent}}\right) - 1}}$$

And the Peclet number Pe_0 is obtained by Equation 3-17[55].

Equation 3-17

$$Pe_0 = \frac{\frac{0.1\,L}{HTU} + 1}{\frac{0.1\,L}{HTU} + \frac{Pe_1}{Pe_2}} \cdot Pe_1$$

Where the correlations for Pe_1 and Pe_2 are shown in Equations 3-18 and 3-19.

Equation 3-18

$$\frac{1}{Pe_1} = \frac{\left(\frac{1}{K_d}\frac{Q_{feed}}{Q_{solvent}}\right)}{Pe_f} + \frac{1}{Pe_s}$$

Equation 3-19

$$\frac{1}{Pe_2} = \frac{1}{Pe_f} + \frac{\left(\frac{1}{K_d}\frac{Q_{feed}}{Q_{solvent}}\right)}{Pe_s}$$

Pe_s is the Peclet number for the solvent phase and Pe_f is the Peclet number for the feed. These can be calculated via these equations where Pe_d and Pe_c are the Peclet numbers for the dispersed and continuous phases, respectively. Therefore substitution of Equations 3-20 and 3-21 into

Equations 3-18 and 3-19 depends on which of the phases is the feed and which one is the solvent.

Equation 3-20

$$\frac{1}{Pe_d} = \frac{E_d \cdot h}{H \cdot V_d}$$

Equation 3-21

$$\frac{1}{Pe_c} = \frac{E_c \cdot (1-h)}{H \cdot V_c}$$

The continuous phase axial mixing coefficients and the dispersed phase axial mixing coefficients used to calculate the continuous and dispersed phase Peclet numbers are calculated with Equations 3-22–and 3-23[51, 56].

Equation 3-22

$$E_c = HV_c\left(0.42 + 0.29\left(\frac{V_d}{V_c}\right) + \left[0.0126\left(\frac{ND_R}{V_c}\right) + \frac{13.38}{3.18 + \left(\frac{ND_R}{V_c}\right)}\right] \times \left(\frac{V_d D_R \rho_c}{\mu_c}\right)^{-0.08} \times \left(\frac{D_C}{D_R}\right)^{0.16} \times \left(\frac{D_C}{H}\right)^{0.10} \times \left(\frac{D_S}{D_C}\right)^{2}\right)$$

Equation 3-23

$$E_d = 0.30\left(\frac{\frac{V_c}{(1-h)} + \frac{V_d}{h}}{\frac{V_d}{h}}\right) + 9.37\left(\frac{ND_R h}{V_d}\right)^{-0.48}\left(\frac{D_R^2\,\Delta\rho\, g}{\gamma}\right)^{-0.64}\left(\frac{D_C}{D_R}\right)^{0.7} h^{-0.9}$$

With the Peclet numbers for the continuous and dispersed phases we can determine Pe_1 and Pe_2 which in turn will correlate to Pe_0. With this Peclet number, the height of a diffusion unit can be obtained and a summation with the height of a transfer unit will give the effective height of a transfer unit. The effective HTU is then plugged in to obtain the height equivalent to a theoretical stage.

RDC-1: Extraction of Caprolactam from Aqueous Ammonium Sulfate

The first of the RDC extraction columns in the series is the ammonium sulfate extraction where residual caprolactam that remains in the 43 weight percent ammonium sulfate in water solution resulting from the Beckmann Rearrangement is extracted with benzene. The resulting ammonium sulfate raffinate which has 0.02 weight percent caprolactam goes to a crystallization unit for further processing of the ammonium sulfate. The extract of this column contains about 3.7 weight percent caprolactam in benzene that overflows from RDC-1 into RDC-2 at stator section 60 of 78. The dimensions of RDC-1 cannot be specified in this report due to the company's non-disclosure confidentiality agreement.

HTU_{eff} and HETS for RDC-1

The partition coefficient, K_d, is significantly impacted by the concentration of ammonium sulfate in the feed as shown in Figure 3-2.

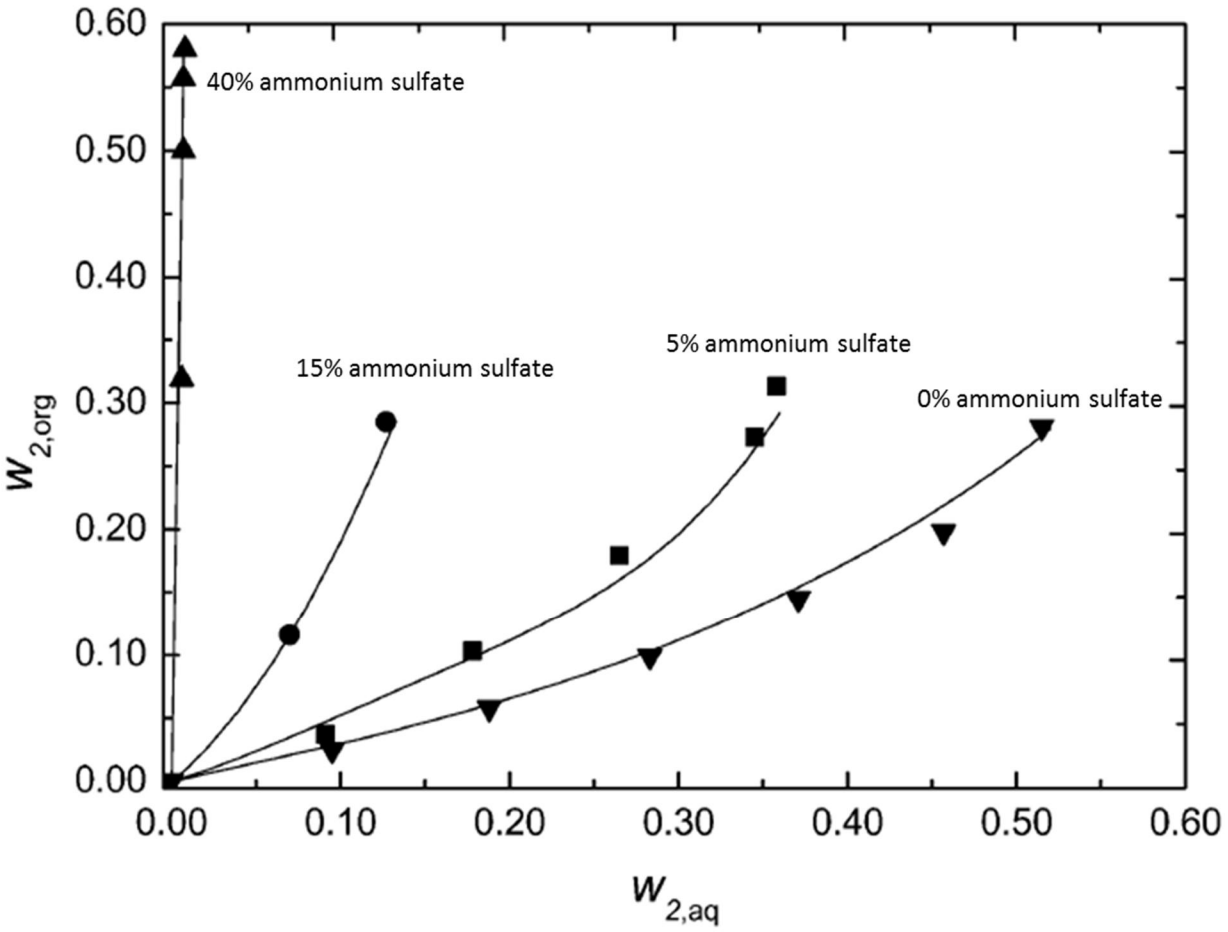

Figure 3-2 Kd vs Ammonium Sulfate Concentration[59]

Approaching the column as a series of mixer-settlers calculates the number of stages in the extraction column to be slightly less than 4 therefore the height of a transfer unit is 3.94 meters. The caprolactam concentrations for the feed and solvent entering and exiting each stage are shown in Table 3-1 for the mixer-settler approach. In this table the caprolactam in the raffinate and caprolactam in the benzene is shown as weight in pounds as well as weight percent for the incoming and exiting flow for each stage.

Stage	FEED	lbs Water	lbs Amm Sulf	CPL in Raffinate	% CPL Raffinate	SOLVENT	lbs Benzene	CPL in Benzene	% CPL Extract	$1/K_D$
1	in	761.52	574.48	9.4	0.70%	out	247.36	9.4	3.66%	
	out	761.52	574.48	3.501953	0.26%	in	247.36	3.501953	1.40%	0.071
2	in	761.52	574.48	3.501953	0.26%	out	247.36	3.501953	1.40%	
	out	761.52	574.48	1.333151	0.10%	in	247.36	1.333151	0.54%	0.071
3	in	761.52	574.48	1.333151	0.10%	out	247.36	1.333151	0.54%	
	out	761.52	574.48	0.511513	0.04%	in	247.36	0.511513	0.21%	0.071
4	in	761.52	574.48	0.511513	0.04%	out	247.36	0.511513	0.21%	
	out	761.52	574.48	0.196954	0.01%	in	247.36	0.196954	0.08%	0.071

Table 3-1 RDC-1 Stages as Mixer-Settlers

Using the approach of the effective height of a transfer unit to determine the number of theoretical equilibrium stages achievable affords graphical depictions of the number of theoretical stages versus flow rates and rotor speeds. Figure 3-3 shows the number of stages achievable at various rotor speeds for the solvent flow to RDC-1 and Figure 3-4 for the total flow to RDC-1.

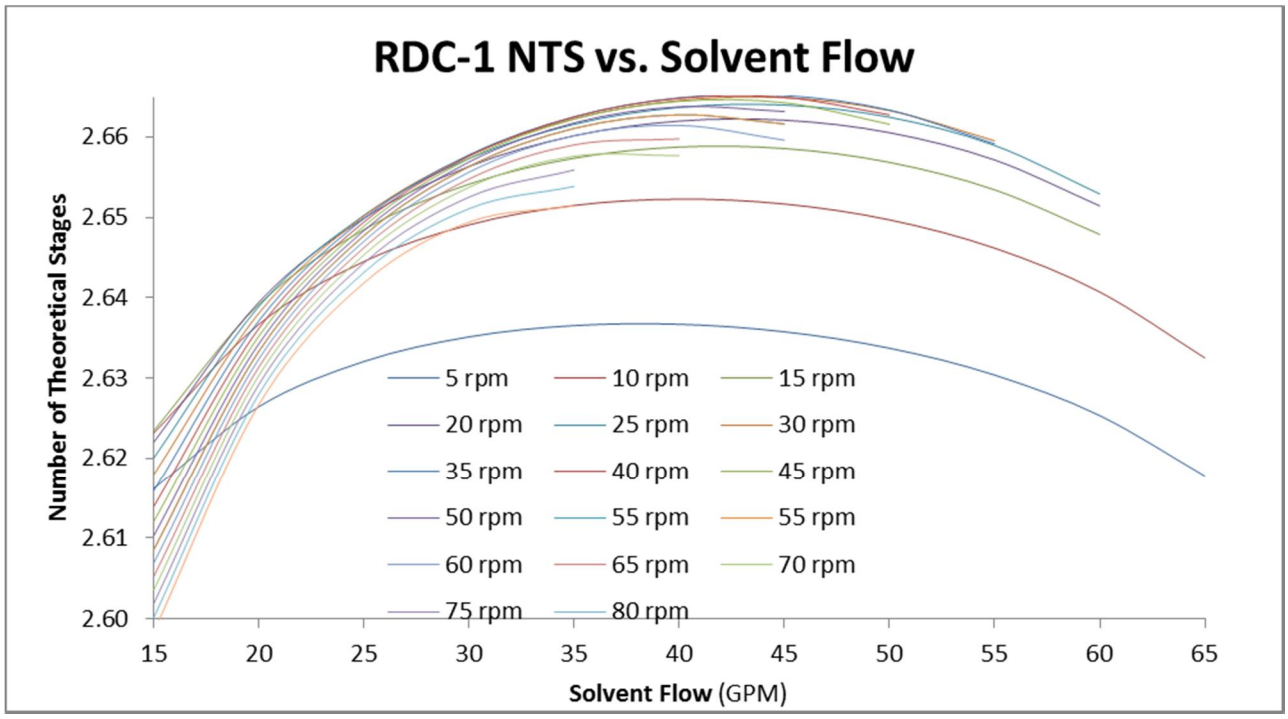

Figure 3-3 RDC-1 NTS vs Solvent Flow at Various Rotor Speeds

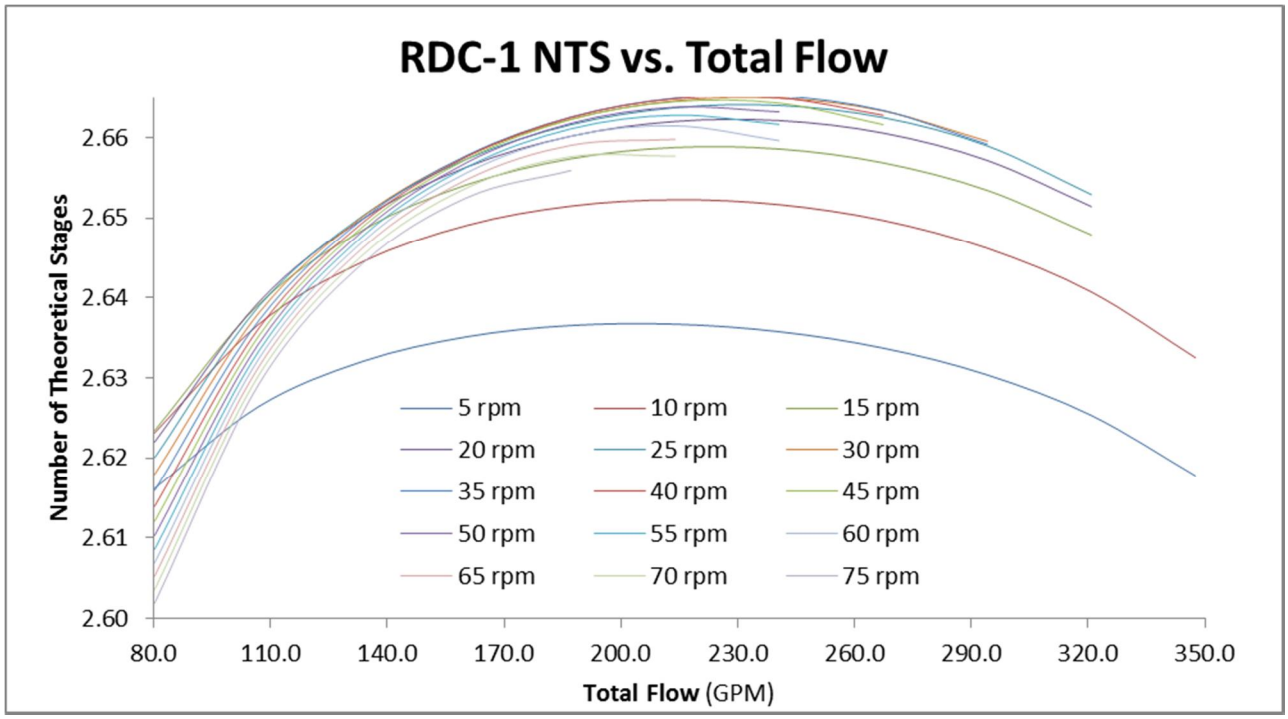

Figure 3-4 RDC-1 NTS vs Total Flow at Various Rotor Speeds

RDC-2: Forward Extraction of Caprolactam from Aqueous Caprolactam Oil

RDC-2 is the forward extraction of caprolactam from the aqueous caprolactam oil that is separated from the aqueous ammonium sulfate solution resulting from the Beckmann Rearrangement. Benzene is the solvent used to extract the caprolactam from the aqueous oil. The feed is fed at 60 gallons per minute of 72.5 weight percent caprolactam and the solvent is fed at 183 gallons per minute of benzene containing approximately 0.04 weight percent caprolactam. The overflow from RDC-1 enters this extraction column at stator section 60 of 72. The extract contains some entrained aqueous phase that separates in the holding vessel between RDC-2 and RDC-3, and this carryover is pumped back to RDC-2 at the feed inlet at approximately 1 gallon per minute of 15 weight percent caprolactam. The dimensions of RDC-2 cannot be specified in this report due to the company's non-disclosure confidentiality agreement.

HTU_{eff} and HETS for RDC-2

The partition coefficient for this extraction is dependent on the concentration of caprolactam in the aqueous phase and temperature as shown in Figure 3-5. The extraction is carried out at 104°F.

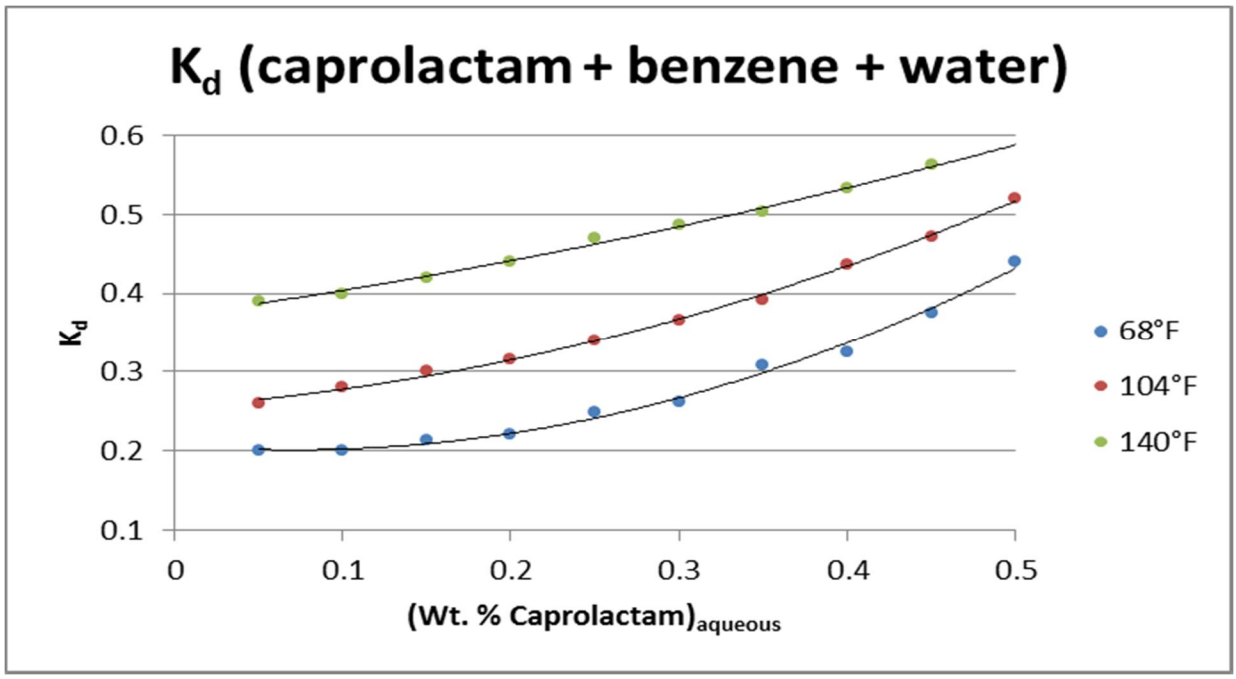

Figure 3-5 Kd Based on Temperature and Caprolactam Concentration[59]

Calculating the number of theoretical stages with the Kremser Equation gives a result of 35.8 stages achieved in RDC-2. This calculation had to be completed with an average partition coefficient of 0.35.

$$N_S = \frac{\ln\left[\left(\frac{0.725-\frac{0.0004}{0.35}}{0.005-\frac{0.0004}{0.35}}\right)\left(1-\frac{1}{\left(0.35\cdot\frac{183}{60}\right)}\right)+\frac{1}{\left(0.35\cdot\frac{183}{60}\right)}\right]}{\ln\left(0.35\cdot\frac{183}{60}\right)} = 35.8$$

Calculating the number of theoretical stages assuming the extraction column acts as a series of ideal mixer-settlers shows that 8 stages are achieved in RDC-2. The concentrations entering and exiting each stage for the mixer-settler approach is shown in Table 3-2 and this accounts for the additional flows from RDC-1 and the return of aqueous carryover. In this table

the caprolactam in the raffinate and caprolactam in the extract is shown as weight in pounds as well as weight percent for the incoming and exiting flow for each stage.

Stage	FEED	lbs Water	lbs CPL in Raffinate	% CPL Raffinate	SOLVENT	lbs Benzene	lbs CPL in Extract	% CPL Extract	K_D
1	in	149.5	376.65	71.6%	out	1662	386.6646	18.9%	0.45
	out	149.5	109.761	42.3%	in	1662	119.7756	6.72%	
2	in	149.5	109.761	42.3%	out	1662	119.7756	6.72%	0.31
	out	149.5	41.35358	21.7%	in	1662	51.36818	3.00%	
3	in	149.5	41.35358	21.7%	out	1414.6	41.86818	2.87%	0.26
	out	149.5	18.55839	11.0%	in	1414.6	19.07299	1.33%	
4	in	149.5	18.55839	11.0%	out	1414.6	19.07299	1.33%	0.26
	out	149.5	8.051448	5.1%	in	1414.6	8.566048	0.60%	
5	in	149.5	8.051448	5.1%	out	1414.6	8.566048	0.60%	0.25
	out	149.5	3.683366	2.40%	in	1414.6	4.197966	0.30%	
6	in	149.5	3.683366	2.40%	out	1414.6	4.197966	0.30%	0.24
	out	149.5	1.863758	1.23%	in	1414.6	2.378358	0.17%	
7	in	149.5	1.863758	1.23%	out	1414.6	2.378358	0.17%	0.24
	out	149.5	1.052013	0.70%	in	1414.6	1.566613	0.11%	
8	in	149.5	1.052013	0.70%	out	1414.6	1.566613	0.11%	0.23
	out	149.5	0.719985	0.48%	in	1414.6	1.234585	0.09%	

Table 3-2 RDC-2 Stages as Mixer-Settlers

The effective height of a transfer unit approach to determine the number of theoretical equilibrium stages achievable affords graphical depictions of the number of theoretical stages versus flow rates and rotor speeds for RDC-2. Since this RDC extraction column has significant differences in the parameters of the feed and solvent streams in the top and bottom portions of the column, using the effective height of a transfer unit approach is best when considering the column as two separate columns and then summing the number of theoretical stages achievable for the two sections. Figure 3-6 shows the number of stages achievable at various rotor speeds for the feed flow to RDC-2 and Figure 3-7 for the total flow to RDC-2.

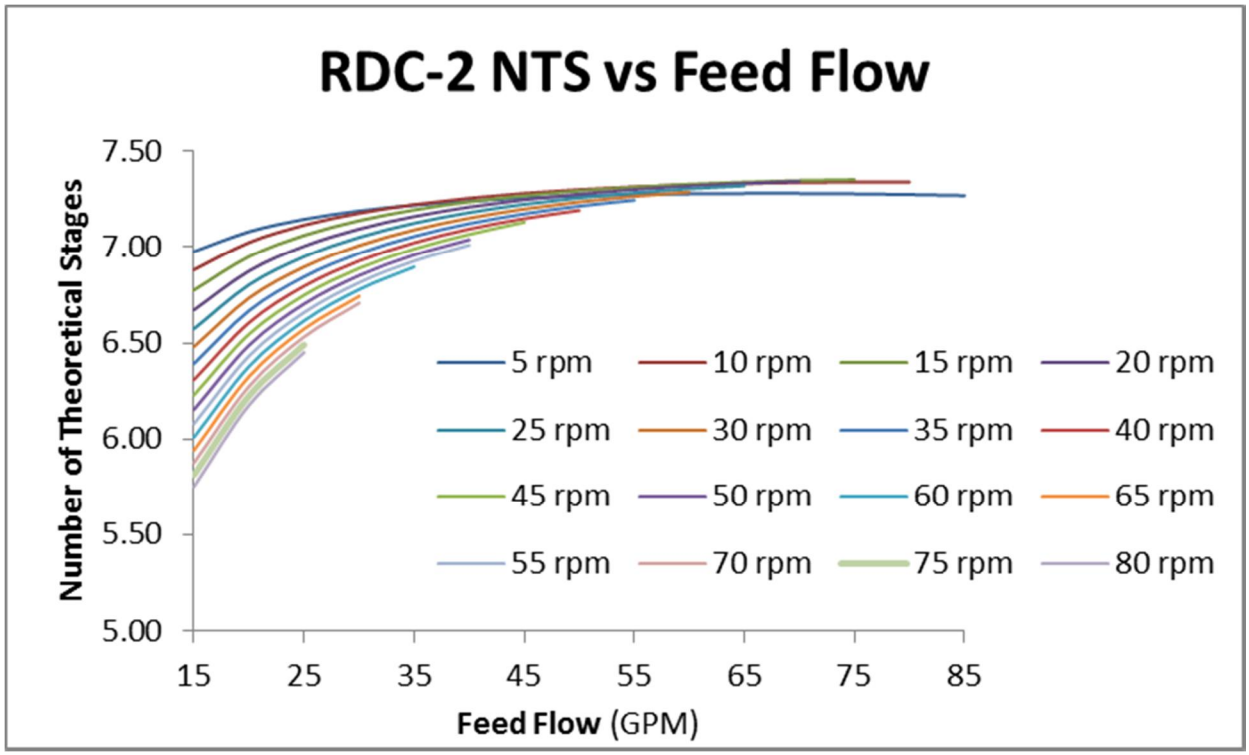

Figure 3-6 RDC-2 NTS vs Feed Flow at Various Rotor Speeds

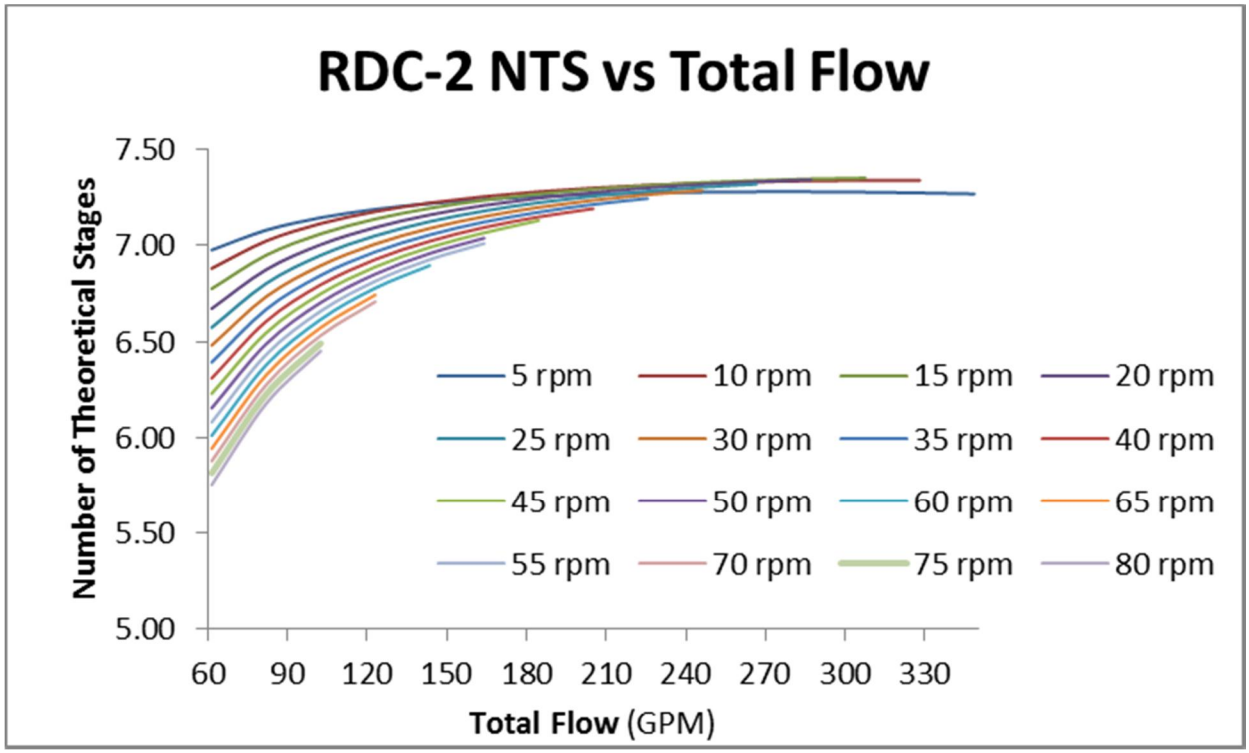

Figure 3-7 RDC-2 NTS vs Total Flow at Various Rotor Speeds

RDC-3: Back Extraction of Caprolactam from Benzene to Water

RDC-3 is the back extraction of the caprolactam from the benzene back into an aqueous solution. Water with residual caprolactam of approximately 0.08 weight percent is used in this extraction which is carried out at roughly 104°F. Temperature is a key factor for back extraction efficiency in that higher temperatures reduce the hydrogen bonding between water and caprolactam molecules thereby more caprolactam remains in the benzene and the back extraction efficiency is reduced. The feed to RDC-3 is 18.9 weight percent caprolactam and the raffinate is 0.1 weight percent caprolactam in benzene which is recycled to RDC-1 and RDC-2 as the solvent. The resulting extract is 41 weight percent caprolactam in water. The dimensions for RDC-3 cannot be specified in this report due to the company's non-disclosure confidentiality agreement.

Calculating the number of theoretical stages with the Kremser Equation gives a result of 3.3 stages achieved in RDC-3. This calculation had to be completed with an average partition coefficient of 3.

$$N_S = \frac{\ln\left[\left(\frac{0.189 - \frac{0.0001}{3}}{0.005 - \frac{0.0001}{3}}\right)\left(1 - \frac{1}{(3 \cdot 0.31)}\right) + \frac{1}{(3 \cdot 0.31)}\right]}{\ln(3 \cdot 0.31)} = 3.3$$

Calculating the number of theoretical stages assuming the extraction column acts as a series of ideal mixer-settlers shows that 5 stages are achieved in RDC-3. The concentrations entering and exiting each stage for the mixer-settler approach are shown in Table 3-3. In this table the caprolactam in the raffinate and caprolactam in the extract is shown as weight in pounds as well as weight percent for the incoming and exiting flow for each stage.

Stage	FEED	lbs Benzene	CPL in Raffinate	% CPL Raffinate	SOLVENT	lbs Water	CPL in Extract	% CPL Extract	K_D
1	in	1662	386.66	18.87%	out	555	385.19	41.0%	2.22
	out	1662	154.5	8.51%	in	555	153.03	21.61%	
2	in	1662	154.5	8.51%	out	555	153.03	21.61%	2.50
	out	1662	58.5	3.40%	in	555	57.03	9.32%	
3	in	1662	58.5	3.40%	out	555	57.03	9.32%	3.01
	out	1662	19	1.13%	in	555	17.53	3.06%	
4	in	1662	19	1.13%	out	555	17.53	3.06%	3.34
	out	1662	5.65	0.34%	in	555	4.18	0.75%	
5	in	1662	5.65	0.34%	out	555	4.18	0.75%	3.71
	out	1662	1.52	0.09%	in	555	0.05	0.01%	

Table 3-3 RDC-3 Stages as Mixer Settlers

The effective height of a transfer unit approach to determine the number of theoretical equilibrium stages achievable affords graphical illustrations of the number of theoretical stages versus flow rates and rotor speeds for RDC-3. Figure 3-8 shows the number of stages achievable at various rotor speeds for the solvent flow to RDC-3 and Figure 3-9 for the total flow to RDC-3.

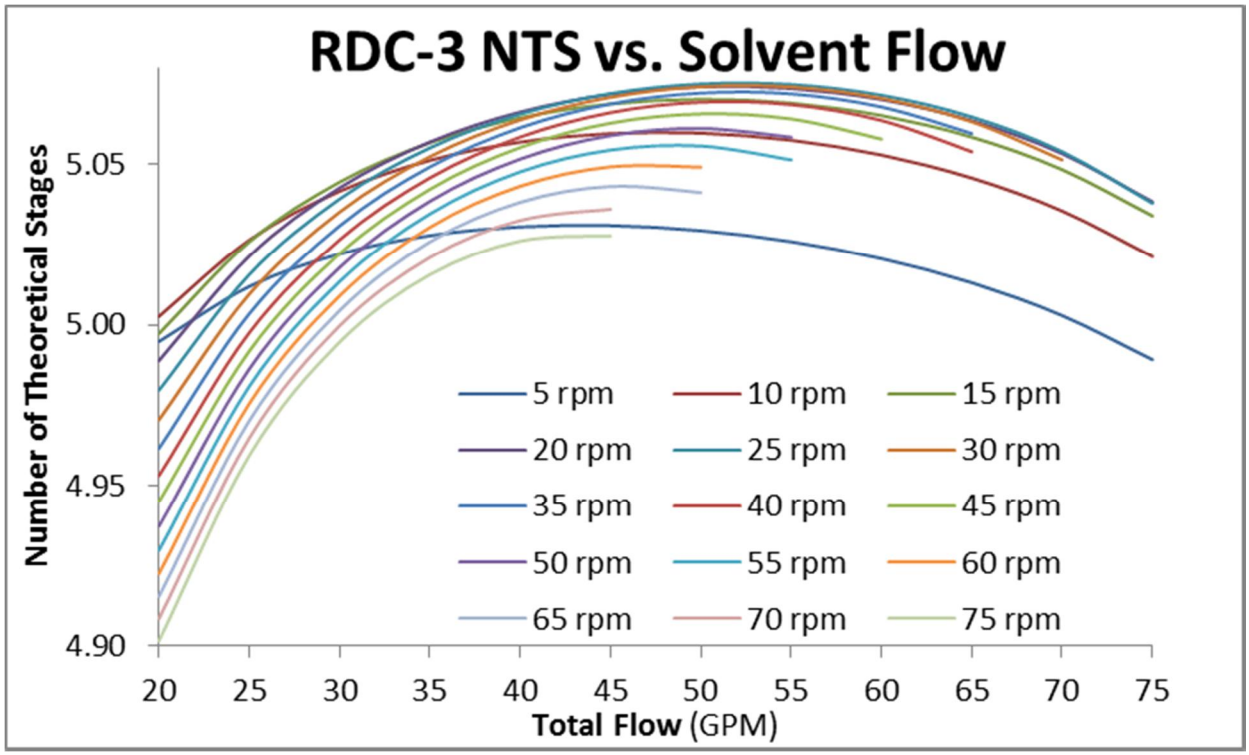

Figure 3-8 RDC-3 NTS vs Solvent Flow at Various Rotor Speeds

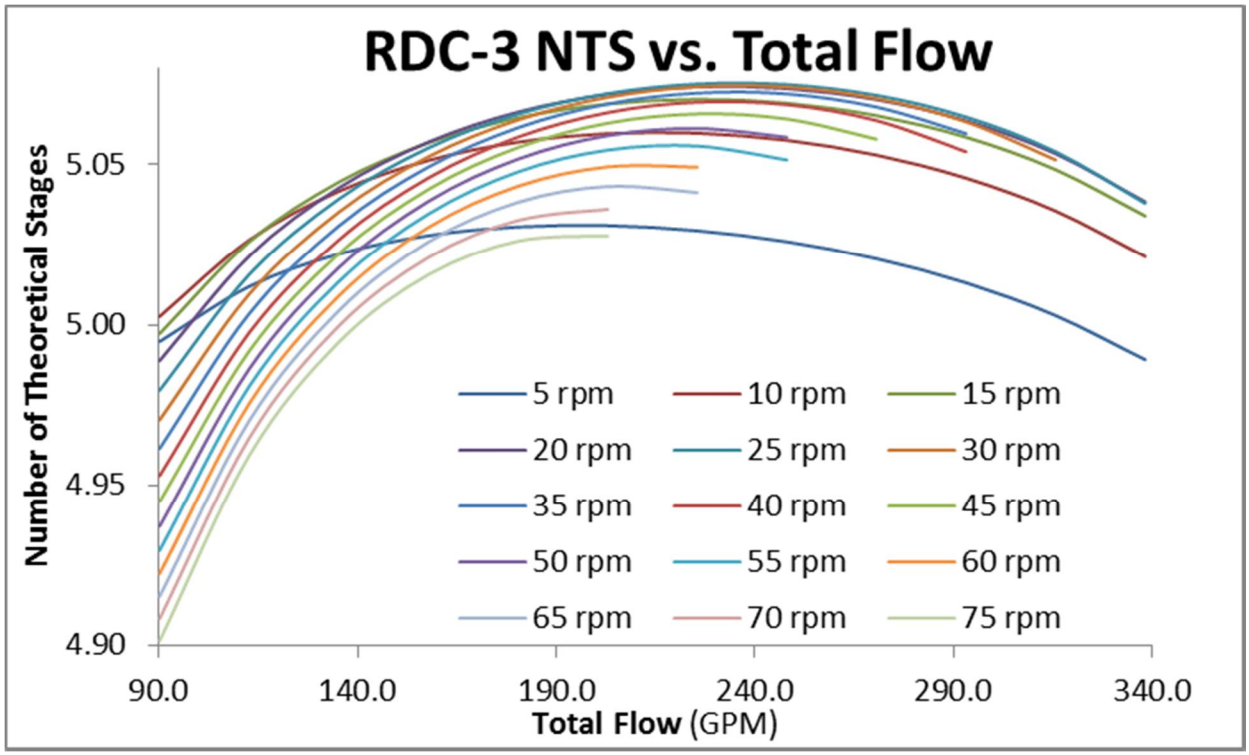

Figure 3-9 RDC-3 NTS vs Total Flow at Various Rotor Speeds

Chapter 4 - Alternative Solvents for Caprolactam Extraction

Caprolactam Extraction

Caprolactam extraction is a key unit operation in the purification of caprolactam produced from a Beckmann Rearrangement of cyclohexane oxime with oleum. The resulting solution from the reaction is neutralized with ammonium hydroxide and separates into an aqueous caprolactam oil and an aqueous ammonium sulfate solution that contains residual caprolactam. Efficient extraction requires an organic solvent that can remove caprolactam from the aqueous ammonium sulfate stream and from the aqueous caprolactam oil. A second back-extraction consists of transferring the caprolactam back into an aqueous stream from the organic stream.

Impurity Profile

Any impurities formed in the Beckmann Rearrangement that have a greater affinity for the aqueous solution will be removed by way of the aqueous waste stream from the extraction of caprolactam into the organic solvent. Impurities that have a greater affinity for the organic phase will remain in said phase when the caprolactam is extracted back into an aqueous stream. Since the organic stream is a continuous loop, heavy impurities in this stream can be removed in a distillation column for the organic solution. Specific impurities that follow the route of caprolactam in the extraction and back-extraction columns are removed in purification steps downstream of the extraction train. The ability of a solvent to selectively extract caprolactam whilst not extracting some of the impurities is an important criterion to consider in solvent selection.

Some impurities that form in the Beckmann Rearrangement of cyclohexane oxime via a side reaction called a Neber Rearrangement. These impurities include aniline, phenol, adipoin,

2-cyclohexenone, and octahydrophenazine. The structures of these compounds are shown in figure 4-1.

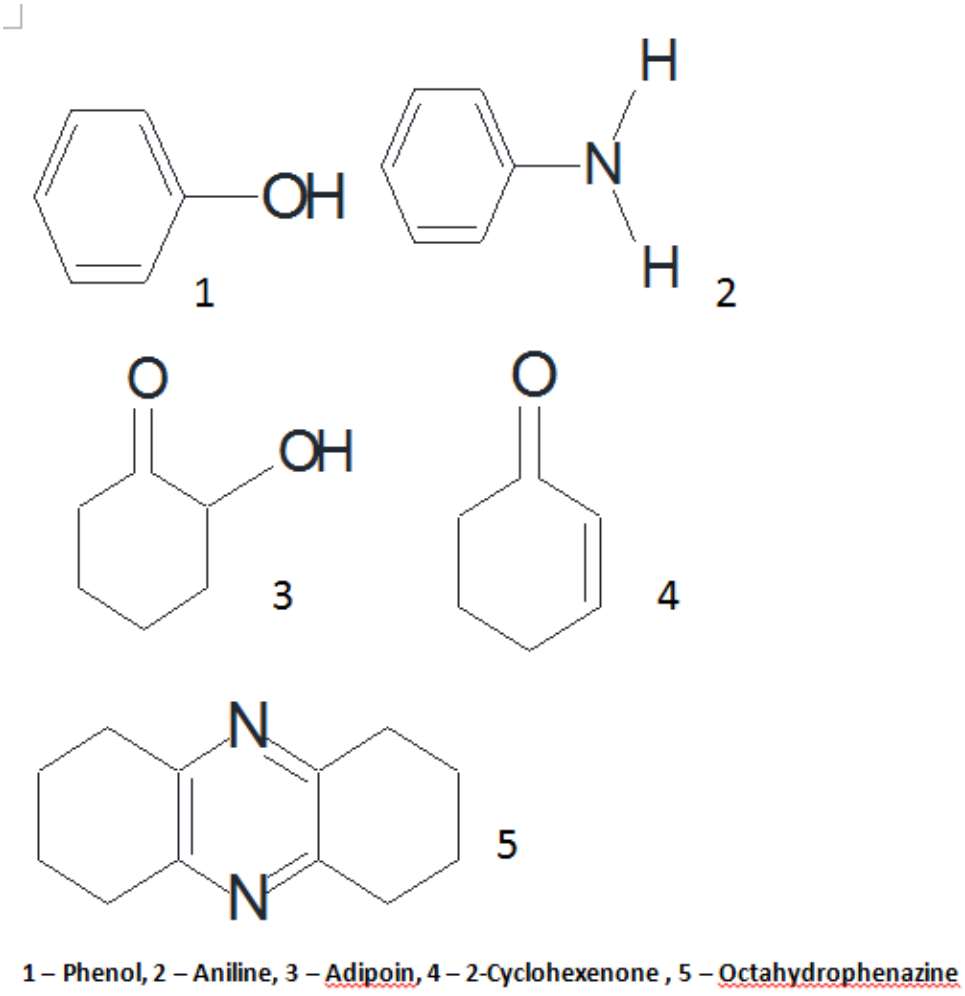

1 – Phenol, 2 – Aniline, 3 – Adipoin, 4 – 2-Cyclohexenone , 5 – Octahydrophenazine

Figure 4-1 Impurities formed by Neber Rearrangement

Some impurities enter the Beckmann Rearrangment with the cyclohexanone oxime as either unreacted species from earlier steps in the synthetic process or as impurities formed within said steps. Typically purification steps are incorporated in the processes to eliminate these impurities in the cyclohexanone oxime however sometimes these impurities will not be separated as efficiently as desired. These impurities can even react with cyclohexane oxime, caprolactam or Neber Rearrangement impurities to form another group of impurities in caprolactam. Some of

the impurities that enter the Beckmann Rearrangment or that are generated by impurities entering this reaction include toluene, cyclohexaonone, aminocaproic acid, OHCO, DODO, and cyclohexenyl cyclohexanone. The latter four of these impurities are shown in figure 4-2.

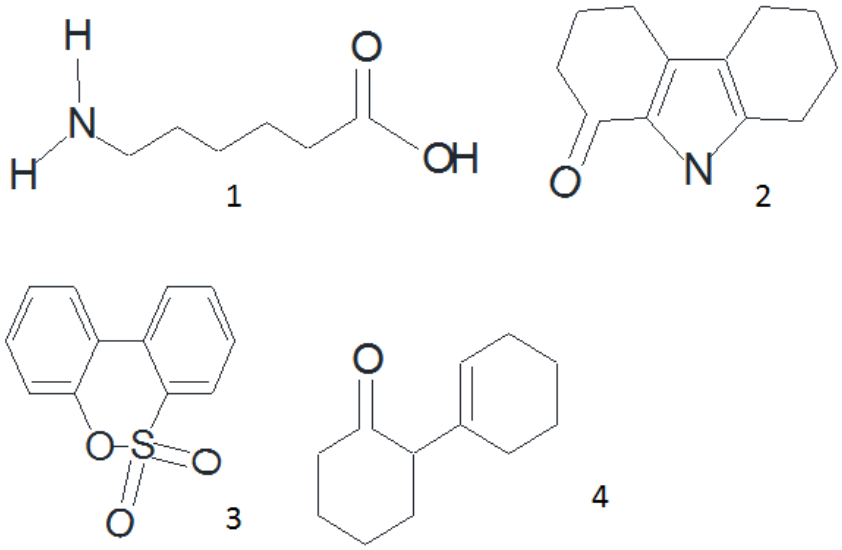

1 – Aminocaproic Acid, **2 –** 2,3,4,5,6,7,8,9-octahydro-carbazol-1-one (OHCO),
3 – Dibenzo[1,2]oxathiine 6,6-dioxide (DODO), **4 –** Cyclohexenyl Cyclohexanol

Figure 4-2 Impurities in Caprolactam due to Purity of Cyclohexanone Oxime

Other impurities that have to be separated from caprolactam include ammonium sulfate, residual ammonia, sulfur dioxide and oligomers formed by polymerization of caprolactam molecules. These impurities have a significant affinity for water over organic solvents and tend to remain in the aqueous raffinate of the extraction of caprolactam from the caprolactam rich oil.

Solvent Selection Requirements

The first fundamental measure for selecting an appropriate solvent is considering the capacity for caprolactam solubility in the solvent. If a solvent has a low capacity then unreasonably large extraction columns are required as well as significant volumes of solvent. The partition coefficient is a ratio of caprolactam concentration in the raffinate and extract

phases at equilibrium. Table 4-1 shows the caprolactam capacity for various solvents at ambient temperature.

Solvent	Weight % Caprolactam
1,2-Dichloroethane	95
1,4-Dichlorobutane	85
Water	82
Cyclohexanol	82
Methyl ethyl ketone	53
Benzene	41
Cyclohexanone	35
Toluene	26
Ethyl acetate	24
p-Xylene	14
Cyclohexane	2

Table 4-1 Caprolactam Solubility Capacities of Various Solvents[58, 72]

Mutual solubility of the organic solvent in the aqueous phase requires fractionation columns that will appropriately recover the organic solvent for reintroduction into the extraction organic loop. This increases costs for the energy required for recovery and for solvent losses. It will also reduce extraction efficiency and increase caprolactam losses via the raffinate. Mutual solubility also increases the probability of impurities that would be selectively removed in extraction to make it through the extraction purification step and into the final product. Minimizing mutual solubility reduces recovery costs and increases product purity.

The density of the solvent has to be considered since more dense solvents would possibly require a redesign of the existing equipment in benzene service. Benzene is lighter than water so the exiting benzene extract or raffinate which entered at the bottom of each column will exit at the column overflow. The difference in the densities of the counter flowing solvents also is the driving force for separations. Viscosity must be considered as well. Higher viscosity in the

continuous phase results in higher drag coefficients for drops, and higher viscosity in the dispersed phase results in higher power requirements for drop breakage. Lower viscosity in the continuous phase results in a reduced resistance for traveling of drops and is helpful for phase separation.

Interfacial tension is of high importance in that this determines the amount of surface area that can be achieved in a solvent system. Higher surface area results in more probable solute transfer which increases extraction efficiency. If the surface area is at or close to minimum, then poor extraction efficiency can be expected. Lower interfacial tension means there will be more droplet breakage and smaller drop size which means more surface area for solute transfer. However higher interfacial tension leads to quicker phase separation. Therefore it is important to find a solvent system that has high enough surface tension to allow for phase separation but low enough so that the droplets of the dispersed phase can be broken by the agitation to increase surface area.

Chemical reactivity and stability should also be considered in selecting a solvent for caprolactam extraction as well as the freezing point and vapor pressure of the solvent. Toxicity and flammability are key characteristics that have to be considered as these two characteristics are the reason for searching out an alternative solvent to benzene.

Solvents

Water

Water is a unique solvent that has a permanent dipole moment and has significant hydrogen bonding between its molecules which leads to the high surface tension. Since water is introduced in the neutralization step after the Beckmann Rearrangment, the caprolactam ($C_6H_{11}NO$) oil that is separated from the aqueous ammonium sulfate contains 25-29% water.

Water and caprolactam have a propensity to have hydrogen bonding among each other as shown in Figure 4-3.

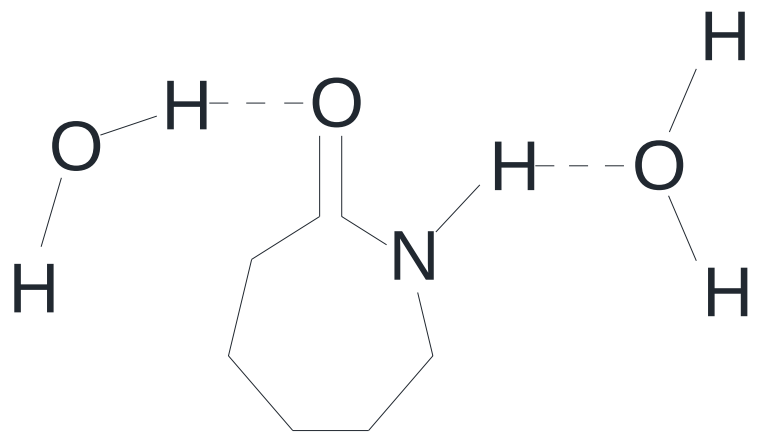

Figure 4-3 Caprolactam - Water Hydrogen Bonding

This hydrogen bonding between caprolactam and water molecules makes for a strong affinity for caprolactam dissolved in water. The carbon based portion of the ring however provides a slight affinity for caprolactam with organic solvents. Higher temperatures increase internal energy among water and caprolactam molecules and leads to a reduction in the hydrogen bonding thereby pushing the partition coefficient more towards the organic phase in comparison to cooler temperatures. Water retains compounds that are able to hydrogen bond yet do not have an organic component such as ammonia, ammonium sulfate, and sulfur dioxide. Some compounds such as aminocaproic acid and caprolactam oligomers tend to stay in the aqueous phase however some will make their way into the organic phase of the extraction process.

Benzene and Aromatic Solvents

Aromatic compounds such as benzene, toluene and xylene have quadrapole moments that tend to have attractive forces on the amide group of caprolactam. These solvents have reasonable capacities for caprolactam solubility with benzene having the higher capacity and

xylene having the lower capacity. The methyl groups on the aromatic ring are activating electron donating substituents that produce a permanent dipole moment in the molecule however these groups reduce packing capabilities due to steric hindrance. Less ability for the molecules to pack more closely reduces the intermolecular forces. The partition coefficient of caprolactam dissolved in the aqueous phase versus caprolactam dissolved in the organic phase also follows the same pattern with benzene having the largest partition coefficient and xylene having the lowest. Nitrobenzene has an electron withdrawing group which is a zwitterion that has more attractive forces with caprolactam in comparison to toluene and xylene, however the functional group also reduces packing abilities; therefore toluene and xylene do not have the caprolactam solubility capacity of benzene.

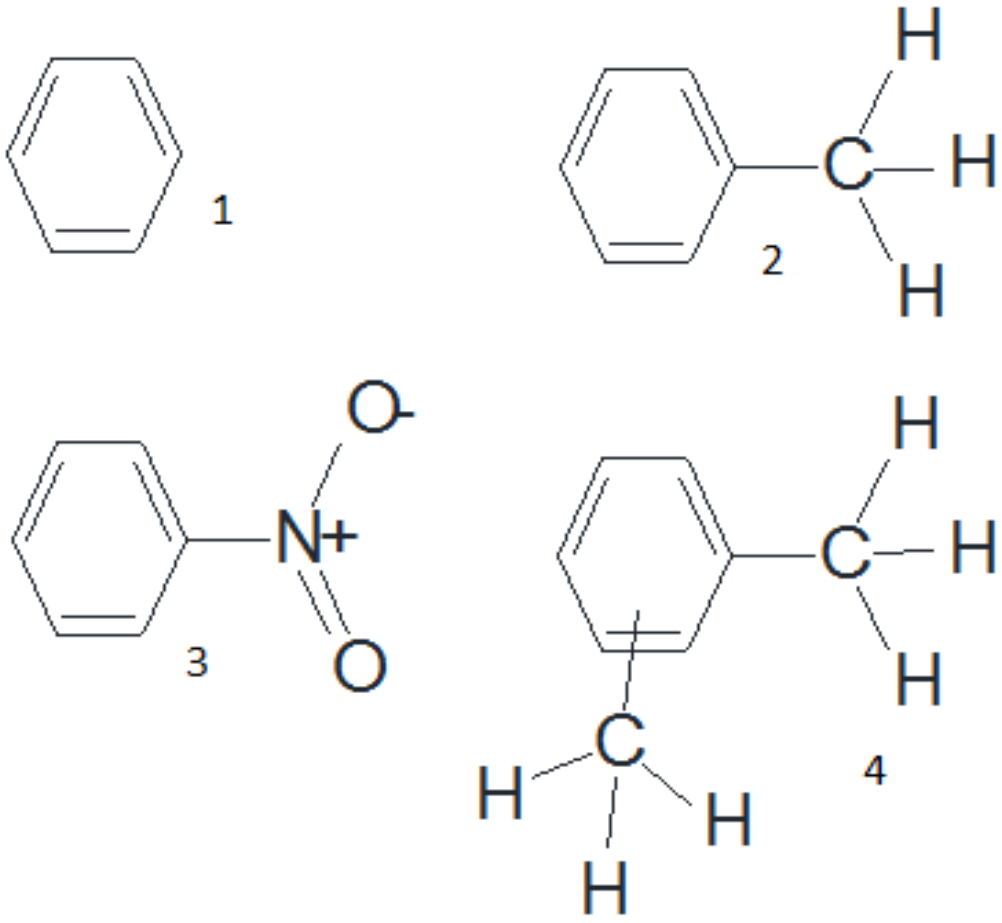

1 – Benzene, 2 – Toluene, 3 – Nitrobenzene, 4 – Xylene

Figure 4-4 Aromatic Solvent Structures

The ternary diagrams of water + caprolactam + solvent for benzene[58, 59, 60, 61, 62], toluene[59, 61, 62] and nitrobenzene[58] with tie-lines are shown in Figures 4-5, 4-6, and 4-7, respectively.

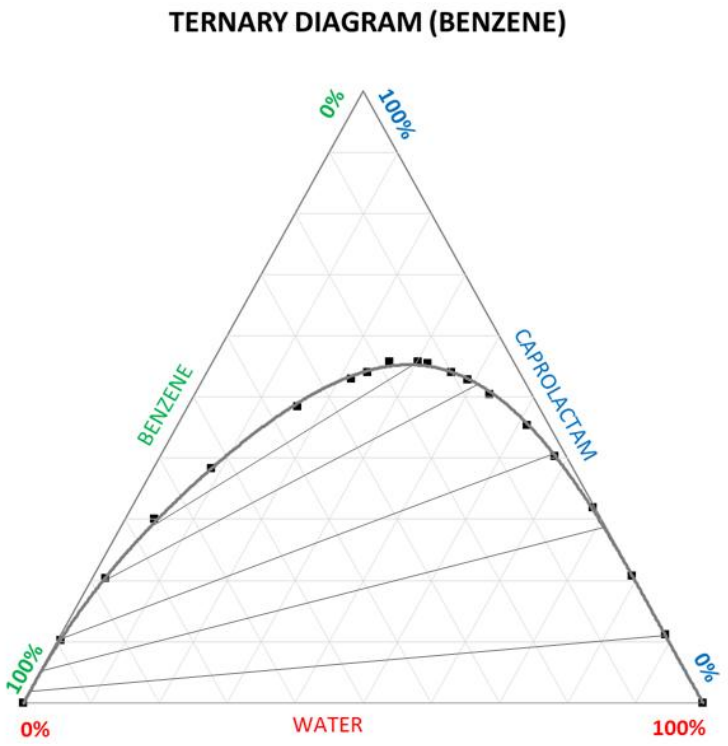

Figure 4-5 Ternary Diagram Water + Caprolactam + Benzene[58]

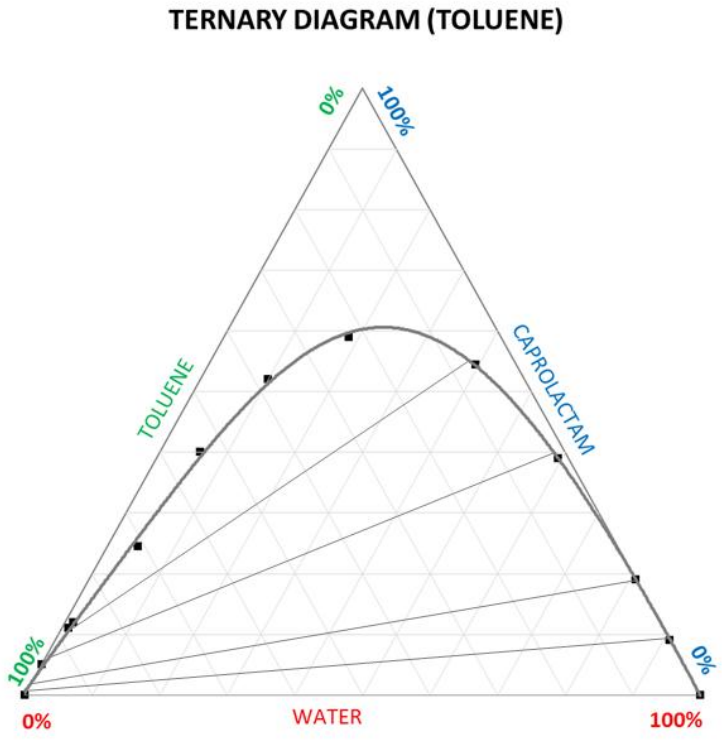

Figure 4-6 Ternary Diagram Water + Caprolactam + Toluene[58]

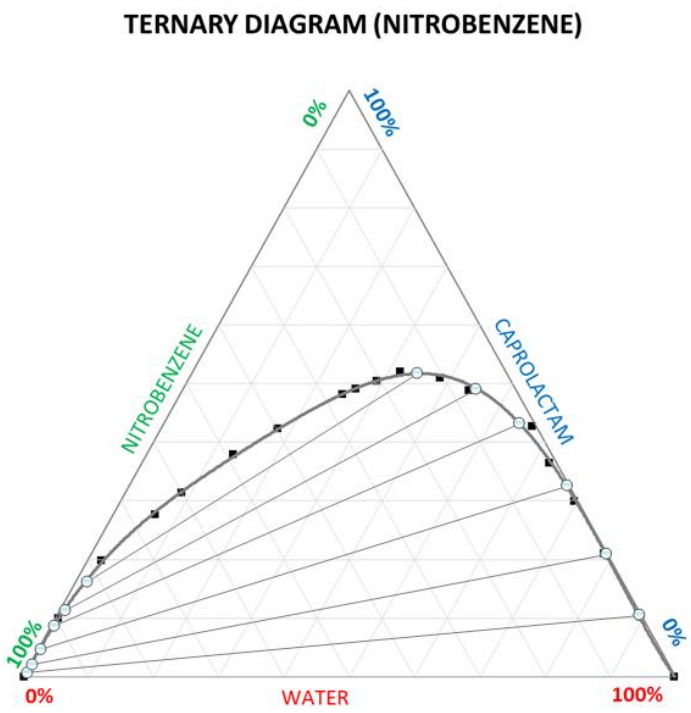

Figure 4-7 Ternary Diagram Water + Caprolactam + Nitrobenzene[58]

Aromatic compounds typically have reduced mutual solubility with water in comparison to more polar organic solvents such as alcohols and alkyl halides. However benzene and water have higher mutual solubility in comparison to xylene and water or toluene and water[63]. This is due to the possible alignment of the water molecules so that the hydrogen atoms of water can interact with the aromatic face of the benzene ring and the oxygen atoms of water can align with the hydrogen atoms of the benzene molecule. The benzene molecule has a quadrupole with the positive hydrogen atoms on the edge of the ring and the negative pi electron cloud of the aromatic ring in the center. Toluene has the methyl group which is an electron donating group and xylene has two methyl groups which inhibit the ability for molecular stacking in comparison to benzene, however these electron donating groups enhance the intermolecular interactions. This is clearly seen by the increase in boiling points: benzene has a boiling point of 176°F, toluene has a boiling point of 231°F and xylene has a boiling point of 281°F. The increase in

intermolecular interactions reduces the potential for interactions with water molecules. Nitrobenzene has the nitrate functional group that similarly to the methyl group reduces the molecule's ability to stack however it allows for hydrogen bonding with water molecules.

Solvent	Solubility in Water (g/L)	Water Solubility in Solvent (g/L)
Benzene	1.8	0.58
Toluene	0.52	0.33
Xylene	0.18	< 0.1
Nitrobenzene	1.9	Unknown

Table 4-2 Mutual Solubility Between Aromatic Solvents and Water[58, 72]

The purpose for attempting to find an alternative solvent for the extraction of caprolactam is due to benzene being a known carcinogen. Nitrobenzene is not a reasonable option as an alternative to benzene because it too is a suspected carcinogen and it is also classified as a reproductive toxin. Toluene and para-xylene are the best options to be considered alternates and since toluene has the highest caprolactam capacity, it is the better choice of the two. Toluene and xylene are considered non-carcinogenic.

The partition coefficient of caprolactam at equilibrium between the organic and aqueous phases shows an increased affinity for benzene in comparison to toluene as shown in Figure 4-8. Therefore caprolactam extraction will require larger extraction columns and more solvent inventories for toluene in comparison to benzene.

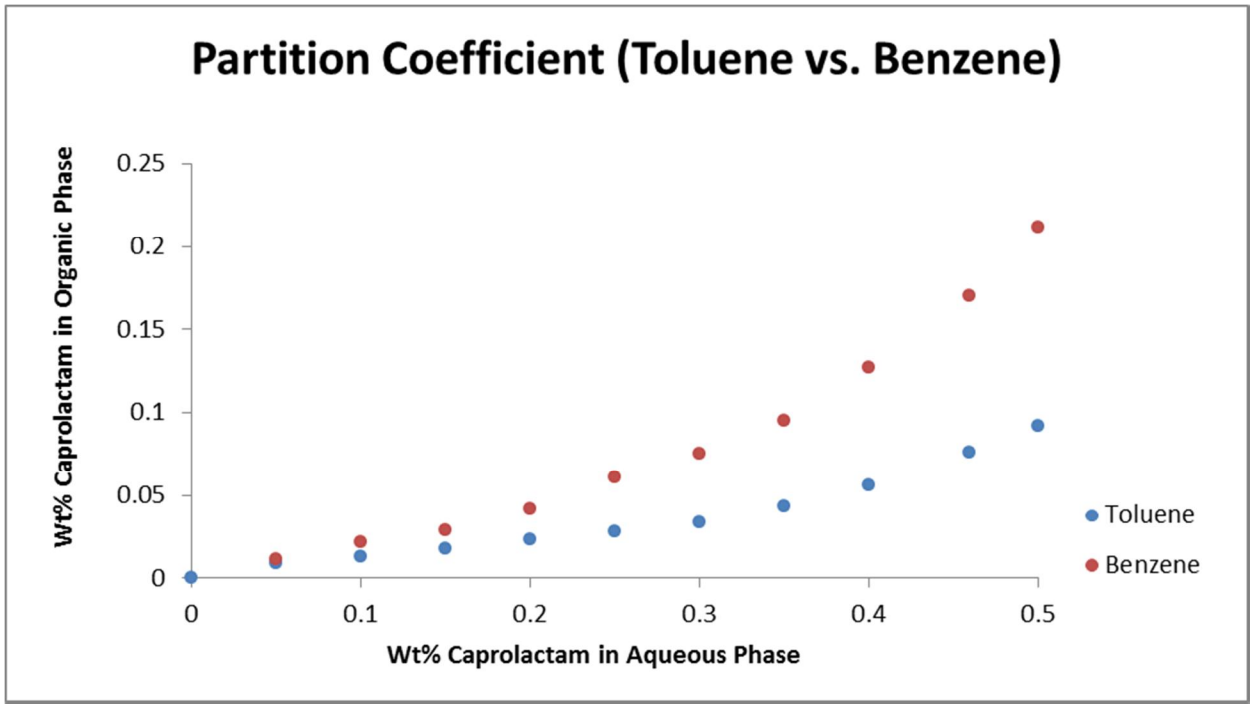

Figure 4-8 Partition Coefficient for Caprolactam (Toluene vs. Benzene)[59]

Alkanes and Cyclic Alkanes

Cyclohexane, methylcyclohexane, hexane, heptane and octane have only carbon-carbon and carbon-hydrogen single bonds that have no potential for hydrogen bonding characteristics. The only affinity between these solvents and caprolactam is due to weak non-polar attraction between the solvent and the aliphatic portion of the caprolactam molecule. This is why caprolactam has a very low solubility capacity in these solvents. Only 2 weight percent caprolactam will dissolve in cyclohexane. In the presence of a water phase, caprolactam will be driven to the aqueous phase due to the much stronger hydrogen bonding forces in comparison to the non-polar interactions.

These non-polar solvents have been considered a potential alternative when used in combination with cyclohexanol or a carbon chain alcohol such as heptanol or octanol.

Chlorinated Hydrocarbons

Several chlorinated hydrocarbons have been investigated for caprolactam extraction. Carbon tetrachloride, chloroform, methylene chloride, dichloroethane and trichloroethylene are some of the solvents that have been investigated[58, 62]. The structures of these compounds are shown in Figure 4-9.

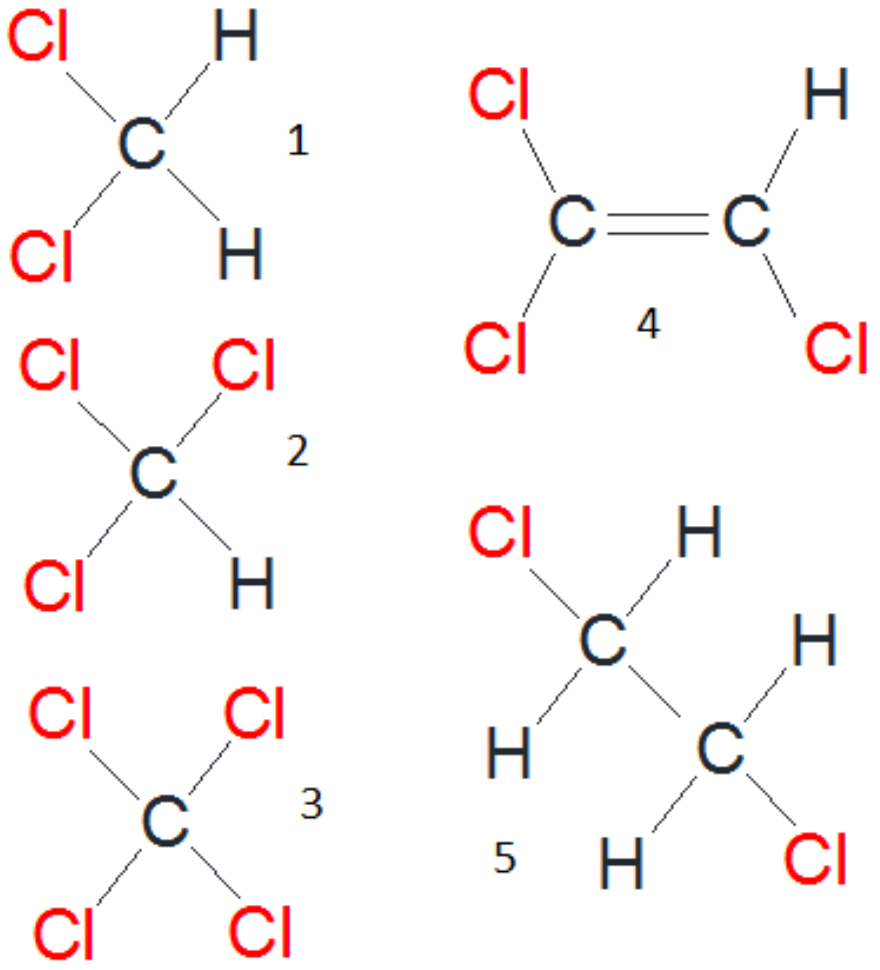

1 – methylene chloride, 2 – chloroform, 3 – carbon tetrachloride,

4 – trichloroethylene, 5 – dichloroethane

Figure 4-9 Chlorinated Hydrocarbons

The ternary diagrams for water + caprolactam + chloroform, water + caprolactam + carbon tetrachloride and water + caprolactam + trichloroethylene are shown in Figures 4-10, 4-11 and 4-12, respectively. The partition coefficient comparisons show that chloroform has the highest equilibrium concentration of caprolactam in the organic phase compared to the aqueous phase and carbon tetrachloride has the lowest equilibrium concentration in the organic phase. This is likely due to the hydrogen bonding capabilities of chloroform molecules. Hydrogen bonding is not possible with carbon tetrachloride due to the lack of a hydrogen atom in the carbon tetrachloride molecule. Trichloroethylene, methylene chloride and dichloroethane show similar partition coefficients for caprolactam to that of benzene as shown in Figure 4-13.

Methylene chloride, 1,2-dichloroethane, 1,1-dichloroethene, chloroform and carbon tetrachloride all fall in the carcinogenic classification therefore they are not considered potential alternatives to benzene for caprolactam extraction. 1,2-dichloroethene has a very low boiling point and is extremely flammable. This solvent also has the potential to be converted to acetylene chloride in the presence of a strong base which is explosive. These properties make 1,2-dichloroethene a poor option to replace benzene. Tetrachloroethane has not been classified as carcinogenic, however it is currently being evaluated as a potential carcinogen[44].

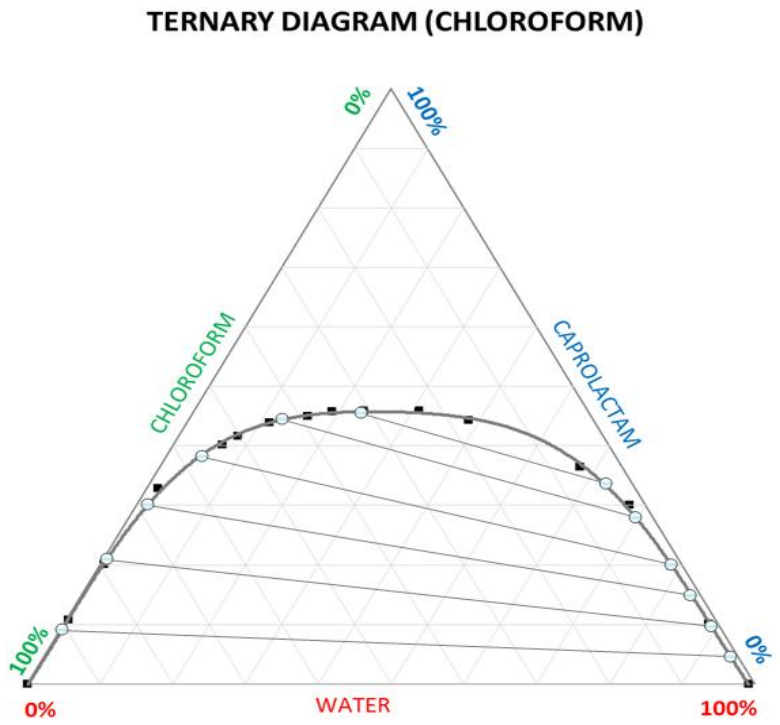

Figure 4-10 Ternary Diagram Water + Caprolactam + Chloroform[58]

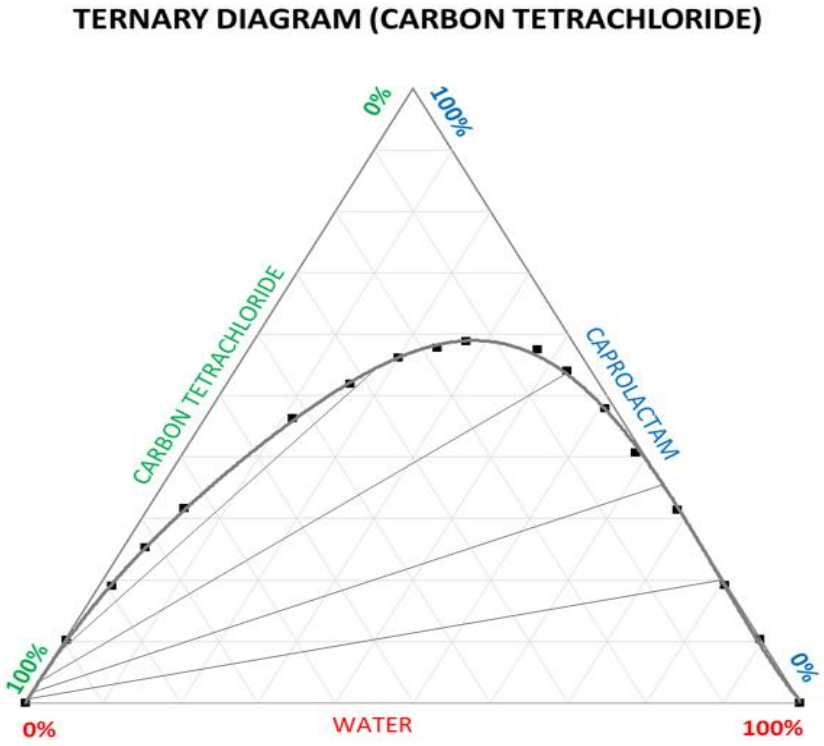

Figure 4-11 Ternary Diagram Water + Caprolactam + Carbon Tetrachloride[58]

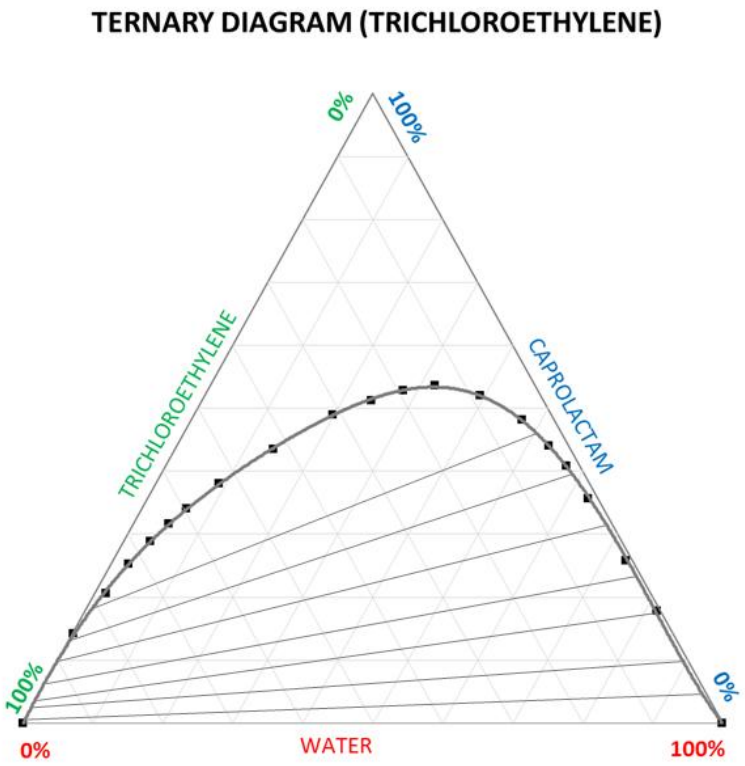

Figure 4-12 Ternary Diagram Water + Caprolactam + Trichloroethylene[58]

Alcohols

Alcohols that have been investigated for caprolactam extraction typically have to contain a large hydrocarbon component to reduce the mutual solubility of the solvent with water. Some alcohols that have been considered include cyclohexanol, 1-heptanol and 1-octanol which are shown in Figure 4-13.

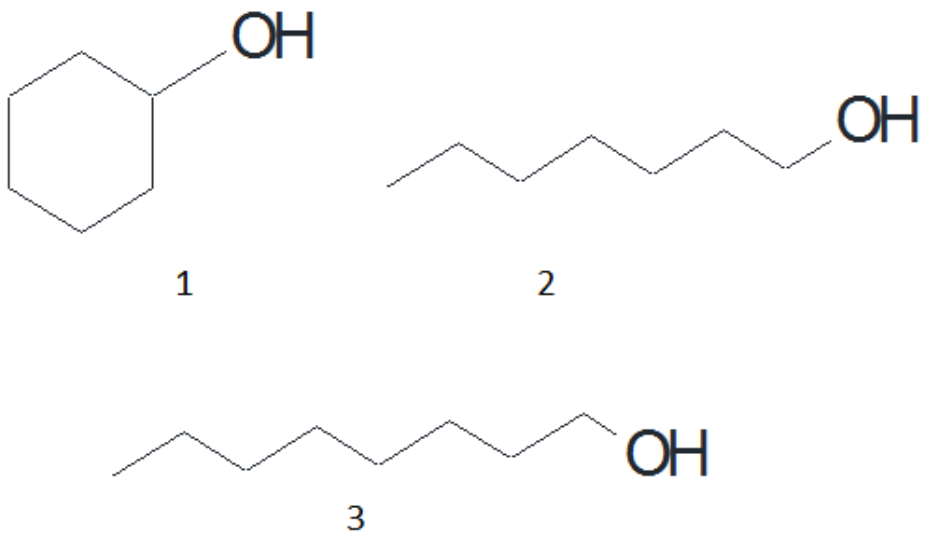

Figure 4-13 Alcohols

Cyclohexanol is a precursor to the caprolactam molecule that has been considered as a potential alternative to benzene as a solvent in extraction. Cyclohexanol has a high capacity for caprolactam however it has a higher solubility in water at roughly 40 grams of cyclohexanol per liter of water. This mutual solubility results in poor separation of impurities, caprolactam losses in extraction raffinates, and it requires extensive solvent recovery units. The ternary diagram for water + caprolactam + cyclohexanol is shown in Figure 4-14[58].

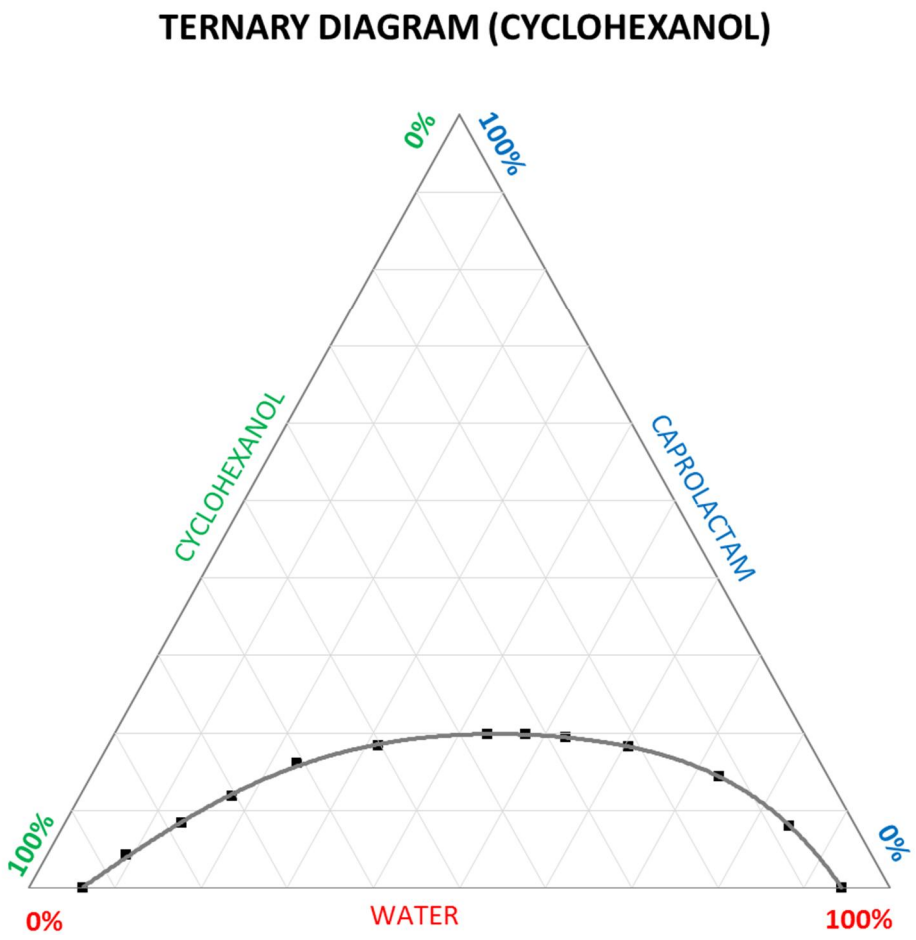

Figure 4-14 Ternary Diagram Water + Caprolactam + Cyclohexanol[58]

Heptanol has a much less mutual solubility with water in comparison to cyclohexanol however the capacity of caprolactam in heptanol is slightly lower than in cyclohexanol. The ternary diagram for water + caprolactam + 1-heptanol is shown in Figure 4-15[64, 65].

Octanol is also being considered in recent research due to a similar capacity for caprolactam in comparison to heptanol with almost negligible mutual solubility with water[66, 67].

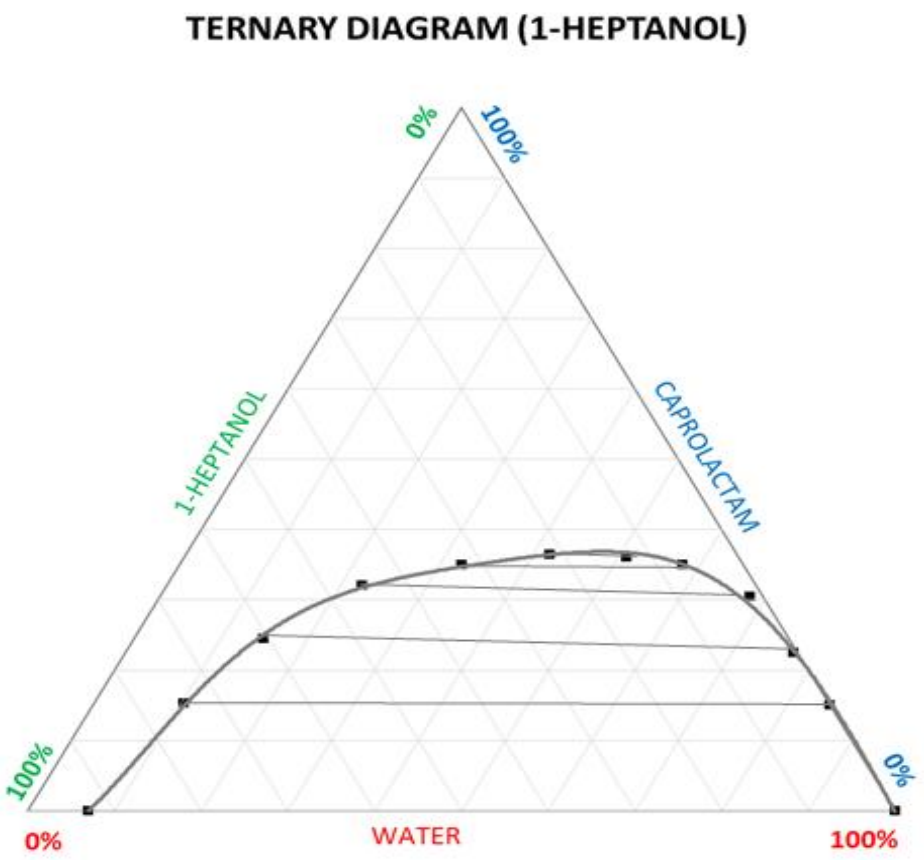

Figure 4-15 Ternary Diagram Water + Caprolactam + 1-Heptanol[64, 72]

Ketones

Like cyclohexanol, cyclohexanone is a precursor to caprolactam that has been considered as a potential alternative solvent for benzene. Cyclohexanone has a 35% solubility for caprolactam, however cyclohexanone has up to 15% solubility in water which make it less efficient in extraction and solvent recovery.

2-heptanone is only slightly soluble in water at 4.3 grams per liter of water making it more acceptable for solvent recovery considerations. This solvent has a slightly higher capacity for caprolactam compared to benzene, and it is less dense than water which would mean that a complete revamp of a current process using benzene as the extracting solvent may not be necessary for conversion. The ternary diagram for water + caprolactam + 2-heptanone is shown

in Figure 4-16[68]. The structures for cyclohexanone and 2-heptanone are shown in Figure 4-17.

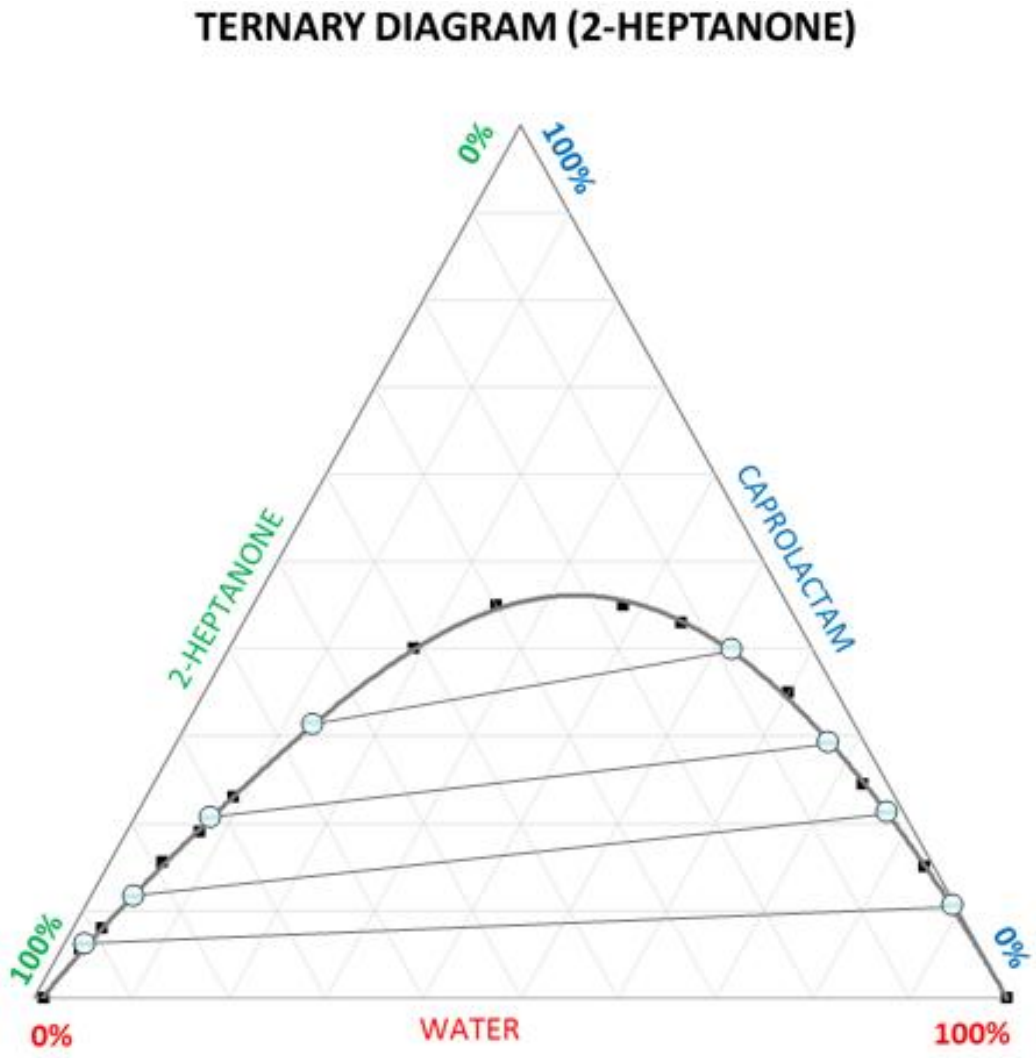

Figure 4-16 Water + Caprolactam + 2-Heptanone[68]

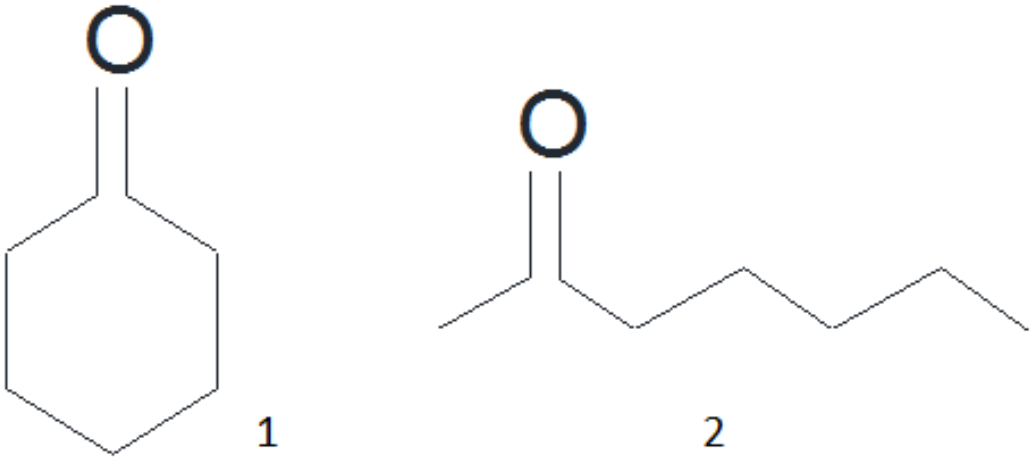

Figure 4-17 Ketone Structures

Ketones are not typically considered potential alternatives for use in the extraction of caprolactam because they possess a carbonyl group. This carbonyl group can be reactive in the process which can lead to the generation of side reactions and further impurities in the product stream.

Solvent Mixtures

Several mixtures have been investigated as potential alternatives for caprolactam extraction. Typically a combination of a non-polar saturated carbon based molecule and a polar carbon alcohol or ketone have been the focus of said studies. The non-polar solvents possess minimal mutual solubility with water however they also reduced capacity towards caprolactam alone[72]. One particular set of solvents include methylcyclohexane and heptanol at various ratios up to 40% heptanol by mass. Another set of solvents investigated included hexane and heptanol at 40% heptanol by mass. Research by van Delden et. al. developed ternary diagrams of water +

caprolactam + 40% heptanol in methylcyclohexane and water + caprolactam + 40% heptanol in heptane[69, 70, 73]. These ternary diagrams are shown in Figures 4-18 and 4-19, respectively.

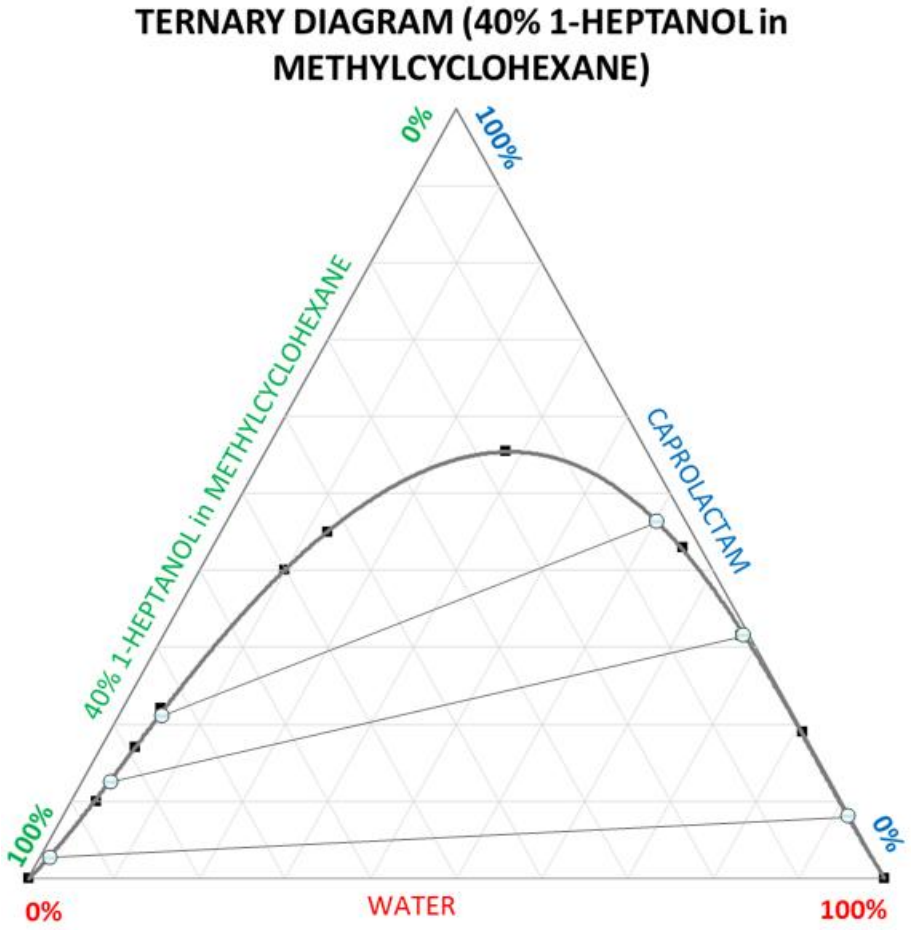

Figure 4-18 Water + Caprolactam + 40% 1-Heptanol in Methylcyclohexane[69]

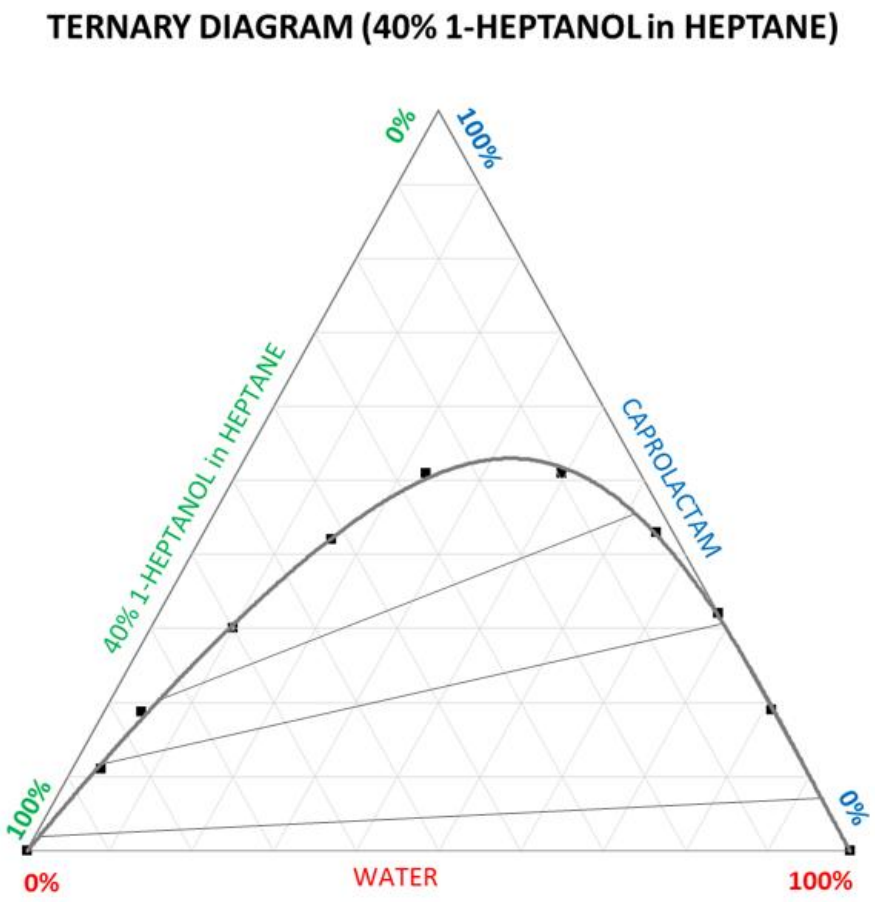

Figure 4-19 Water + Caprolactam + 40% 1-Heptanol in Heptane[69]

Another pair of solvents investigated as potential alternatives to benzene are 1-octanol in a non-polar organic solvent. The set of non-polar organic solvents includes cyclohexane, hexane, heptane and octane and the weight percent of 1-octanol ranged from 50-60%[67].

Recent research has also included investigation in performing caprolactam extraction with ionic liquids[71]. Selection of a proper alternative solvent to benzene in caprolactam extraction is not a simple task. For production facilities that are currently using benzene in the purification of caprolactam, there are significant costs to consider for conversion to an alternative solvent. Once a solvent is deemed sufficient for caprolactam solubility capacity and has a reasonable partition coefficient with caprolactam in the presence of water, then there are other

parameters such as surface tension in the presence of the solute, density of the solvent, amount of solvent required to perform the extraction, flammability of the solvent, and recoverability of the solvent among many others. The thought process in swapping solvents has to include whether or not the current extraction columns are sized appropriately, will the raffinate and extract end up on opposite locations due to variation in density of the alternative compared to benzene, or if the current solvent recovery system has sufficient heating capacity to recover a solvent with a higher boiling point than benzene. Extensive modifications may come with expensive price tags for plants hoping to convert from benzene to a more benign solvent for the extraction of caprolactam, however new caprolactam plants currently in the design phase should have sufficient literature and background on the investigation into alternative solvents or solvent systems that they can go another route from the selection of benzene for their processes.

Toluene seems to be the better alternative for caprolactam extraction as it does not pose the same health risks as benzene. Even though toluene does not have the same capacity for caprolactam, it does provide similar impurity separation and can be readily recovered via a solvent recovery system comparable to applications in benzene recovery.

Chapter 5 - Conclusions

Caprolactam Extraction

Caprolactam extraction is a key unit operation in the purification of caprolactam. The forward and back extraction of caprolactam from the aqueous caprolactam oil is essential for effective removal of both organic and aqueous soluble impurities that are formed in the Beckmann Rearrangement, the neutralization step or enter into the process with one of the raw materials. The entrainment of said impurities into the caprolactam final product stream leads to poor quality Nylon 6 polymer products. Efficient extraction in all three columns is essential to minimize caprolactam losses in the waste streams. The loss of caprolactam in the waste stream results in an increase in the variable cost per unit of production.

RDC Extraction Columns

Caprolactam extraction can be achieved by way of a variety of extraction column options. Pulsed-packed columns, rotating disk and doughnut columns, and rotating disk contactor extraction columns are the most widely employed technologies for the extraction of caprolactam. However the propensity to form emulsions or have phase carryover in the forward extraction of caprolactam lends a preference for the RDC extractor because the high shear mixing can be readily reduced by slowing the rotation of the rotor. The RDC is also more suitable for fouling materials, and it is the better option for liquid-liquid systems with low interfacial tension. The RDC extraction column is the preferred choice due to its high throughput, low cost, low driving power, high efficiency per unit height and high operational flexibility[57].

Rotor Speed Curves

The speed at which the rotor and disks are rotated within the RDC extraction column is an important factor in achieving the most efficient solute transfer as the energy input into the

system is proportional to the interfacial area between the solvents in the system. Increased rotor speed at higher flows can lead to increased dispersed phase hold-up in the column and increases in axial mixing which reduces the driving force of the concentration differential. Reduced rotor speeds lead to channeling of the dispersed phase and minimal droplet breakage which reduces interfacial area for solute transfer thereby decreasing extraction efficiency.

The rotor speed curves clearly show that at reduced flow rates, higher rotor speeds are necessary to attain proper droplet breakage. The curves for RDC-1 and the bottom of RDC-2 show a higher required rotor speed which is understandable as these two have the liquid systems with the higher interfacial tension. The rotor speeds for the top section of RDC-2 are significantly lower than those required in the bottom section of RDC-2. To minimize holdup and carryover in the top section of RDC-2, the rotor speed curves developed for the top section have to be the target rotor speeds for the column rather than the ones generated for the bottom section. Unfortunately this means the bottom section of RDC-2 may not receive the energy input necessary to have proper droplet breakage and this could result in reduced extraction efficiency in the latter stages of forward extraction. The rotor speed curves for RDC-1 and RDC-3 are very similar with RDC-1 having slightly higher speed requirements due to the higher interfacial tension of the aqueous ammonium sulfate + benzene + caprolactam system.

Theoretical Extraction Stages

Calculation of the theoretical stages for each extraction column based on flow rates and rotor speeds provided insight on how to achieve higher efficiency for extraction based on the process conditions. In each case, the higher rotor speed curves have much larger slopes at the lower flow rates whereas the lower rotor speeds have flatter slopes. As the flow rates increase in each case, the lowest rotor speeds tend to fall below the middle range rotor speeds in achievable

extraction stages. Comparison of the number of theoretical stages achievable with the rotor speeds in the 75-85% dispersed phase holdup range from the rotor speed curves affords the most efficient rotor speed to target based on feed and solvent flow rates to each extraction column.

Alternative Solvents for Caprolactam Extraction

Benzene has been the preferred choice for extraction of caprolactam for a majority of the industrial processes due to its capacity for caprolactam and high efficiency in solvent recovery, however benzene poses undesired health risks as it is a known carcinogen. There has been considerable investigation in determining possible alternative solvents for the caprolactam extraction process. A number of halogenated solvents have been studied and seem to work well, however many pose their own health and environmental concerns. Alcohols and ketones have shown a high capacity for caprolactam though these solvent have too high mutual solubility with water which results in product losses and impurity issues as well as the requirement for a robust solvent recovery system. Non-polar hydrocarbons alone do not have the capacity for caprolactam, but mixtures of a non-polar hydrocarbon with alcohols or ketones have shown promise. Ensuring the appropriate component ratio in a solvent mixture for a continuous process can require significant process control schemes that could be costly. Toluene does not have the same capacity for caprolactam as benzene yet it is comparable. Toluene shows very similar impurity separation and can be readily recovered in a similar solvent recovery system as that used for benzene. Since toluene does not pose the health risks associated with benzene, toluene seems to be the best choice as an alternative solvent for caprolactam extraction.

Nomenclature

English

$A - area$

$A^H - Helmholtz\ Free\ Energy$

$A_J - Jasper\ coefficient$

$A_{sz} - Szyzkowski\ adsorption\ coefficient$

$a - activity\ coefficient$

$a_0 - standard\ activity$

$B_{sz} - Szyzkowski\ adsorption\ coefficient$

$C - concentration$

$$C_R - constant = \left(\frac{D_S}{D_C}\right)^2$$

$$C_1 - constant = \frac{24 \cdot \mu_c}{0.53 \cdot d_{32} \cdot \rho_c}$$

$$C_2 - constant = \frac{4 \cdot d_{32} \cdot g \cdot \Delta\rho}{1.59 \cdot \rho_c}$$

$$C_3 - constant = \sqrt{{C_1}^2 + \frac{4 \cdot C_2 \cdot (1 - \phi_f)}{1 + 4.56 \cdot {\phi_f}^{0.73}}}$$

$C_\psi - constant, = 1.0\ if\ solute\ transfer\ is\ from\ continuous\ to\ dispersed\ phase,$

$= 1.29\ if\ solute\ transfer\ is\ from\ dispersed\ to\ continuous\ phase$

$d_{32} - Sauter\ mean\ droplet\ diameter$

$D_C - column\ diameter$

$d_{cr} - critical\ drop\ size$

$D_R - rotor\ disc\ diameter$

$D_S - stator\ opening\ diameter$

$d_S - stator\ ring\ opening\ diameter$

$d_T - column\ diameter$

$E_c - continuous\ phase\ axial\ mixing\ coefficient$

$E_d - dispersed\ phase\ axial\ mixing\ coefficient$

$F - force$

$G_f = \left(\frac{z_c}{D_R}\right)^{0.9} \left(\frac{d_S}{D_R}\right)^{2.1} \left(\frac{D_R}{d_T}\right)^{2.4} column\ geometry\ factor$

$g - gravitational\ constant$

$H - height\ of\ compartment, distance\ between\ stators$

$h - dispersed\ phase\ holdup = \phi$

$H_c - height\ of\ column$

$h_c - continuous\ phase\ height$

$HDU - height\ of\ a\ diffusion\ unit$

$HETS - height\ of\ theoretical\ stage$

$h_f - dispersed\ phase\ holdup\ at\ flooding = \phi_f$

$HTU - height\ of\ a\ transfer\ unit$

$K_d - partition\ coefficient = \frac{weight\ \%\ solute_{Phase\ 1}}{weight\ \%\ solute_{Phase\ 2}}$

$L - length, column\ height$

$N - rotor\ speed$

$N_{cr1} - first\ critical\ rotor\ speed$

$N_{cr2} - second\ critical\ rotor\ speed$

$N_P - dimensionless\ power\ number\ of\ the\ rotor$

$N_S - number\ of\ stages$

$P - pressure$

$Pe_0, Pe_1, Pe_2 - Peclet\ Number$

$Pe_c - continuous\ phase\ Peclet\ Number$

$Pe_d - dispersed\ phase\ Peclet\ Number$

$Pe_F - feed\ Peclet\ Number$

$Pe_S - solvent\ Peclet\ Number$

$P_W - power$

$Q_c - volumetric\ flow\ of\ continuous\ phase$

$Q_d - volumetric\ flow\ of\ dispersed\ phase$

$Q_F - volumetric\ flow\ of\ the\ feed$

$Q_S - volumetric\ flow\ of\ the\ solvent$

$R - gas\ constant$

$\check{R} - volumetric\ phase\ ratio = \frac{Q_d}{Q_c}$

$Re_R - rotor\ Reynolds\ number = \frac{N \cdot D_R^2 \cdot \rho_c}{\mu_c}$

$S - entropy$

$T - temperature$

$U - internal\ energy$

$\bar{u}_0 - characteristic\ velocity\ of\ droplets$

$V - volume$

$V_c - superficial\ velocity\ of\ the\ continuous\ phase$

$\bar{V}_c - actual\ velocity\ of\ the\ continuous\ phase\ through\ the\ stator\ opening$

$V_{c,f} - superficial\ velocity\ of\ the\ continuous\ phase\ at\ flooding$

$V_d - superficial\ velocity\ of\ the\ dispersed\ phase$

$\bar{V}_d - actual\ velocity\ of\ the\ dispersed\ phase\ through\ the\ stator\ opening$

$V_e - effective\ slip\ velocity$

$V_s - slip\ velocity$

$We_D - disc\ Weber\ number$

$w_{2,aq} - Caprolactam\ concentration\ in\ aqueous\ phase$

$w_{2,org} - Caprolactam\ concentration\ in\ organic\ phase$

$X_F - solute\ weight\ fraction\ in\ the\ feed$

$X_R - solute\ weight\ fraction\ in\ the\ raffinate$

$Y_S - solute\ weight\ fraction\ in\ the\ solvent$

$z_c - compartment\ height$

Greek Letters

$\beta - coefficient$

$\Gamma_i - interfacial\ excess\ concentration$

$\gamma - surface\ tension\ or\ interfacial\ tension$

$\Delta\rho - difference\ between\ the\ density\ of\ the\ continuous\ and\ dispersed\ phases$

$\varepsilon, \epsilon - mechanical\ power\ dissipation\ per\ unit\ mass$

$\mu_c - viscosity\ of\ the\ continuous\ phase$

$\mu_i - viscosity\ of\ species\ i$

$\mu_i^0 - viscosity\ of\ species\ i\ at\ standard\ conditions$

$\mu_w - viscosity\ of\ water$

$\rho_c - density\ of\ the\ continuous\ phase$

$\phi - dispersed\ phase\ holdup = h$

$\phi_f - dispersed\ phase\ holdup\ at\ flooding\ = h_f$

References

1. Dutta, B. K. (2007). Principles of Mass Transfer and Separation Processes. PHI Learning Pvt. Ltd., 8.3 Solvent Selection (pp. 434-436). New Delhi.

2. Butt, H-J.,Graf, K., Kappl, M. (2013). Physics and Chemistry of Interfaces. Wiley-VCH Verlag GmbH & Co. KGaA, 3.3.5 Interfacial Excess Energies (pp. 44-46). Weinheim, Germany.

3. Ghosh, P. NPTEL – Chemical Engineering – Interfacial Tension [pdf module]. Retrieved from E-Learning Course Website: http://nptel.ac.in/courses/103103033/8

4. Antonoff, G. On the Validity of Antonoff's Rule. J. Phys. Chem. 46 (1942) pp. 497-499

5. Butt, H-J.,Graf, K., Kappl, M. (2013). Physics and Chemistry of Interfaces. Wiley-VCH Verlag GmbH & Co. KGaA, 3.5.2 Interfacial Excess Energies (pp. 49-53). Weinheim, Germany.

6. Dukhin, S., Kretzschmar, G., Miller, R. Dynamics of Adsorption at Liquid Interfaces: Theory, Experiment, Application. Elsevier Science B.V. (1995) 2.5 Treatment of the Langmuir Adsorption Isotherm as Introduction to Adsorption Dynamics (pp. 47-48). Amsterdam, The Netherlands

7. Jasper, J. The Surface Tension of Pure Liquid Compounds. J. Phys. Chem. Ref. Data. 1 (1972) pp. 841-1009

8. Wu, H. Chung, T. (2011) Effect of Surface Tension on Mass Transfer Devices, Mass Transfer in Multiphase Systems and its Applications, Prof. Mohamed El-Amin (Ed.), ISBN: 978-953-307- 215-9, InTech, Available from: http://www.intechopen.com/books/mass-transfer-in-multiphase-systems-and-itsapplications/effect-of-surface-tension-on-mass-transfer-devices

9. Bakker, C., van Buytenen, P., Beek, W. Interfacial Phenomena and Mass Transfer. Chem. Eng. Sci. 20 (1966) pp. 1039-1046

10. Haydon, D. Oscillation Droplets and Spontaneous Emulsification. Nature 176 (1955) pp. 839

11. Davies, T. Mass-Transfer and Interfacial Phenomena Proc. Roy. Soc. (London) A243 (1958) pp. 483

12. Sternling, C., Scriven, L. Interfacial Turbulence: Hydrodynamic Instability and the Marangoni Effect. AIChE J. 5 (1959) pp. 514-523

13. Treybal, R. Liquid Extraction, 2nd Edit., McGraw-Hill, New York (1963)

14. McFerrin, A., Davison, R. The Effect of Surface Phenomena on a Solvent Extraction Process. AIChE Journal. 17 (1971) pp. 1021-1027

15. Stevens, G. Interfacial Phenomena in Solvent Extraction and its Influence on Process Performance. Tsinghua Sci. & Tech. 11 (2006) pp.165-170

16. Groothius, H., Zuiderweg, F. Influence of Mass Transfer on Coalescence of Drops. Chem. Eng. Sci. 12 (1960) pp. 288

17. MacKay, G., Mason, S. Some Effects of Interfacial Diffusion on the Gravity Coalescence of Liquid Drops. J. Colloid Sci. 18 (1963) pp. 674

18. Hanson, C. Recent Advances in Liquid-Liquid Extraction. Pergamon Press Ltd. (1971) 6.6 Coalescence and Break-up of Drops in Extraction Equipment (pp. 579-584). Oxford, England.

19. Drew, T. Advances in Chemical Engineering Volume 4. Academic Press, Inc. (1963) 1. Mass-Transfer and Interfacial Phenomena (pp. 1-49). London, England.

20. Jeffreys, G., Davies, G. Recent Advances in Liquid-Liquid Extraction. Elsevier Ltd. (1971) Chapter 14 – Coalescence of Liquid Droplets and Liquid Dispersion. pp. 495-584

21. Lee, J., Hodgson, T. Film Flow and Coalescence – Basic Relationships, Film Shape and Criteria for Interfacial Mobility. Chem. Eng. Sci. 23 (1968) pp. 1375-1397

22. Ramaswamy, S., Huang, H-J., Ramarao, B. (2013) Separation and Purification Technologies in Biorefineries. John Wiley & Sons Ltd. 3.4.2 Types of Extractors (pp. 67-70). Chinchester, West Sussex, United Kingdom.

23. Moris, M., Diez, F., Coca, J. Hydrodynamics of a Rotating Disc Contactor. Separation and Purification Tech. 11 (1997) pp. 79-92

24. Lo, T., Baird, M., Hanson, C. Handbook of Solvent Extraction. John Wiley & Sons Ltd. (1983) 13.3 Scheibel Columns (pp. 419-429). New York, United States of America.

25. Rousseau, R. Handbook of Separation Process Technology. John Wiley & Sons, Inc. (1987) 7.7 Performance and Efficiency of Selected Contactors (pp. 441-446). New York, United States of America.

26. Lo, T., Karr, A. Development of a Laboratory-Scale Reciprocating Plate Extraction Column. Ind. Eng. Chem. Process Des. Dev. 11 (1972) pp. 495-501

27. Dongaonkar, K., Clive Pratt, H., Stevens, G. Mass Transfer and Axial Dispersion in a Kuhni Extraction Column. AIChE Journal 37 (1991) pp. 694-704

28. Yang, Y., Fei, W., Sun, J., Wan, Y. Hydrodynamics and Mass Transfer Performance of a Modified Rotating Disc Contactor (MRDC). Trans IChemE, Vol 80, Part A, (2002) pp. 392-400

29. Rozkos, B., Mizek, T., United States Patent C 3,495,947 Asymmetric Rotating Disc Contactor. Prague, Czechoslovakia.

30. Torab-Mostaedi, M., Azadollahzadeh, M. Mass Transfer Performance in an Asymmetric Rotating Disc Contactor. Chem. Eng. Res. and Des. 94 (2015) pp. 90-97

31. Speegle, M. (2011). Process Technology Systems. Delmar Cengage Learning., 13 Extraction Systems (pp. 179-189). Clifton Park, New York, United States of America.

32. Reman, G., Olney, R. The rotating disk contactor – a new tool for liquid-liquid extraction. Chem. Eng. Prog. 51 (1955) pp. 141.

33. Garthe, D. Fluid Dynamics and Mass Transfer of Single Particles and Swarms of Particles in Extraction Columns. Ph.D. Thesis (2006) Technische Universitat Munchen, Munchen

34. Cauwenberg, V., Degreve, J., Slater, M. The Interaction of Solute Transfer, Contamininants and Drop Break-Up in Rotating Disc Contactors: Part II. The Coupling of Mass Transfer and Breakage Process via Interfacial Tension. Can. J. Chem. Eng. 75 (1997) pp. 1056-1066

35. Schmidt, S., Simon, M., Attarakih, M., Lagar, L., Bart, H. Droplet Population Balance Modeling – Hydrodynamics and Mass Transfer. Chem Eng.Sci. 61 (2006) pp. 246-256

36. Haderer, T., Marr, R., Martens, S., Siebenhofer, M. Design of Rotating Disc Contactors; Implementation of CFD Tools. Presentation at the 2004 Annual Meeting, Austin, TX, Nov. 7-12

37. Godfrey, J., Houlton, D., Ramlochan, K., Slater, M. Single Phase Axial Mixing in Rotating Disc Contactors, Trans. IChemE, 79 (2001) pp.156-162

38. Laddha, G., Degaleesan, T., Kannapan, R. Hydrodynamics and Mass Transport in Rotary Disc Contactors. Can. J. of Chem. Eng. 56 (1978) pp.137-150

39. Khadivparsi, P. Simulation of Rotary Disc Contactors for Industrial and Semi-Industrial Processes. M.Sc. Thesis, University of Tehran, (1993)

40. Molavi, H., Hosseinpoor, S. Bahmanyar, H. An Investigation on the Effect of Continuous Phase Height on the First and Second Critical Rotor Speeds in a Rotary Disc Contactor, International Journal of Chemical, Molecular, Nuclear, Materials and Metallurgical Engineering. 4 (2010) pp. 37-42

41. Kumar, A., Hartland, S. Prediction of Drop Size in Rotating Disc Extractors. Can. J. of Chem. Eng. 64 (1986) pp. 915-924

42. Kamath, M., Subba Rau, M. Prediction of Operating Range of Rotor Speeds for Rotating Disc Contactors. Can. J. of Chem. Eng. 63 (1985) pp. 578-584

43. Alessi, V., Penzo, R., Slater, M., Tessari, R. Caprolactam Production: a Comparison of Different Layouts of the Liquid-Liquid Extraction Section. Chem. Eng. Technol. 20 (1997) pp. 445-454

44. Schmidt, M. Analysis of Alternatives (Public Version) Industrial Use as an Extraction Solvent for the Purification of Caprolactam from Caprolactam Oil. DOMO Caproleuna GmbH (2014)

45. Lo, T., Baird, M., Hanson, C. Handbook of Solvent Extraction. John Wiley & Sons Ltd. (1983) 18.4 Extraction of Caprolactam (pp. 557-567). New York, United States of America.

46. Alessi, V., Penzo, R., Slater, M., Tessari, R., Caprolactam Production: A Comparison of Different Layouts of the Liquid-Liquid Extraction Section. Chem. Eng. Technol. 20 (1997) pp. 445-454

47. Kumar, A., Hartland, S. Unified Correlation for the Prediction of Drop Size in Liquid-Liquid Extraction Columns. Ind. Eng. Chem. Res. 35 (1996) pp. 2682-2695

48. Kumar, A., Hartland, S. A Unified Correlation for the Prediction of Dispersed-Phase Hold-Up in Liquid-Liquid Extraction Columns. Ind. Eng. Chem. Res. 34 (1995) pp. 3925-3940

49. Strand, C., Olney, R., Ackerman, G. Fundamental Aspects of Rotating Disk Contactor Performance. AIChE J. 8 (1962) pp. 252-261

50. Kumar, A., Hartland, S. Empirical Prediction of Operating Variables in Liquid-Liquid Extraction Equipment, Godfrey, J., Slater, M. Eds., Wiley, Chichester, U.K., pp 625-735

51. Kumar, A., Hartland, S., Design of Liquid-Liquid Extractors. Min. Pro. Ext. Met. Rev. 17 (1997) pp. 43-79

52. Molavi, H., Hosseinpour, S., Bahmanyar, H., Mojtaba, S. Modified Correlations for the First and Second Critical Rotor Speeds, as well as Break Up Probability in a Rotary Disc Contactor. Can. J. Chem. Eng. 89 (2011) pp. 1236-1246

53. Vogel, H., Todaro, C. Fermentation and Biochemical Engineering Handbook (Second Edition); Todd, D. Solvent Extraction. Ch. 8 pp.348-381

54. Laitinen, A., Kaunisto, J. Hydrodynamics and Mass Transfer in a Rotating Disk Supercritical Extraction Column. Ind. Eng. Chem. Res. 37 (1998) pp. 2529-2534

55. Lo, T., Baird, M., Hanson, C. Handbook of Solvent Extraction. John Wiley & Sons Ltd. (1983) 13.1 Rotating-Disk Contactor (pp. 391-404). New York, United States of America.

56. Kumar, A., Hartland, S. Prediction of Axial Mixing Coefficients in Rotating Disc and Asymmetric Rotating Disc Extraction Columns. Can. J. Chem. Eng. 70 (1992) pp.77-87

57. Molavi, H., Hosseinpour, S., Bahmanyar, H., Mojtaba, S. Investigations on Local and Average Static Hold-Ups in Liquid-Liquid Systems in a Rotary Disc Contactor. Can. J. Chem. Eng. 89 (2011) pp.1464-1472

58. Tettamanti, K., Nogradi, M., Sawinsky, J. Equilibria of the Ternary System Caprolactam / Water / Organic Solvent, in the Liquid State. Periodica Polytechnica. 4 (1960) pp. 201-217

59. van Delden, M., Kuipers, N., de Haan, A. Liquid-Liquid Equilibria and Physical Properties of the Quaternary Systems Water + Caprolactam + Ammonium Sulfate + Benzene and Toluene. J. Chem. Eng. Data 49 (2004) pp. 1760-1770

60. Tuinier, R., Krooshof, G. Interfacial Tension Between Benzene and Water in the Presence of Caprolactam. J. Colloid Int. Sci. 382 (2012) pp.105-109

61. van Delden, M. Caprolactam Extraction in a Pulsed Disc and Doughnut Column with a Benign Mixed Solvent. Ph.D. Thesis, University of Twente, The Netherlands, 2005

62. Glazko, I., Yu, A., Levanova, S. Performance and Selectivity of Organic Solvents in Extraction of Caprolactam from Lactam Oil. Russian J. Appl. Chem. 80 (2007) pp. 941-944

63. Kirchnerova, J., Cave, G. The Solubility of Water in Low-Dielectric Solvents. Can. J. Chem. 54 (1976) pp. 3909-3916

64. Wijtkamp, M., van Bochove, G., de Loos, Th., Niemann, S., Fluid Phase Equilib. 158-160 (1999) pp. 939-947

65. Poraicu, M., Davidescu, C., Pacurariu, C. Hydroquinone Extraction from Acid Solutions. Chem. Bull. Politechnica. 42 (1997) pp 139-143

66. Gong, X, Lu, Y., Li, M., Ma, X., Ni, Q., Luo, G. Liquid-Liquid Equilibria of the Quaternary System Water + Caprolactam + 1-Octanol + Ammonium Sulfate. J. Chem. Eng. Data. 52 (2007) pp. 851-855

67. Gong, X, Lu, Y., Li, M., Ma, X., Ni, Q., Luo, G. Selection and Evaluation of a New Extractant for Caprolactam Extraction. Chin. J. Chem. Eng. 16 (2008) pp. 876-880

68. van Bochove, G., Krooshof, G., de Loos, Th. Fluid Phase Equilib. 194-197 (2002) pp. 1029-1044

69. van Delden, M., Kuipers, N., de Haan, A. Selection and Evaluation of Alternative Solvents for Caprolactam Extraction. Separation and Purification Tech. 51 (2006) pp. 219-231

70. van Delden, M., Vos, G., Kuipers, N. Extraction of Caprolactam with an Alternative Benign Solvent in a Pulsed Disc and Doughnut Column. Solvent Extraction and Ion Exchange 25 (2007) pp. 639-664

71. Chen, D., OuYang, X., Wang, Y., Yang, L., He, C. Liquid-Liquid Extraction of Caprolactam from Water Using Room Temperature Ionic Liquids. Separation and Purification Tech. 104 (2013) pp. 263-267

72. van Bochove, G. Two- and Three-Liquid phase Equilibria in Industrial Mixed-Solvent Electrolyte Solutions. Ph.D. Thesis, DUP Science, Delft, 2003

73. Gong, X., Lu, Y., Luo, G. Phase Equilibrium Calculations in Mixtures Containing Caprolactam with a UNIFAC Model. Chin. J. Chem. Eng. 18 (2010) pp. 286-291

74. Lo, T., Baird, M., Hanson, C. Handbook of Solvent Extraction. John Wiley & Sons Ltd. (1983) 13.4 Oldshue-Rushton Column (pp. 431-439). New York, United States of America.